Multi-case Evaluation of Empirical Methods for Satellite-Derived Bathymetry

Shore Monitoring & Research

TU Delft

Deltares

Master Thesis

TU Delft
Author: Sean Zandbergen
4179153

Multi-case Evaluation of Empirical Methods for Satellite-Derived Bathymetry
Committee:

- Prof.dr.ir. S.G.J. Aarninkhof
- ir. R.C. de Zeeuw
- Dr. ir. A.P. Luijendijk
- Dr. R.C. Lindenbergh

Date: June 4, 2020

Summary

Research on the physical, ecological and environmental processes in the coastal zone often rely on the availability of accurate bathymetric information. The traditional method to acquire these data is by conducting depth soundings from a vessel, which is a very accurate way for measuring bottom elevations in all kinds of water, but has as a downside that the acquisition of data is slow. The rate data collection is limited by the vessel speed and swath, which for instance results in months of surveying to accurately map the entire Dutch coastal zone. Therefore, it is mostly applied in targeted surveys where bathymetric information is required for instance in construction project or detailed coastal analysis and modeling. It is not also feasible to conduct an entire survey for such projects and therefore remote sensing data has gained popularity in the past decades.
Multiple methods of bathymetry derivation from satellite data has been topic of investigation, One of those is the concept of light attenuation, which was already covered in publications from the 1970s but is still used in many (coastal) researches. A simplification of the complex radiative transfer theory was made by assuming a log-linear relationship between reflected radiance and water depth. This simplification implies that calibration with known elevation data is needed to obtain an accurate bathymetry. These empirical Satellite Derived Bathymetry (SDB) methods were successfully used in multiple researches the past years, but those mostly focused on single locations with typical good SDB conditions (clear water with a high reflective bottom).

The main goal of this research was to gain insight in the possible applications and limitations of empirical SDB methods when optical conditions are not as ideal as in previous researches. A multi-case evaluation of these methods was conducted at several different locations on earth with each having particular conditions that affected the reflected radiance ranging from the "most ideal" case with clear water to a case where SDB is hardy possible because of high levels of turbidity.

Promising results were obtained in cases where one can be certain that the measured reflectance is coming from the bottom, so in clear waters with hardly any suspended sediment and waves that disturb the path of light to the bottom. The results, with vertical errors below 50 cm, were in accordance to earlier researches. Also in more complex cases, where water clarity was affected by some levels of turbidity, a reliable bottom was still derived, but vertical errors where increasing. The determining factor whether it was possible to use SDB was if measured reflectance was coming from the sea floor.

The full potential of a single satellite image was further analyzed by spatial analyses which showed that a small amount of data already gives enough information of calibrate a model to an accurate SDB. However, these results all rely on the initial reflectance values measured by the satellite's sensor These initial values were analyzed more elaborately without the use of calibration data. The concept of the attenuation of light in water was applied to satellite images to assess the bottom derivation without performing any calibration of the algorithm. It was found that, even after correction for atmospheric effect, measured reflectances on images that were captured at different time varied per image, which hindered the temporal analysis. With the addition of ground-truth data, these fluctuations are eliminated by vertically shifting the bottom to the absolute correct level, but when no data is available, differences in measured reflectance does not necessarily be caused by vertical bottom changes. A contribution of these fluctuations was found in the solar zenith angle, which is differs over the year.

With SDB it is possible to derive accurate bathymetric maps under good optical condition. When these conditions get more challenging, the uncertainty in the bottom reflection increases, resulting in an increase of uncertainty in SDB as well.

List of Abbreviations

CATZOC	Category Zone of Confidence
CDOM	Color Dissolved Organic Matter
CED	Canny Edge Detection
ESA	European Space Agency
EO	Earth Observation
GEE	Google Earth Engine
GSD	Ground Sample Distance
LAT	Lowest Astronomical Tide
MSL	Mean Sea Level
NDWI	Normalized Difference Water Index
NDVI	Normalized Difference Vegetation Index
NIR	Near-Infrared
NOAA	National Oceanic and Atmospheric Administration
OLI	Operational Land Imager
SBES	Single Beam Echo Sounding
SDB	Satellite Derived Bathymetry
TSM	Total Suspended Matter
SWIR	Short Wave Infrared
WGS84	World Geodetic System 1984

Contents

1 Introduction

Around 40 percent of the world population lives within a distance of 100 kilometers from the coast and 10 percent lives in areas that are 10 meter or less above sea level (United Nations, 2017). The barrier between land and water, the coastal zone, is therefore of major importance for the protection against floods. Besides that, it also functions as habitat for a wide variety of flora and fauna and it fulfills an important recreational function. Too understand the behavior of this highly dynamic area, measurements and modeling are a key part in the coastal zone management. Bathymetric information is vital to perform sufficient analysis on coastal areas. It is used in hydrodynamic models and to assess coastal morphological development and therefore, proper monitoring of these areas is important for the coastal security.

Bathymetric surveying is the way to obtain the required information of the sea bed. However, carrying out these surveys can be challenging. The conventional way to acquire bathymetric data is by performing in-situ measurements, for example by depth sounding. Despite giving accurate results with high spatial resolution, this method is costly and slow and therefore not suitable in many large scale cases. Only a small area can be mapped at once, so in research on larger areas or global scale the use of this method is often impossible. Also in the shallow parts of the coast, sounding has its limitations, since the survey vessels are not able to reach that areas close to the coastline. Therefore, innovative ways to obtain bathymetry are topic of many researches recently.

Remote sensing has been playing a big part in the monitoring of coasts all over the world. With the increasing computational power and the rise of cloud computing, processing large amount of remote sensing data (big data) is getting more and more accessible. The use of satellite imagery is a form of remote sensing that has gained a lot of attention, because of these technological developments. Multi- and hyper-spectral imagery is utilized in monitoring and measuring a variety of phenomena in the coastal zone, such as vegetation, development of the shoreline and bathymetry mapping.

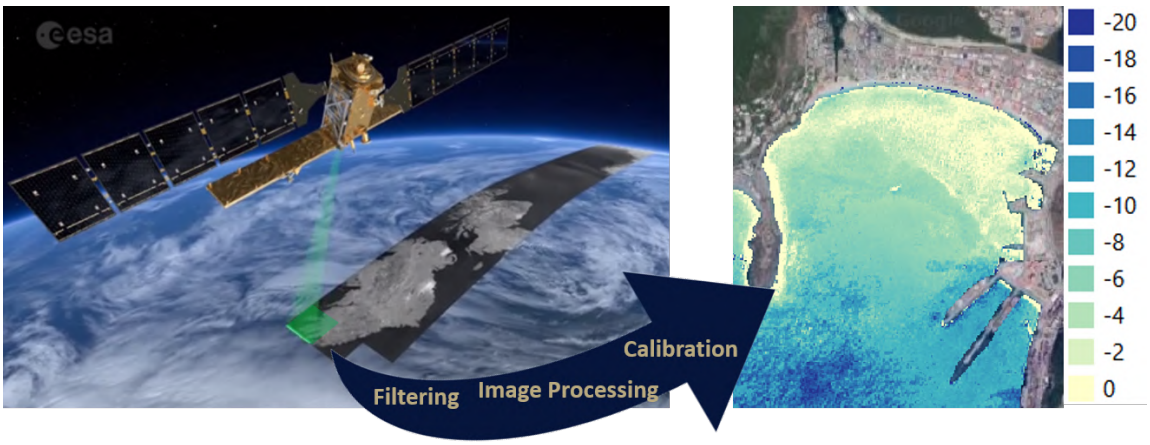

Figure 1.1: Concept of Satellite Derived Bathymetry.

The last decades, several algorithms have been developed to obtain bathymetric information from multi-spectral images. These methods can be distinguished as empirical based and physically based. The empirical methods require ground-truth data to calibrate the pixel values in the image to a value for water depth. Physically based methods make use of the spectral properties of the water

for different frequency bands of the light spectrum. In clear water and under uniform conditions without bed variations, these methods perform well. However, in areas with suspended sediments, changing bed material or other variabilities in the image, Satellite Derived Bathymetry (SDB) is harder to obtain.

1.1 Problem definition

Over the past decades, a number of methods have been developed to obtain water depth information out of multi-spectral images. Most of these methods are based on the principle of light attenuation in water. The physical processes that play role in this phenomenon are highly complex and can therefore only be derived semi-analytically using the radiative transfer equation (Ocean Optics Web Book, 2019). Knowledge on the inherent optical properties of water that cause for absorption, scattering and light attenuation is required to use this technique of water depth derivation. These properties could be obtained via in-situ measurements on turbidity concentration, water clarity, water color and atmospheric conditions, but it is required that these measurements are conducted exactly at the time the satellite passes over the area of interest. The return frequency of Sentinel-2 satellites is well defined, but atmospheric conditions like clouds or haze are not so predictable. Therefore, timing of in-situ measurements is extremely challenging, especially in remote areas where.
To completely remove the need for field data, physical-based methods parameterize these properties by using numerical models that are able to derive optical properties in water given a number of area-dependent specifics (location on earth, time-of-day, etc.). However, this does not take account for local deviations in optical conditions like sediment clouds and applies the same parameters to the entire image.

Another widely used way of deriving water depth from multi-spectral satellite images is using empirical SDB methods. These are a simplification of the radiative transfer equation by assuming a log-linear relationship between measured radiance and water depth. Those methods were developed and assessed in researches over the past years and have proven their performance in optical clear waters. However, they require the addition of ground-truth elevation data to calibrate the models for accurate bathymetric retrieval.

Concluding from a large number of researches on this topic, variations in bottom material and suspended sediment are the two major sources of error using empirical SDB. However, the limitations and optimal processing steps under these different circumstances have never been topic of research. Therefore, this research focuses on defining the limits of empirical methods to derive bathymetry, the accuracy one can expect in certain locations and what considerations should be taken in order to achieve the best results.
Another aspect that is treated in this research, is the use of satellite images for the purpose of temporal morpho-dynamic analysis. In this application, in-situ training data is not necessarily required, because also the relative differences can be a valuable source of information for the qualitative analysis of elevation changes in sea bottom.

The problem definition is translated into the following objectives:

- Define the shortcomings and limitations of empirical SDB methods
- Develop an optimal strategy to obtain a satellite derived bathymetry under various circumstances.

1.2 Research Questions

1.2.1 Main Question

The research objective is transferred to the following research question:

"To what level can empirical SDB methods be used to give optimal bathymetry under various (optical) conditions?""

The *various conditions* for this research are areas where optical water properties and bottom material vary within the defined area of interest.

1.2.2 Sub Questions

The following sub-questions are defined that lead to the answer on the main research question.

1. What are results of SDB methods without vertical tuning and are there SDB applications without providing calibration?
2. What methods are available to derive bathymetric information from multi-spectral satellite imagery and how do they perform with respect to each other?
3. What is the performance of the methods when they are extrapolated in time and space?
4. How do water properties (turbidity, bottom type) influence the results of the SDB algorithms?
5. What is the applicability of the investigated SDB method?

2 Literature Review

In this section, the background research for this thesis is presented. Further on in the report, at times reference is made to the information given in this chapter.The literature research covers an overview of coastal monitoring and the applications and processing of satellite data for hydraulic engineering purposes.

2.1 Coastal Monitoring

Understanding the behavior of a coastal system starts with the availability of data to analyze. A variety of methods and techniques has been used to gather information about above- and under water elevation all within their own levels of accuracy. The choose of measuring technique depends on the expected use of the data. For instance, to sufficiently analyze sediment balances, which are often centimeter variations in sea floor, an accurate measuring technique is required, but for a general understanding of the local shape of the bottom the tolerances could be less strict.

The most common and accurate method to measure the bathymetry is by sounding. A vessel, equipped with an echosounder, sends a sound pulse to the seafloor. The sound waves that are reflected by the bottom return to the device that measures the time period between sending and receiving the pulse. With a known sound velocity in water, a measure of the water depth is obtained. Echo sounding comes in two varieties, using single-beam and multi-beam. A single-beam echo sounder can be easily mounted to small vessels that can reach shallow waters, therefore it is widely used for nearshore bathymetry mapping. The downside of single-beam echo sounding is the position of the bottom is measured with small detail. Therefore, small bottom features are often not captured. This technique is mostly applied in transect measurements where with a regular frequency points are measured along a pre-defined transect. To obtain a grid from these transects, some form of interpolation is needed between the transects, which may cause errors in the areas where no direct data is available. A multi-beam, which is basically a configuration of multiple single-beam echo sounders positioned in different angles, can be used to cover a whole area at once. Using this technique, small bottom features can be measured. However, it is less suitable for the use in very shallow water.

LiDAR is another method that is used for the mapping of the coastal zone. An airplane or UAV, equipped with a laser scanner, flies over the area of interest while the laser measures the distance with the ground. Some types of lasers are able to penetrate the water and retrieve bathymetric information up to 50m water depth. However, the use of these bathymetric LiDAR systems is expensive and results depend on the clarity of the water. In turbid waters, the laser is not able to penetrate the water column until the bottom.

Because of the price and the limited temporal resolution of mentioned techniques, the use of remote sensing data is gaining popularity. Development in technology and cloud computing make it possible for researchers to work with large quantities of satellite data. The most used satellites are equipped with optical- or radar sensors, that either capture the reflected solar radiance from the earth (optical) or transmit and receive an electromagnetic signal (radar). Applications of both sensors are explained in more detail in chapter 2.4.

2.2 Satellite Products

According to the UCS Satellite Database (Union of Concerned Scientists, 2019) there are around 760 satellites orbiting the earth with the purpose of earth observation. These can be equipped with a variety of sensors depending on the purpose of the mission. The majority of satellites either have optical- or radar sensors to monitor the earth. Lately, also LiDAR sensors are used, for instance for

measurements of ice thickness in the arctics (ICESAT). The synthetic-aperture radar (SAR) is the most common radar sensor on a satellite. With SAR, a two-dimensional image of the earth's surface can be obtained. A big advantage of radar is the independence of clouds and other atmospheric effects on the measurements, because of the low frequency of electromagnetic waves of the emitted pulse. Optical sensors measure the intensity of the reflected solar radiation from the earth within certain spectral bands. Most of them capture the wavelengths corresponding to visual light to create an image of the earth's surface. Depending on the type of sensor and height of the satellite above the surface of the earth, images with a ground sample distance (GSD) as small as 30 centimeter per pixel can be obtained.

There are several satellite products available that can be used for the purpose of satellite derived bathymetry. The cooperation between The U.S. Geological Survey (USGS) and NASA resulted in the Landsat program, which still offers the longest continuous global record of the surface of the Earth. Its first satellite mission, Landsat1, with the goal of earth observation dates already from the early 1970s. Because of its open access, high temporal resolution and moderate spatial resolution, the Landsat images are widely used in scientific research for many years. Currently Landsat 7 (equipped with the Enhanced Thematic Mapper Plus (ETM+) sensor) and Landsat 8 (equipped with the Operational Land Imager (OLI) sensor) are operational and are in orbit with a revisit time of around 16 days. The images captured by the OLI sensor have a spatial resolution of 30 meters in visible, NIR and SWIR frequency bands. In table 2.1 all frequency bands are listed.

Another earth observation satellite mission which images are freely accessible is operated by the European Space Agency (ESA). The Sentinel-2 mission consists of two identical satellites that are equipped with the Multispectral Instrument (MSI) and capture radiance within the bands specified in table 2.2. Since 2015, these two satellites are in a sun-synchronous orbit to obtain images during daylight with a revisiting time of about 5 days. Because of this high frequency imagery and the higher resolution than Landsat, the use of Sentinel images is increasing in scientific research.

Table 2.1: Landsat 8 OLI bands

Band Number	Central wavelength [μm]	Bandwidth [μm]	Resolution [m]
1	0.443	0.02	30
2	0.482	0.065	30
3	0.561	0.075	30
4	0.655	0.05	30
5	0.865	0.04	30
6	1.609	0.1	30
7	2.201	0.2	30
8	0.590	0.18	15
9	1.373	0.030	30
10	10.8	0.6	100
11	12	1.0	100

Table 2.2: Sentinel-2 MSI bands

Band Number	Central wavelength [μm]	Bandwidth [μm]	Resolution [m]
1	0.443	0.021	60
2	0.492	0.066	10
3	0.560	0.036	10
4	0.665	0.031	10
5	0.704	0.015	20
6	0.741	0.015	20
7	0.783	0.02	20
8	0.833	0.106	10
8A	0.865	0.021	20
9	0.945	0.02	20
10	1.374	0.031	60
11	1.614	0.091	20
12	2.202	0.175	20

2.2.1 Satellite Data Providers

Google has developed a platform which enable users to perform cloud-based processing on a large catalog of satellite image products (Gorelick et al., 2017). Considering the large size of satellite images, this platform is of great contribution to the accessibility of satellite data processing. Satellite products of the Landsat and Sentinel satellite missions are available in the catalog, including some processed versions where raw data is already translated to Radiance and Top of Atmosphere reflection values.In a web-based user interface, custom processing scripts can be written in JavaScript or build-in algorithms can be used in satellite image processing. The map makes it able to visualize calculated raster interactively.
With the Python API, Google made it possible to use the Google Earth Engine (GEE) in combination with Python. A number of additional Python modules were available that improve the workflow of GEE with Python and give similar interactive experience as the JavaScript IDE.

Images with a higher spatial resolution ($<$ 10m) are offered by commercial companies like Maxar (DigitalGlobe) or Planet. Therefore, they are not included in the GEE open catalog. Examples of satellites that capture Hi-Res image are WorldView, QuickBird and TripleSat. However, their increase in spatial resolution is associated with a decrease in spectral resolution compared with Sentinel-2 and Landsat8 (see chapter 2.2.2). Most of them contain measured radiance in four frequency bands (RGB + NIR) with larger bandwidths compared with Sentinel or Landsat images. Another disadvantage of high resolution imagery is the high price. One high-resolution image tile can cost hundreds of euros.

2.2.2 Resolution

Satellite images can be specified into four types of resolution: spectral-, spatial-, temporal- and radiometric resolution. The **spectral** resolution is a measure of the amount of spectral bands and the wavelength range within the bands. An image with a high spectral resolution has many bands which allows for narrow bandwidth. A smaller wavelength band give more detailed information about what radiance of wavelength is reflected.

The area that is covered by one pixel is considered **spatial** resolution. There is a large range of multi spectral satellite product with resolutions varying between 1000m and 0.3m. Obviously, performing processing on a higher resolution image, requires more computational power than for a low-res image of the same area. Depending on the desired application, a product with a certain spatial resolution is chosen. The satellites considered in this research are in orbit around the world and revisit any location on earth with a certain time. This time varies per satellite and is defined as the temporal resolution. For the purpose of monitoring high dynamic processes, a small revisit time is necessary, thus a high **temporal** resolution.

Finally there is **radiometric** resolution. This is governed by the accuracy a sensor is able to collect data and is expressed in bits. Regular images often are in a 8-bits format, which means that every pixel can have one of the 2^8 values (so a value between 0 and 255). Landsat and Sentinel respectively have a 16- and 12 bit radiometric resolution, which means that for Landsat 8 (OLI)every pixel on every wavelength band can have a value between 0 and $2^{16} = 65{,}536$ and for Sentinel-2 (MSI) 4,095. Because the pixel could have more values between the minimun and maximum value, an image with a higher radiometric resolution has a more detailed measurement in every pixel. However, this high bit depth also results in larger data size of these images.

The level of resolution is a trade-off between the four mentioned resolutions. A high temporal resolution image is paired with a low spatial resolution, because that requires a large earth-satellite distance. High resolution images often have a moderate spectral resolution because of the large data

size a high resolution image requires. Based on the goal of the used image, a product with certain resolutions is selected.

2.3 Disturbances of Reflectance

Light that is captured by the satellite's optical sensor has traveled a long distance through the atmosphere and, if the image is over water, the water column. The path of light can be disturbed by many factors in the atmosphere and water that reflect or absorb light before it reaches the sea bottom. For the purpose of SDB, the reflected radiance from the sea floor is the one of interest. Reflectance from other sources cause noise in the SDB signal.
Generally, four sources are accountable for the reflectances of light during its path to the sea floor: atmosphere, water surface, water column and the sea bottom itself. The observed radiance as function of wavelength can be expressed as a composition of a few different sources (Kanno et al., 2011). With V the in-water scattering, B the bottom reflectance, S the surface reflectance and A the scattering in the atmosphere:

$$L(\lambda) = V(\lambda) + B(\lambda) + S(\lambda) + A(\lambda) \tag{2.1}$$

This is schematized in figure 2.1. An important step in pre-processing of satellite images is the removal of all measured reflected radiance that is not coming from the sea bottom.

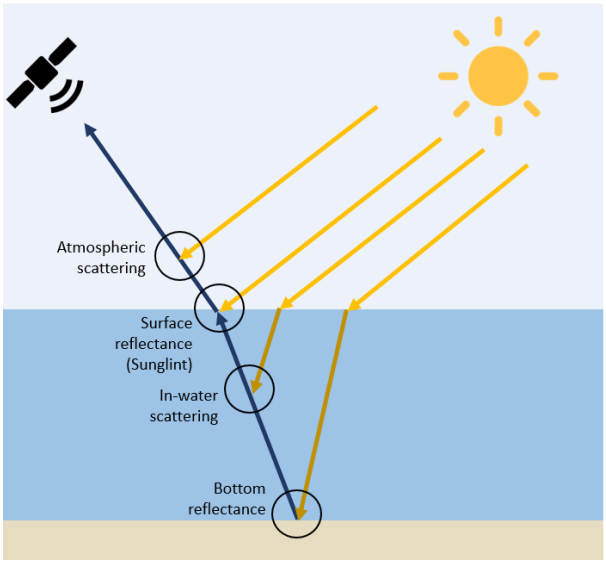

Figure 2.1: Different sources of measured radiance

2.3.1 Atmospheric

Light that is traveling through the atmosphere can either be scattered, absorbed or transmitted without the path being affected. The first two cause artifacts in the image like haziness and the adjacency effect (scattered light affects neighboring pixels). Absorption of light in the atmosphere is caused by aerosols like water vapor, ozone, oxygen, carbon dioxide and methane. Clouds are an extreme type of atmospheric disturbance caused by water vapor where almost all light is blocked from continuing its path and is reflected from the top of the cloud. Water vapor in smaller concentrations let some light pass while some fraction is scattered.
Other factors that mainly cause scattering of light are small particulates like smoke, smog and dust. These are mostly concentrated around highly polluted areas or, in the case of dust, around deserts. Also natural phenomena like volcano eruptions bring large concentrations of particulates in the atmosphere.

For the atmospheric correction of satellite images, numerous algorithms were developed. Most of them are based on the basis of the radiative transfer theory. This equation analytically describes the scattering and absorption of solar radiance. However, solving this equation for all contributing constituents has never been achieved. Therefore, several models with assumptions of parameters and lookup tables are made. Examples of well-known models are 6S, MAJA, ACOLITE. Comparative research of some models Sola and Llovería (2018) with in-situ spectral measurement on land showed small difference between the performance of atmospheric correction models. Their performance mainly depends on the land cover.

Since late 2018, Sentinel provides images that are atmospherically corrected as Level-2A processed images in GEE. These images are processed with ESAs SEN2COR module. If an image is corrected for atmospheric effects, the resulting values are called the Surface Reflectance (SR). For application on land, this correction is already sufficient to perform analysis, but for application in water, the water surface and water column also contribute to light scattering and absorption that requires correction.

2.3.2 Water Column

As opposed to atmospheric correction, there are not many algorithms that correct for the effects of water on measured radiance. It is challenging to derive a correction for all the water that is captured by the image. This is mainly because of the presence of small scale effects. Atmospheric correcting algorithms apply their correction on the entire image, often assuming uniform conditions over the whole covered area. In water, on the other hand, large differences can occur locally by sediments discharged by rivers, hydrodynamic forcing on beaches, dredging or currents. Therefore, conditions in the water column can already be significantly varying within a small area.

The radiative transfer theory can also be applied in water, where the properties of absorption and scattering are described by the Inherent Optical Properties (IOP) of the water Ocean Optics Web Book (2019). However, the magnitude of the contribution of these different IOPs is often not known for the considered image (location and time of capturing). By timing in-situ measurements with the satellite overpass, these values can be added to the radiative transfer equation to derive the contribution of scattering and absorption. To capture the spatial differences in IOPs over an image, many measurements are needed at multiple locations. Another way of retrieving IOP values is by using numerical models like HYDROLIGHT with estimated parameters of certain types of waters. Because of the variability of water properties, for the application on large areas (e.g. entire satellite image) there is less benefit in terms of accuracy compared with simpler methods to estimate bottom reflectance.
One of those simple methods is Dark Object Subtraction (DOS) developed by Chavez (1988). With this method it is assumed that pixels over deep water don't include any reflected radiance from the bottom anymore from any wavelength, because of absorption of radiative energy. So, all the signal the sensor measures is coming from other sources than the sea bottom. If this deep water pixel values are then subtracted from all the water pixels in the image, it is assumed only the value of bottom reflectance remains. Kanno et al. (2011) adjusted this method by stating that the deep water reflectance can be estimated by a linear function of the near-infrared frequency band such that:

$$L(\lambda_i)_\infty = \alpha_0 + \alpha_1 L(\lambda_{NIR}) \tag{2.2}$$

Using linear regression with the deep water pixels of band i as dependent variables, the coefficients α_0 and α_1 can be derived.

2.3.3 Sun Glint

The third source of error in measured bottom reflectance is the reflectance of the water surface. If the sensor of the satellite is facing the same angle with the earth's surface (zenith) as the solar radiance is reflected, a phenomenon called sun glint occurs. In that case, the water surface acts as a mirror that reflects the sun light directly back to the sensor. This appears as a bright spot in the image, so the reflectance values are high. Correcting for sun glint is only possible in areas where the effect is small. Locations with severe sun glint are not usable for SDB, because all measured reflectance is originating from the water surface. Therefore, detecting and filtering images containing sun glint seems a better solution than correcting for it in the image.

Figure 2.2: Sunglint on a drone image appears as a bright spot in the water

2.4 Satellite Applications

Products from earth observation satellites are used in many fields of research. Just for the coastal zone, there are ample applications to use satellites for monitoring and inspection. In this section, some of those applications are presented.

Bathymetry

Bathymetric information is vital for many applications within the coastal zone management. Traditional methods are relatively slow and expensive (chapter 2), so remote sensing techniques to obtain bathymetry are gaining interest. Satellite products are used in a variety of ways. A common method is to detect crests of waves to determine the local wave length. Using the relation of wave dispersion in shallow water, the water depth under the wave can be obtained. This method requires the use of high spatial resolution satellite images, because the GSD has to be smaller than the wavelength to capture the wave crests. This method is only applicable in areas where waves are present and the noise due to short wind-waves is limited. A large advantage of this method is that it does not rely on the optical properties, which makes it possible to retrieve the water depth even in very turbid waters.
Another way to define bathymetry from satellites is using under-water stereo photogrammetry (Hodúl et al., 2018). Some satellites are capable to capture a stereo-pair of images of an area by tilting the sensor when passing. Because objects in the image are captured from different directions, a 3D representation can be made using triangulation. This algorithm looks for the same object in both

images and finds the intersection of two projection rays. In coastal engineering, this technique is widely used for terrestrial 3D mapping of coastal structures (see **Topography** below). However, in water application of photogrammetry becomes challenging because of refracting light. Also characteristics of the water surface (waves) and water column (turbidity) make it difficult to derive a 3D underwater map.
Radar measurements are also used to derive the bathymetry in waters with depths ranging from 10 to 100 meters. Satellites equipped with a Synthetic Aperture Radar (SAR) sensor, measure the back scatter from an emitted electromagnetic microwave signal. In swell condition without the influence of wind waves or other disturbances, the wave crests can be measured. Using the dispersion relation, the relation between water depth and wave frequency. For water shallower than 10 meters, non-linear effects are contributing more to the wavelength and therefore linear wave theory is no longer applicable.

Vegetation

The presence of vegetation plays an important role in the development of coastal dunes. The most seaward part of the dune, the foredune, is formed by sedimentation due to aeolian sand transport. The growth of vegetation forms a trap for the sand, so it accumulates in these vegetated patches (Durán and Moore, 2013). Therefore, monitoring of vegetation plays an important role in the analysis of dune development.
There is an extensive amount of research performed on the use of (satellite) imagery to monitor vegetation health. The first satellite mission for earth observation, the Landsat 1, was even launched with the goal of monitoring vegetation. Satellite imagery is widely used for years already in agriculture and research on forestry. Therefore, there are ample methods available to investigate vegetation with the use of images. The question is whether these methods are transferable to be used in the coastal zone. The amount of research on that is much more scarce. De Giglio et al. (2017) did research on the use of images from an UAV and high resolution satellite images and was able to classify the vegetation in a coastal dune. Most of the dune vegetation is on a smaller scale than the resolution of public available satellite products. With more high-resolution (sub-meter) satellite images coming available, their application in research within the coastal region will probably increase the coming years.

Shoreline

The position of the shoreline is an important parameter that can used in the analysis of the dynamics of the coast (García-Rubio et al., 2015) as well as assessing the local water level. Whether the coast is accreting or eroding can be determined based on the horizontal location of the water line.
On global scale, a satellite derived shoreline (SDS) has been used to do research on erosion and sedimentation of sandy beaches (Luijendijk et al., 2018). This was done using the entire Landsat 8 collection (approximately 40 years) which has a spatial resolution of 30 meters and it was found that the majority of sandy shorelines around the world showed an eroding pattern over these 40 years of analysis. Using images with greater GSD, shoreline changes can be mapped more accurately.
With the addition of data of a local gauge, shore line tracking can also be used to retrieve bathymetric information of the inter-tidal zone. The position of the water line is connected to a measured water elevation. When using this method on multiple images, captured at different moments within the tidal cycle, the bottom profile of the inter-tidal area is build up. Especially in areas with large tidal range and large inter-tidal areas, with this method large scale, accurate bathymetry can be obtained.

Topography

Multi-spectral satellite images can be used to map the topography from terrestrial areas. The technique for this, stereo photogrammetry, requires a stereo-pair images looking from different

angles to the same area. Most of the time, aerial images from airplanes or UAV are used to apply this technique because of their high spatial resolution and the possibility to acquire more overlapping images. When using images from a satellites, mostly only a single pair of the same area is captured. Because objects in the image are required to perform the triangulation, only high resolution satellite images are capable to use for photogrammetry. These images need to be captured as close in time as possible to each other. Based on the different perspective on the same objects in the image, an elevation map can be produced. Solazzo et al. (2018) is a publication where the elevation of a large area was successfully mapped using high-resolution satellite images.

Water Quality

The optical properties of water can be affected by the occurrence of suspended sediment, CDOM (color dissolved organic matter), algae/phytoplankton or pollutants. In the case of the latter, pollution of a body of water can be detected by satellite images if it affects the color or clarity of the water. These applications are important for ecological and environmental purposes, so poluted water can be detected rapidly and measures can be taken to protect for instance vulnerable habitats or drinking water extraction.
Increased concentration of either of the constituents, changes the manner light travels through the water, so more light energy will be absorbed with larger concentrations. Also different frequencies of light are influenced differently than other. There are several publications on the matter of measuring concentration of total suspended matter (TSM) with multispectral images. Dekker et al. (2002) published a method to quantify TSM by using the radiative transfer equation. They defined that the green and red Landsat bands were most suitable for the estimation of suspended matter. The quantification of sediment required numerical parameterization. Lymburner et al. (2016) used Ecolight 5.0 to obtain the parameters for the concentration calculation. They also developed the TSM index as initial, simple measure of turbidity concentrations. This relation provided an indication of areas where concentrations were high and was defined as:

$$TSMindex = (green + red)/2 \tag{2.3}$$

Turbid water has the largest influence on the accuracy of a satellite derived bathymetry (Gao, 2009). Due to suspended particles in the water, the path of radiation is (partly) blocked. In that case, the light reflects from the top sediment instead of the bottom, which leads to a underestimation of water depth. In Tripathi and Rao (2002), a correction factor is applied to the model to take account for turbidity by dividing the measured reflectance with the suspended sediment concentration.

2.5 Optical Bathymetry Methods

2.5.1 (Semi-)Analytical

Theoretically, water depth can be obtained by analytically solving the radiative transfer equation. This equation connects the optical properties of the water body and the light within the water. However, even for very simple situation (no scattering of light) an analytical solution is not possible (Ocean Optics Web Book, 2019). Therefore, the radiative transfer equation can only be solved numerically and requires parameterization of a large number of variables. (Lee et al., 1999) (Dekker et al.) and Hedley et al. (2005) did researches that are focused one these analytical methods. The advantage of this method is that it can be solved for all properties of water, so not only water depth, but also for instance for bottom albedo, sediment concentration and algae concentration. The model requires a very accurate atmospheric correction which is often very hard to derive.

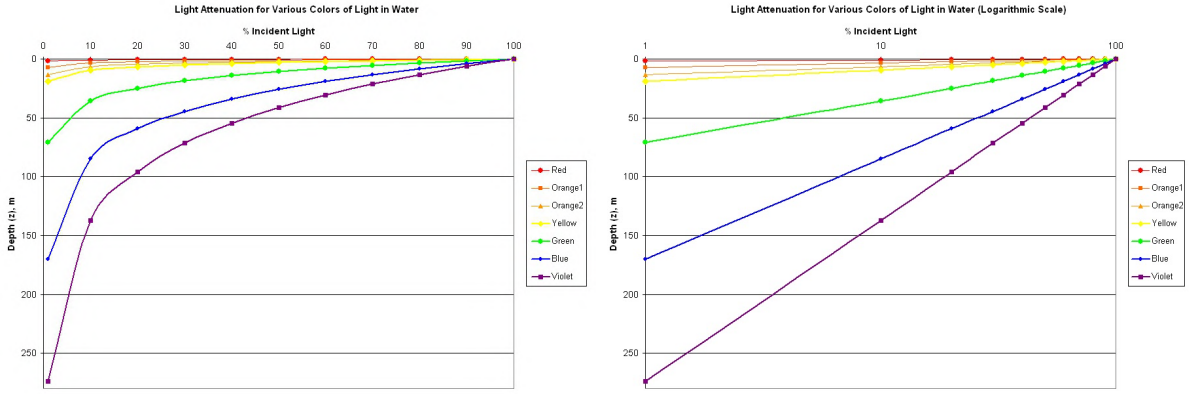

Figure 2.3: Light attenuation, right figure shows the log-linear relation between reflectance and water depth (Leah Moore, 2010)

2.5.2 Empirical

When light enters water, its intensity decreases. In this phenomenon, which is called light attenuation, energy of light decreases exponential with the water depth (Figure 2.3). The intensity of light that is left after traveling through water and the corresponding water depth follow a relationship described by Beer's Law. In clear water, light of different wavelengths is absorbed differently. The shorter wavelengths (green, blue, violet), that contain more energy, penetrate deep into the water, whilst the longer wavelengths (yellow, red, orange) hardly penetrate the water at all and are absorbed high in the water column. In nature this phenomenon is noticeable when looking at the color of the sea. The wavelength that corresponds to blue light is the one that is attenuated the least when traveling through water. Therefore, of all the different wavelengths, the largest portion of reflected light consist of the blue wave length and that is why a clear ocean has a blue color. In coastal areas, the occurrence of more phyto-plankton and suspended sediments results in a reduction of blue-light penetration and more reflections in the green spectrum. The color of the water will therefore be more green or brown. This wavelength depended attenuation of light can be described with the following formula:

$$L(z) = L(0)e^{(-Kz)} \tag{2.4}$$

Where *z* is the water depth, and *K* the attenuation coefficient, which depends on the the wave length of the light. *L(0)* is the incident amount of radiation and *L(z)* is what is left after traveling through a water column of depth *z*. This is under the assumption of a fully reflective bottom where no light energy is absorbed.
Empirical bathymetry methods make use of this theory of light attenuation. The earliest linear transform method, originally developed in Lyzenga (1985), makes use of the relation between sensor measured radiance and in-situ measured water depths (e.g by sounding). He found a correlation of water depth and radiance in a single wavelength band if water optical properties and bottom reflectance are uniform. The measured radiance of a certain frequency band is transformed to the following equation:

$$X_i = ln(L_i - L_\infty) \tag{2.5}$$

L_i and L_∞ are the pixel intensity and the mean of pixel intensities in deep water. This subtraction is a way to correct for disturbances in the water column and is explained in more detail in section 2.3.2. In this simplest case, the water depth is a function of the transformed reflection of only one wavelength band. In that case, the equation for water depth will be:

$$Z = \alpha_0 + \alpha_i * X_i \tag{2.6}$$

Where the alpha-coefficients should be obtained by applying (linear) regression using in-situ bathymetric data. When only one band is used in the calculation, the result is dependent on the reflectance of the bottom which should be uniform and very reflective. In practical situations, where a sea floor can consist of many different materials, this hardly occurs. Every material has its own measure of reflectance and absorption, which is expressed in its albedo value: the percentage of light that is being reflected by a body. Bright surfaces like snow or white sand have high albedo values, thus most of the incident light is reflected, whilst darker objects like vegetation and rock absorb a great portion of light. When there are variations in bottom reflectance, this single frequency method is sensitive for small disturbances of albedo and is therefore only applicable on homogeneous bottoms. For more practical situations, multiple bands of the image are used to adept for (small) albedo variations. For instance, the linear relation between three log-transformed wavelengths X_i , X_j and X_k and the water depth is then defined as:

$$Z = \alpha_0 + \alpha_i * X_i + \alpha_j * X_j + \alpha_k * X_k \tag{2.7}$$

An alternative method was published by Stumpf et al. (2003) and was based on the ratio between two wavelength bands. It was found that a change in bottom albedo has a similar effect on two bands, but a change in depth causes one band to be more absorbed than the other. Therefore, the change in ratio between two bands should be more affected by changes in depth than changes in bottom reflectance, so this method should by applicable on a sea bottom with more strongly spatial variations in albedo.

$$Z = \alpha_0 + \alpha_i * \frac{ln(nL(\lambda_i))}{ln(nL(\lambda_j)} \tag{2.8}$$

These two methods, which are used in a large number of scientific publications on satellite derived bathymetry (e.g. Pacheco et al. (2015),Kabiri (2017),Traganos et al. (2018)), rely on the availability of in-situ depth information to calibrate the algorithm. The most common method of obtaining the alpha-coefficients is using a least squares linear regression. Some researches use the previous methods in combination with other regression techniques like (Adjusted) Geographically Weighted Regression (Yrigoyen et al. (2008),Su et al. (2013) Vinayaraj et al. (2016), Poliyapram et al. (2017)).

Regression

A linear relationship between some target data and one or more predictor variables can be obtained via a method called linear regression. Goal of this method is to find the line that has the best fit for the data points. In simple linear regression this line will follow the form: $y_{pred} = a_0 + a_1 * X$, where a_0 and a_1 are the coefficients that needs to be determined, X is the predictor variable and y_{pred} the predicted target value. Least-squares is the most common method to find the line that is closest to all data points. For each data point, the vertical distance to the regression line is calculated and all there "errors" are squared and summed. Iteratively, the line with the least squared error is the best linear fit for this data set.
The performance of the linear regression can be analyzed using several metrics. The most used one to measure the overall performance is the R-squared, which indicates the amount of correlation between the data and the regression line. As seen in Figure 2.4, regression lines of red, green and blue are differently correlated with the in-situ data. The log-transformed green band shows the best correlation, so its R-squared value is close to 1. The regression line of red is not following the in-situ data so well, so that regression has a low R-squared score.

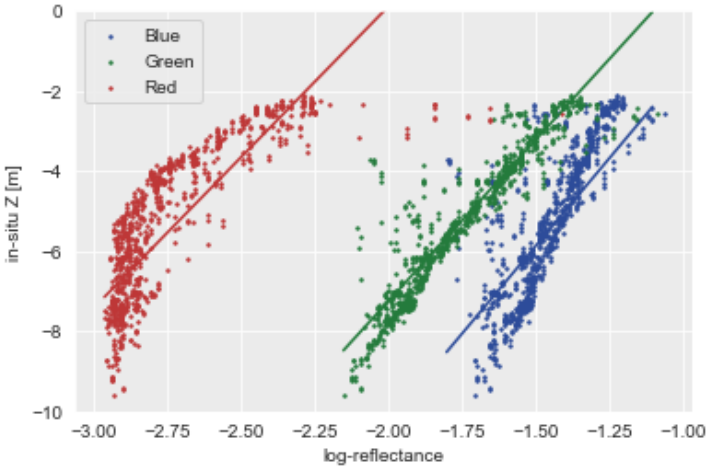

Figure 2.4: Linear regression between reflectance and in-situ calibration data on three wavelength bands

Other methods of regression are also possible. The red wavelength it might be better to use a non-linear method like polynomial regression that can capture the curve better than a straight line. However, the assumption that the relation between reflected light and water depth is log-linear is then not used anymore.

3 Methodology

An elaborate description of the steps that were taken in this research is presented in this section. First the choice of algorithms and satellite products is elaborated. Next, the locations that were used as case study are presented including a description of their characteristics. After that, all the steps that were followed to go from satellite image to bathymetry are treated. This includes downloading, filtering and pre-processing images with the use of the GEE Python API and validation of the results. And finally, the strategy to give answer to the research questions is presented.

3.1 Model- and satellite selection

In chapter 2.2 was explained that there are a numerous amount of satellites equipped with multi-spectral image sensors, all with their own specifications. For the decision which sensor to use, factors like availability, amount of historic data, ground sampling distance (GSD) and price are taken into account. Images from Landsat and Sentinel satellites are openly available and are provided in GEE. Images with a higher spatial resolution are mostly provided by commercial companies which charge per unit area. Because in this research, a large amount of areas (and thus images) were processed, commercial images were not used. In the choice between Landsat-8 and Sentinel-2, the better spatial- and temporal resolution and the proven performance in other researches were the deciding factor for the use of Sentinel-2 images.

For the derivation of bathymetry from satellite images, empirical SDB methods were used in this research. In chapter 2.5.2 was explained that the two main variants of these methods are linear- and ratio transform. Both rely on the same principle of the attenuation of light in water. However, the ratio method contains an additional benefit over the linear method, because it uses the ratio between frequency bands to give a measure for the depth. Theoretically, this should reduce the influence of varying albedo, since the difference in albedo should be about the same in both wavelengths. By using multiple bands in the SDB methods, a large number of band combinations can be made. A selection of combinations that are proven in other researches was made. Both methods were assessed in the analysis of the initial SDB performance. After that, the best performing method was used in further assessment of bathymetry derivation.

3.2 Case Studies

Characteristics of water (clarity, color, bottom material) are of influence on the ability to use satellite images for SDB, but they vary per location on earth. In many existing SDB publications, focus lies on one area to perform and assess a certain SDB algorithm and is often done in areas where the optical condition of the water are good. In this research, goal was to find an optimal way to achieve the best results using empirical SDB methods under various circumstances. Therefore, a number of locations with varying (optical) characteristics were assessed. The requirement for these areas was that there should be accurate in-situ bathymetric information available to calibrate and validate the results from satellite derived bathymetry.
In this section, an overview is presented of all areas that were assessed in this research. To present the characteristics of the different areas, they were scored based on six categories: Bottom reflectance, turbidity, cloudiness, hydro- and morpho-dynamics, and tidal range. Some of these scores were subjectively assigned to the area by comparison of satellite images, however they provide a measure of how the locations differ from each other. In later chapters, reference will be made to these areas when they are used for various analysis.

3.2.1 Scoring criteria

The level of **turbidity** was scored by a combination of visually checking a number of satellite images and comparing the Total Suspended Matter (TSM) score (equation 2.3). In a similar way, the **cloudiness** was scored. Both by comparing the scores and visual check. A high score of cloudiness corresponds with a high presence of clouds. When clouds are within the region of interest, it is not possible to obtain a bathymetry. In some areas around the world it is hard to derive bathymetry only because of the large presence of clouds. For instance, during the rainy season, parts of the world have a small number of cloudless pictures.

Tidal- and hydrodynamic properties were gathered from a variety of websites that provide tide- and wave information https://www.tide-forecast.com/ and https://magicseaweed.com . Based on this information, tide and hydrodynamics were scored high for high tidal range and big waves and currents. The tidal range is important, because SDB measures water depth. Therefore, a correction of the tide has to be done to calibrate and validate the satellite bathymetry with the in-situ measurement.
A high score for **bottom reflection** was assigned to high reflective bottoms, like very white sand. Because SDB methods work on the principle of light reflection, the albedo of the bottom material is of significant influence on the final results. Areas where the seabed consists out of multiple materials, and thus multiple albedo values, were scoring low.
Lastly, a score for the level of **dynamically in the morphology** was assigned based on time series analysis of the satellite images and, if available, by assessing in-situ data over multiple surveys.

3.2.2 Study Areas

The locations that were selected are displayed in Figure 3.1 and their characteristics in Table 3.1. Below that, a more elaborate description is given per location with more information of local condition and the ground-truth data that is available.

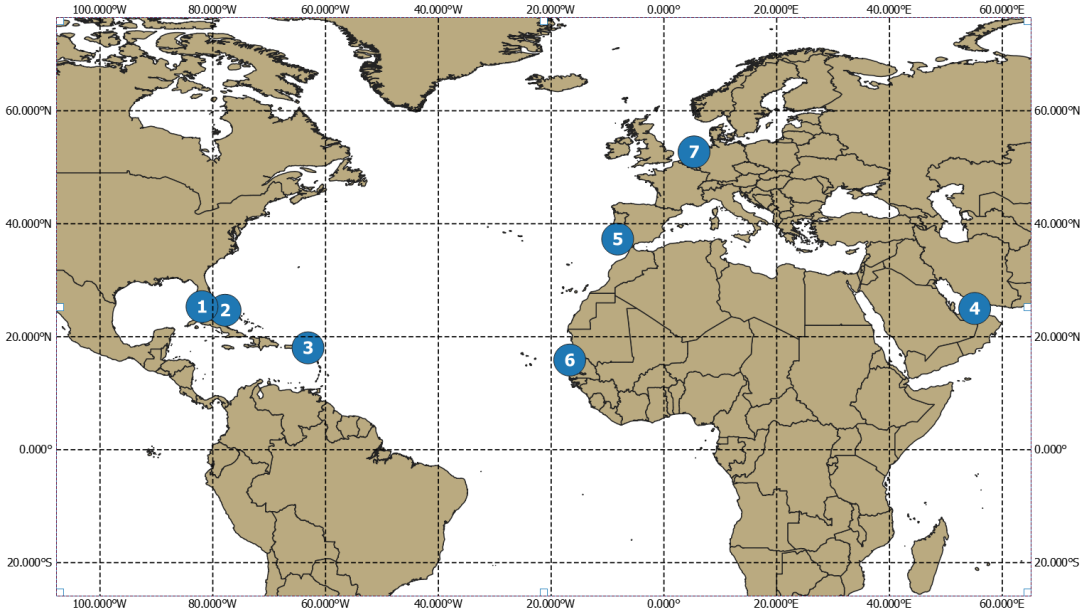

Figure 3.1: Locations of the cases around the world [latitude, longitude]. Numbers correspond with cases in Table 3.1

Table 3.1: Locations of case studies with their properties. Green colored properties are favorable for the use of SDB, red unfavorable. The brightness of color shows the importance of the property.

Location	Case	Water clarity	Bottom	Waves	Data
1. Bahamas	Clear water, reflective bottom	Good	Sand	Minimum	Chart
2. Key West	Clear water, less reflective bottom	Good	Sand/Reef	Minimum	LiDAR 2016
3. Sint Maarten	Clear water, varying albedo	Good	Sand, Reef, Vegetation	Moderate	SBES 2011
4. UAE	Deep water, bottom not visible	Moderate	Sand	Moderate	MBES 2018
5. Rio Formosa	Deep, turbid water	Moderate	Sand	High	LiDAR 2013
6. St Louis	Deep, turbid, morphodynamic	Bad	Sand	High	SBES 2018
7. Markermeer	Lake, turbid	Bad	Clay,Sand	Minimum	SBES 2016

Bahamas

The Bahamas is a group of more than 700 islands located in the Atlantic Ocean. The waters around these islands have great ability to be used for SDB, because of their crystal clear water and a high reflective sea bottom material. The shallow parts around the Bahamas provide such conditions and are not too deep ($<$ 20m). Under these circumstances, the SDB was obtained without the need of taking account for albedo differences and turbidity. An accurate bathymetric data set was not available in this area, so validation was done using chart data (Navionics, 2019). During the time of this research, a hurricane hit the Bahamas, which might have resulted in some bottom changes. That is why this case study is also used to investigate the possibly to use satellite images to capture morphological changes after a storm without the addition of in-situ values.

Key West, USA

Key West is located at the most southern point of Florida, USA. This location is characterized by small islands surrounded by shallow waters. Because of its clear water, this location is really suitable for the application of satellite derived bathymetry. In 2016 the National Geodetic Survey (NGS) conducted a comprehensive topographic and bathymetric LiDAR survey of large parts US coast including Key West. This dataset is publicly available via the National Oceanic and Atmospheric Administration (NOAA) data portal. Caballero and Stumpf (2019) used this data already in their research on using Sentinel-2 imagery for SDB. The dataset was used in the current research to compare the results with the results of the recent state-of-the-art publication of Caballero and Stumpf (2019). Moreover, a large area is covered by the data, which made it possible to validate the SDB model on a large area of the satellite image. The presence of (small) clouds and their shadow on the earth's surface makes it difficult to

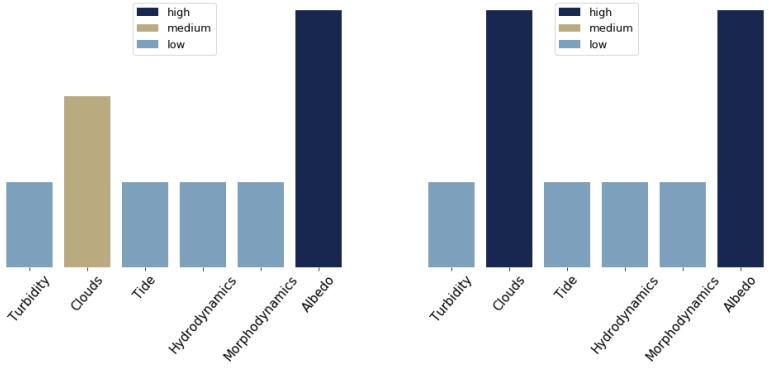

(a) Bahamas **(b)** Key West, USA

Figure 3.2: Scores of six categories per area in the Bahamas and Key West

Sint Maarten

The island of Sint Maarten, which is divided into a French and a Dutch part, is part of the Antilles Islands and located in the Carribean Sea. Wave- and current condition are mild, so the water is very clear. In the Dutch part of the Island (South), a single-beam echo sounding survey was conducted in order to map the entire south coast of the island. From 0 to about 20 meters below mean sea level, data was acquired on cross-shore transects. Because of the heterogeneity in the sea floor composition, this case study was also included for the assessment of the variation in albedo.

Rio Formosa, Portugal

One of the most cited researches on satellite derived bathymetry is the one from Pacheco et al. (2015). In their research, the bathymetry of several areas around the Portuguese coast at Faro was determined using Landsat 8 satellite images. The results of this research were compared with the findings of this paper. In this research only Sentinel 2 images were used, so a comparison can be made between the two satellite products. Because of the occurrence of high wind- and wave forces and presence of tidal inlets and river mouths, this area is characterized by large amounts of suspended sediments, which make bathymetry derivation from satellite images challenging. Therefore, this data set was used in multiple analyses (turbid-water case and temporal- and spatial extrapolation).

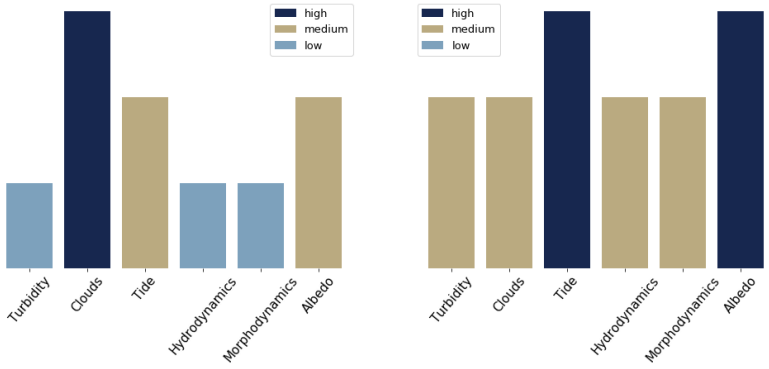

(a) Sint Maarten **(b)** Rio Formosa, Portugal

Figure 3.3: Scores of six categories per area in Sint Maarten and Rio Formosa

United Arab Emirates

The water in the Persian Gulf has optical properties that make this area suitable for SDB. Because of the mild hydraulic conditions, not much sediment gets in suspension by wave and current action,

so light penetrates relatively deep in the water column. This case study was used to assess the deep water performance of the SDB technique. Also some deep dredged channels were present, that were used to check if satellite images are able to detect these features.

St Louis, Senegal

On the west coast of Africa, beach erosion is a big concern for villages and cities located near the shore. One of these cities is St. Louis in Senegal. The problems of this city and neighboring villages was aggravated due to a man-made breach to bring the river mouth closer to the city. Since then, a long spit is developing southwards resulting in large areas of sedimentation and erosion. The pace of the morphological development in this area is high, concluding from satellite image time series and two bathymetric surveys 6 months apart.
Because of the availability of these data sets and the rapid morphological development, St Louis was used as case study in the temporal analysis of this research (chapter 3)

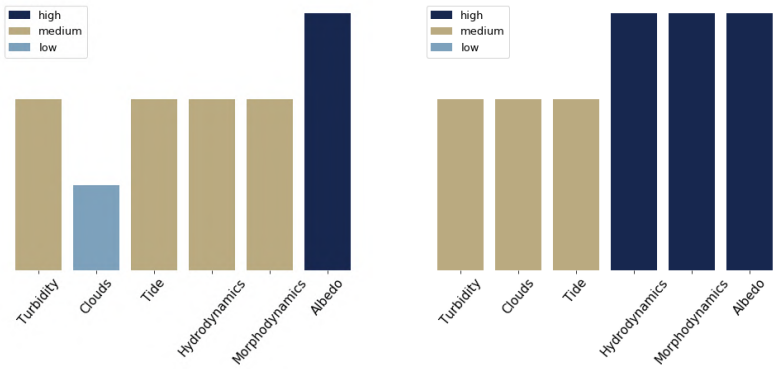

(a) United Arab Emirates **(b)** St, Louis, The Netherlands

Figure 3.4: Scores of six categories per area in UAE and Senegal

Markermeer, The Netherlands

The Dutch IJsselmeer and Markermeer are separated by the Houtribdijk. This dike protects low laying (reclaimed) land around these lakes from high water levels and wave action. Recently, a project has been carried out to strengthen this dike by constructing a gently sloping, sandy foreshore. In 2014 a small pilot site was constructed to assess the morphological behavior of a sandy foreshore and beach in front of a dike. For three years a stretch of about 500 meters of dike was monitored intensively by monthly bathymetric and topographic surveys. Insights of the pilot project were used in the design of the final dike reinforcement, which is completed at the end of 2019. One of the findings in the pilot was the formation of a wide plateau between two more steeply sloping bottoms than initially constructed.

This case study was chosen because here, in contrast to the other areas, a lake environment was considered. This implies other hydro-dynamic conditions, possibly difference in water constituents and thus water color and difference in bottom material. For the SDB application on temporal changes, the multi-year bathymetric monitoring data was used.

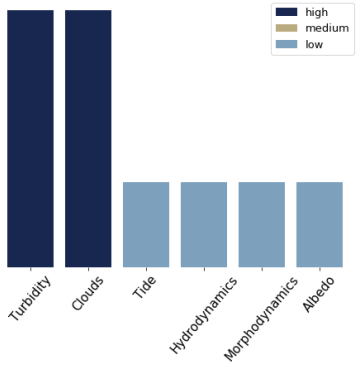

(a) Markermeer, The Netherlands

Figure 3.5: Scores of six categories per area in the Markermeer

3.3 Image Acquisition

Google Earth Engine is used for downloading and processing of the Sentinel-2 satellite images. With GEE, Google has provided a platform to easily access a large variety of satellite products and perform computations in the cloud. Earth Engine provides two Sentinel-2 data products: Level-1C (Top of Atmosphere) and Level-2A (Surface Reflectance). The level indicates what processing the images has been undertaken already. To get from Level-1C to Level-2A (TOA to SR), an atmospheric correction algorithm was applied (Sen2Cor). This algortihm is comparable with the 6S atmospheric correction applied in this research, however only images after December 2018 are provided in Level-2A state. Therefore, in this research the Level-1C images are used and are manually corrected for atmospheric and water column effects. The difference between the products and a description of GEE is explained in detail in the literature review (chapter 2.2).

By using the Python API, all GEE functionalities are available to use in a Python environment. Most of the computing can take place at the Google server, but for some computations it is necessary to download the information and treat the images as matrices in Python. Therefore, for this research a custom Python toolbox is build by which the SDB computations can be performed in a structured manner.

3.4 Filter Collection

The Sentinel-2 image collection consists out of hundreds of thousands of images, so it was challenging to find images that were suitable of SDB. Filtering is an important step in the workflow to reduce the collection to only good quality satellite images. The Sentinel-2 satellites pass each location on earth about every 5 days, which results in around 70 images per year. However, only a small amount of those images are suitable for SDB, because of the presence of clouds, cloud shadows or other artifacts in the image. Therefore applying filters to the collection to reduce the number of unusable images is an essential first step.

GEE allows users to filter a satellite image collection based on the parameters in the metadata that are attached to every image. First of all, an area of interest (AOI) and a date range were defined. The date range is important, because the image capturing time should be sufficiently close to the time of in-situ acquisition, especially at a morphological dynamic location. However, selecting a large date range, results in large image collections, which take long time to process until they are ready to use for SDB. The area of interest was defined by creating a polygon as a shape-file with the use of GIS software. This file is then used to define the AOI where the image is filtered with. An additional filter is added to remove images from the collected where the AOI is only partly covered by the image. Next, only images were selected where the overall image was already not cloudy

using the provided cloud percentage in the meta data. This percentage was varied for different sites, because sometimes, with a strict filter, few images remained.

3.5 Pre-Processing

After the first step, an image collection remains containing only images that have passed the defined filters. Before these images can be used to derive bathymetry, they first have to go through pre-processing steps. These steps consist out of clipping the image, separate water from land, create a mask for clouds and correct for effects of the atmosphere and water column.

3.5.1 Area of Interest

A single Sentinel-2 image covers an area of about 100 by 100 kilometers. The area that was assessed was often a fraction of the image and therefore the region of interest was defined. The geometry of this area was used to clip the satellite image. This is beneficial for the processing steps hereafter, since we are working with a smaller image. Beside optimization in processing, reducing the area also contributes to less variations in optical properties of the water. The process of scattering and absorption of light water column is more uniform on smaller areas and therefore the error caused by these variations reduces.

3.5.2 Land/Water mask

The next step was masking out all elements on the image that are not water. If the defined region of interest already contained only water, this step was not necessary. But in some cases, to precisely cut out the coastline, a mask to leave only the pixels of water in the image and remove the land-pixels was created. This was done using an algorithm based on normalized difference water index (NDWI), a Canny Edge Detection(CED) algorithm and Otsu thresholding presented in Donchyts et al. (2016). The NDWI was calculated for the entire (clipped) image using the following equation with the green and short wave infrared wavebands:

$$\text{NDWI} = \frac{X_{GREEN} - X_{SWIR1}}{X_{GREEN} + X_{SWIR1}} \tag{3.1}$$

In most applications, to create a binary image, one would apply the thresholding directly after this step, but to improve the accuracy, first a CED algorithm was used to find the steep gradients in NDWI values. These gradients are located on the border of water (high NDWI) and land (low NDWI), so represent the waterline in the image. A buffer of 5 pixels on both sides of this line is made and the histogram of the pixels within this buffer were used in Otsu's method to find the threshold NDWI value to create the binary, land-water image. Otsu's method iterates through all threshold values in the histogram of the image and finds the optimal value to classify the image into two classes (Otsu, 1979). This is done based on minimizing the variance within a class. For every threshold value in the iteration, the variance of the class to the left and to the right is calculated and added together (within class: mean/standard deviation).

3.5.3 Cloud mask

The presence of clouds affects the usability of satellite images for the calculation of bathymetry, because they (partly or completely) block the reflection of radiance from the earth's surface below, so the sensor won't capture it. Moreover, small clouds in the image cause shadows on the clear parts of the image. Depending on the solar angle, these shadows could be located some horizontal distance away from the cloud. Because of the difference in reflected radiation between shadowed and non-shadowed areas, in shadowed areas bathymetry can not be derived based on reflected radiance. Preferably, the image that is used should be clear from any clouds, which was tried to accomplish in the filtering stage. However, in certain areas where the amount of useful, cloud-free images was

already small, a good image with the presence of a few small clouds was still valuable by applying a cloud mask.
Sentinel-2 1C images are provided with a QA band containing information on cloud cover. By extracting the cloud bits from that band, a mask image (containing ones for the values to keep and zeros for the value to mask out) was created. In the areas under the clouds, gaps in bathymetry will occur, that, in the case of small clouds, were filled by interpolation.

3.5.4 Atmospheric Correction

Despite being an atmospheric effect, clouds were treated separately as explained in the previous step. This is because they often are a complete obstruction of light to reach the earth's surface and therefore need to be masked out of the image. For all other atmospheric effects that were treated in chapter 2, an atmospheric correction algorithm was used.
After the previously explained steps, the image only contained pixels where water is present, but the reflectance values still give a representation of the reflection at the top of the atmosphere, where all the effects of the light traveling trough the atmosphere are still present. In the literate review, an explanation is given about atmospheric effects and how to correct for them. Here, the practical implementation of the correction method is presented.

The goal of the atmospheric correction was to obtain the reflectance values from the surface instead of what the sensor measures at the top of the atmosphere. To do that, the S6 correction algorithm was used. This radiative transfer model simulates the effect of light passing though the atmosphere, so the reflectance values at the surface were obtained. Based on the location on earth and the time it was captured, several empirical correction factors for water vapor, ozone and aerosols were acquired from look up tables. These values were then used to convert the TOA values to SR values. A Python implementation of this model (PyS6) was used to obtain the surface reflectance of the clipped satellite image.

3.5.5 Water Column Correction

The water column correction was the final correction that was applied. Correcting for constituents in the water column is also the most challenging to do, because of the large spatial differences of IOPs of the water and the sea floor albedo due to differences in bottom type. For instance an area of shallow water with dark sea grass has similar reflectance as a part with deep water and sand. There are some models that simulate and numerically derive the inherent water properties (IOP) at the considered location, but these models require calibration and validation using local data at the time of image capture.

Because of the necessity to process many images and the lack of in situ data of optical water properties, the simplest method to correct for effects in the water column was used: Dark Object Subtraction (DOS). This method assumes that pixels of deep water ($>$30 m) do not contain any reflectance from the sea floor anymore, because all light energy was absorbed before it reached the bottom. Therefore, all reflectances that were measured by the sensor of these pixels are disturbances caused by scattering in the water column. It was assumed that these properties are uniform over the area of interest. The median value of those deep water pixels was subtracted from the other water pixels to leave only bottom reflection values on the shallow water pixels. The estimations made in this method were rough, but the areas that were considered in this research are relatively small, so it is the closest approximation when no actual data of water properties is available.

A polygon of a small area over water where the depth is sufficiently large was defined and saved as a shape file. At locations with clear water (Bahamas, Sint Maarten) deep water can easily been located from the satellite image. At other locations where the water is less clear, a chart (Navionics

Navionics (2019)) or the in-situ data was used to find areas of deep water. The shape was used in GEE to obtain the median values of all pixels within the polygon.

3.5.6 Noise Reduction

Some images appeared to contain a noisy signal, especially in the blue and red frequency bands. A smoothing filter can be applied on the image to ruduce the noise and obtain a cleaner signal. However, this results in a decrease of spatial resolution. Therefore, in this research, the pixels that are not between the 5th and 95th percentile were removed from the image.

3.6 SDB Methods

As presented in the literature review (section 2.5.2), two main variations of empirical SDB methods can be distinguished: linear transform and ratio transform. Both rely on the same principle of light attenuation, but use the wavelength bands in a different way of obtaining bathymetric information out of them. Ample scientific research was done applying both methods, some of them including a comparison. However, not a clear favorable method could be determined from the literature research, so therefore a comparison between both linear- and ratio transform was done in this research to assess their performance. After this assessment, the best performing one was used in the remainder of this research.

Table 3.2: Empirical SDB methods.

Paper	Method	Regression
Lyzenga (1985)	Linear Transform	Linear regression
Stumpf et al. (2003)	Ratio Transform	Linear regression

Because in both methods, several combinations between wavelength bands can be made. An assessment on the differences in performance of both methods using multiple combinations of wavebands is presented in section 3.8.3. The variants that were used in this research are listed in table 3.2 and chosen based on experiences in excising literature.

3.7 Calibration and Validation

Empirical SDB methods need calibration with ground-truth data to be vertically tuned to the correct bottom level. In this research the importance of this calibration step will be assessed by comparing results with and without addition of in-situ data. For the locations that were used as case study, data from various sources is available, consisting of chart-, SBES-, MBES- and (bathymetric) LiDAR data. For the calibrated assessment, the data set to use to train the model has to be prepared properly. This starts with the data selection. That can be done either randomly from the data set or by selecting the points manually. During the research a manual selection of transects appeared to give the best resulting satellite derived bathymetry and is also a good representation of the real world acquisition of (training) data. A cross-shore transect covers a larger variety of depths than selecting random points within the AOI.

Just like creating the training data set, validation data was selected from the total data set. Again, this could either be done by selecting transects or by random sampling. By random sampling, the chances of having multiple validation points in the same pixel are smaller, so there is less chance on validating the same sample multiple times with different values. Therefore, for validation, random points from the in-situ data set were used. In Figure 3.6, the separation between calibration and validation data is visualized.

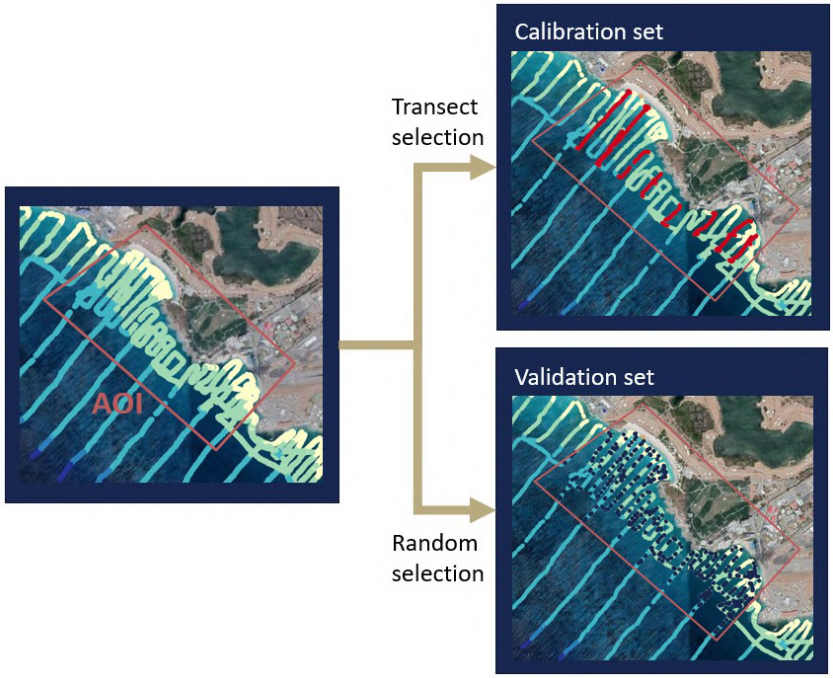

Figure 3.6: Workflow calibration and validation split

The validation data is grouped in bins of 1 meter water depth. For each of these groups, the root-mean-square error (RMSE) was calculated. This metric of accuracy was chosen over the mean absolute error (MAE), because it gives higher weight to large errors due to squaring. In SDB, an accuracte bottom level at every pixel is desirable and therefore large errors should be penalized more in the accuracy assessment. The Category Zones of Confidence (CATZOC) was used to assess the accuracy of the SDB results. A CATZOC value is used in nautical charts to provide information on the level of confidence of the presented water depths, so vessels can take that uncertainty into account when determining their under keel clearance. CATZOC is divided in five categories with a specific positional- and depth accuracy. In Table 3.3 the different CATZOC classes are listed with their corresponding requirements.

Table 3.3: CATZOC classes

CATZOC	Position Accuracy [m]	Depth Accuracy [m]
A1	5	0.5 + 0.01d
A2	20	1 + 0.02d
B	50	1 + 0.02d
C	500	2 + 0.05d

3.8 Research Strategy

In chapter 1.2.1, the main research question and the associated sub-questions were formulated. The strategy to give answer to these questions is presented in this section. The steps elaborated in the previous sections were done for every. If in these strategies "pre-processing" is mentioned, it means that the steps of chapter 3.5 were done.

3.8.1 Before calibration: Light Attenuation

For the optimization of the use of existing SDB methods, first their initial performance was assessed. These empirical methods rely on the concept of attenuation of light energy in water. In

theory, with knowledge about surface- and sea bottom reflectance, using only this concept should give an estimation of the water depth. Empirical SDB are generally calibrated with the use of some ground-truth data to obtain an accurate absolute bottom derivation. In this analysis, the calibration is not done to obtain insight in the raw signal and investigate the possibilities of using satellite images without the availability of data of the area of interest. The assessment was performed on an area in the Bahamas where the water clarity is high. To include the influence of variation in sea bottom composition, also Sint Maarten was used as a case study (see section 3.2.2 and 3.2.2 for a detailed elaboration of this area's characteristics). For a period of a year, all suitable satellite images at this location were acquired and processed according to the steps presented in the previous sections.

In the light attenuation theory, water depth is estimated using light of a single frequency. The Sentinel-2 image doesn't provide single frequencies in the bands, but channels with a certain bandwidth of frequencies. Therefore, a choice had to be made between multiple bands. As shown in the literature review (section 2.5), light with a shorter wavelength (blue, green) penetrates deeper in the water than the light with longer wavelengths. Therefore, only the blue and green channels of the satellite images were used during this assessment. A comparison between the two was made to assess the potential of both wavelengths for the use in SDB.

Because a detailed data set of an area with clear water and high reflective sea floor, like in this case the Bahamas, was not available, water depth information of the online chart Navionics was used to perform a rough validation of the results in this step. In Sint Maarten, were an accurate data set is available, the water is also very clear, the bottom is less homogeneous. Therefore, patches of sandy bottom were manually selected to use in this analysis. Furthermore, this data was used to investigate the influence of bottom material on measured reflectance.
Finally, the capability of Sentinel-2 images for the detection of typical bottom features was analyzed. Therefore, multiple areas were used where:

1. a typical beach slope was present, or
2. deep (dredged) channels occurred, or
3. nearshore sandbars were located

3.8.2 Before calibration: Temporal Analysis

The morpho-dynamic behavior of the sea bottom is an important aspect in the assessment of the development of the coast. To obtain insight in the way bottom material is transported, the use of satellite images is very valuable. Regular methods to get information of the sea floor require to perform a survey with a vessel or aircraft. Therefore, for large areas, a data set with high temporal resolution is often not feasible (economically and practically). Satellites return to the same location on earth every few days regularly, so if images can be used in the assessment of the sea floor, it is possible to make a time series of the development of the local morphology with high temporal resolution.

To analyze if changes in bottom profile correlate with changes in bottom reflectance, an area in the Bahamas was considered again. It was assumed that morphological changes in the Bahamas were negligible over the course of a year, but during this research, in September 2019, hurricane Dorian hit the Bahamas, which might have caused morphological changes. Therefore, a one-year period before the hurricane was assessed to eliminate influence of morphological development in the resulting SDBs. After that, an assessment on the effects of Dorian in the sea bottom was done. Therefore, images after September 2019 were obtained and processed. The differences in reflectance values pre- and post-hurricane images were then analyzed for the detection of morphological changes.

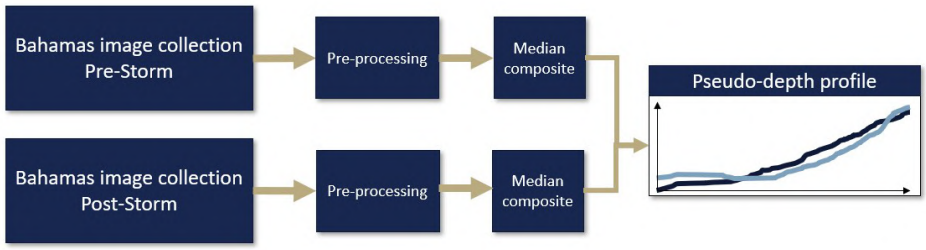

Figure 3.7: Scheme of temporal bottom assessment Bamahas. Pre-Storm and Post-Storm. Displayed bottom profile is illustrative

The absence of actual bathymetric data made it difficult to be certain if differences in reflectances after the storm were caused by morphological changes. Therefore, the same procedure was done in an area where two data sets were available separated approximately 6 months apart. This area located near St. Louis, Senegal (section 3.8.4) is a very morphological active area where a large spit is developing rapidly (4km in 4 years), causing the river mouth to move southward (Figure 3.8). Because of the changes in sea bottom, at many times the suspended sediment concentration is high, which made the capture of bottom reflectance difficult. To compensate for that, all images within a month of the survey data are captured, processed and combined into a median composite to filter out sediment plumes. Figure 3.9 shows the workflow that was followed for this analysis.

Figure 3.8: Four years of morphological development (2016-2020) captured with Sentinel-2 satellite images of St. Louis, Senegal. Left: 2016, middle: 2020 and right: the difference of green signal between two images. Red areas show locations of sedimentation, blue areas is where erosion occurred

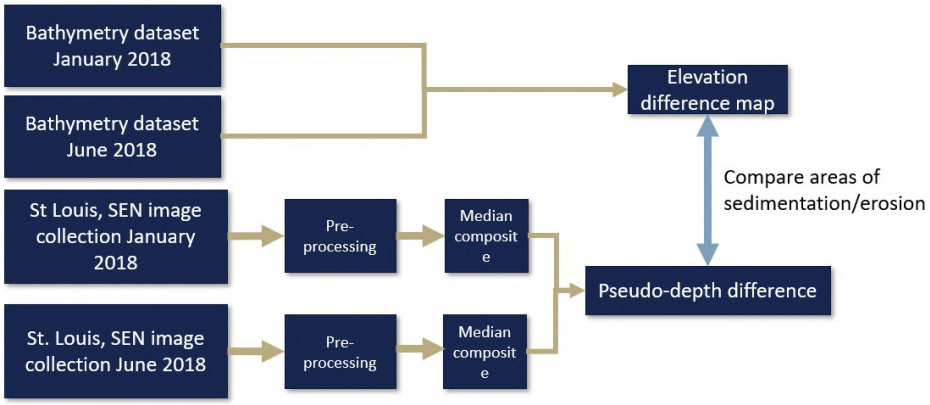

Figure 3.9: Scheme of temporal bottom assessment St Louis, Senegal. Januari vs June 2018

3.8.3 After calibration: Method Comparison

In the previously presented sections, the potential of using satellite images for bathymetric analysis without the addition of in-situ data was investigated. However ,empirical SDB methods rely on ground-truth data that is used to calibrate the model. Only then, an good absolute bathymetry was obtained.
First, a comparative research was done between different empirical methods. The linear transform and ratio transform methods were used. In chapter 2 the background of this methods is explained in detail. In both, multiple combinations of wavelengths can be used to obtain bathymetry. In table 3.4 the different combinations that were used are listed.

Table 3.4: Bands combinations of Empirical SDB Methods

Method	Name	Combination
linear	L-B	log(blue)
linear	L-G	log(green)
linear	L-BG	log(blue) + log(green)
linear	L-BGR	log(blue) + log(green) + log(red)
ratio	R-BG	log(blue)/log(green)
ratio	R-GR	log(green)/log(red)
ratio	R-BR	log(blue)/log(red)
ratio	R-BGGR	log(blue)/log(green) + log(green)/log(red)

All of these methods are used on images of the same area. The sandy area in Sint Maarten was used for the initial assessment in clear water with a well reflecting sea bottom, because an accurate data set of the bathymetry was available. Figure 3.10 shows the steps that were followed for every method.

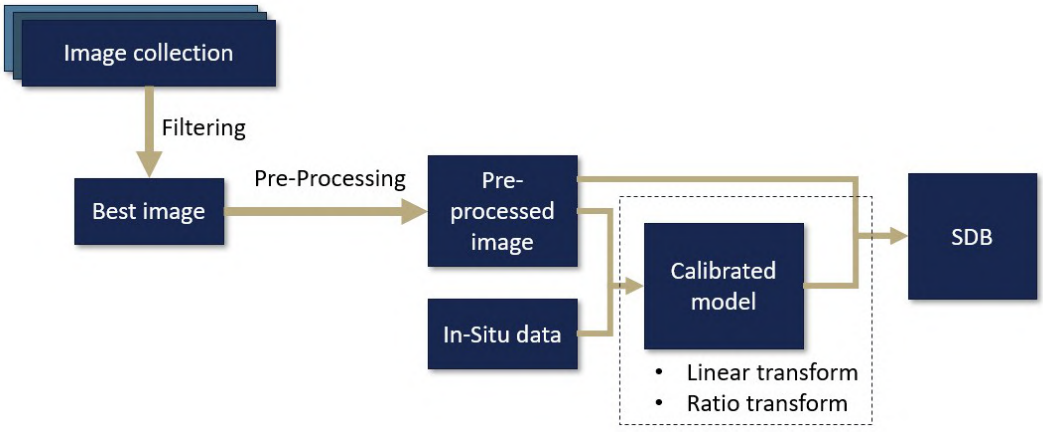

Figure 3.10: Scheme for workflow of assessment empirical SDB methods

3.8.4 After calibration: Assessment in Multiple Conditions

A direct comparison of empirical SDB on multiple cases with significantly different circumstances has not been part of any research yet. Therefore, a number of sites were selected (presented in section 3.2) and used to assess the performance of SDB under their particular conditions. Figure 3.11 shows the workflow and the locations that were used. For all of them, accurate bathymetry data was available to perform the calibration and validation of the model. An image collection per site was created with images that are captured as close as possible to the survey date. After filtering,

the best image for every site was pre-processed to be ready to be used in calibration of the SDB model.

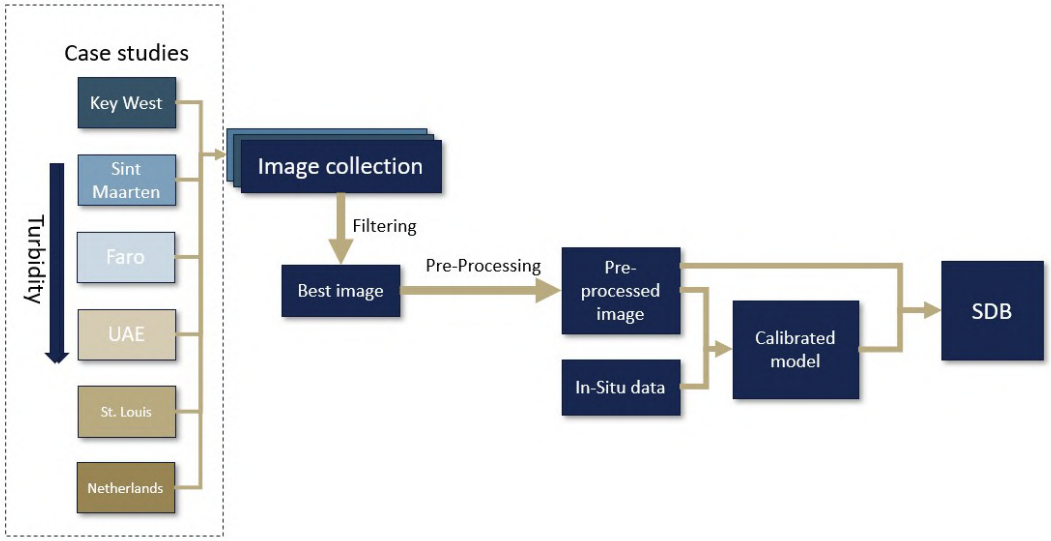

Figure 3.11: Workflow for multiple case studies

In each area, the available data is split into a calibration and validation data set. The processing of these data was explained in section 3.7. For each location, the same ratio of calibration and validation data was used to make sure an equitable comparison was made.

The calibrated SDB model was then applied to the image to obtain absolute bottom levels in the datum of the in-situ data. Next, this SDB was assessed on overall root mean squared error (RMSE), RMSE per depth class (in 1 meter bins) and spatial error.

3.8.5 Calibration Data: spatial and temporal extrapolation

A great potential of SDB is that the bathymetry of large areas can possibly be obtained from a single satellite overpass. Calibration data however, is most likely situated at a relatively small area in the image. Therefore, good understanding of the obtained SDB in areas some distance from the calibration area is needed before one can be certain about the quality of the derived bathymetry.
Typically, the performance of a trained algorithm depends on the amount of data the model is trained with. Conceptually, this is shown in figure 3.12. When a certain amount of training points is reached, the model results won't get any better by increasing the amount of training data.

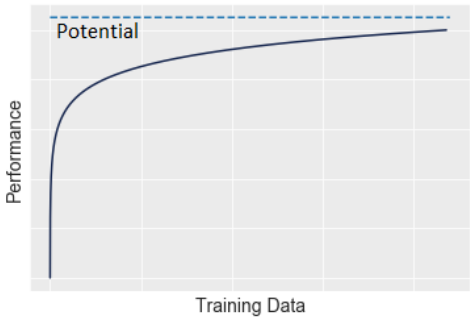

Figure 3.12: Concept of learning curve for regression

To assess the influence of the number of training points, for the case of Sint Maarten, the amount of calibration points was reduced. The initial calibration set was created in such a way that it covers all water depths. Reducing the set causes for gaps in calibration data at certain depths. In areas where the bottom slope is relatively gentle, there is a higher probability of still having calibration

data at the most common depth. However, if the bottom is sloping, missing data at some depths can cause miscalculation of bathymetry, because they are not included in the regression.
After every reduction, the SDB was made and the errors per depth class were obtained. The data set was further reduced until the vertical errors became significantly large. The same procedure was done for Faro, Portugal. In that area, the bottom has a relatively gentle slope until 20 meters water depth.

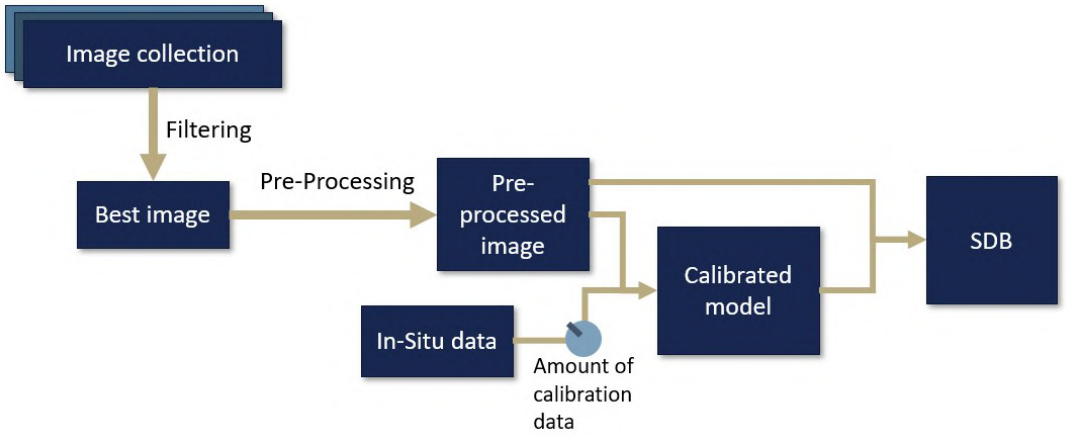

Figure 3.13: Workflow for the assessment of calibration data

For the further analysis on spatial extrapolation, validation of the calibrated image was done using data at locations with increasing distance from the calibration site. Therefore, the data set of Faro was used again, because it covers a large area and has sheltered and non-sheltered patches from waves. A calibration site was selected where no turbidity due to a river outlet was present. On three different areas within the same image, but at increasing distance from the calibration data, the model was validated. The validation areas were selected such that turbidity effects won't disturb the assessment on the spatial effect.

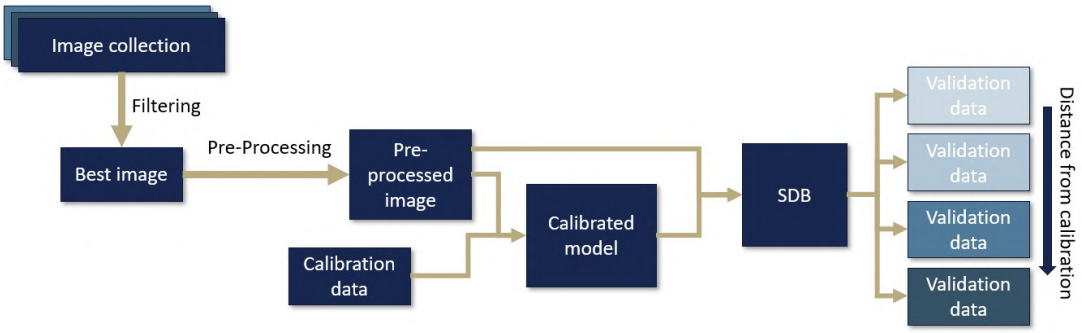

Figure 3.14: Workflow for the assessment of spatial extrapolation

4 Results

In this section, the results of the steps defined in the research strategy (chapter 3.8) are presented. First, the theoretical light attenuation principle was assessed to investigate the initial performance of SDB and to check how the method holds when it is used in temporal analysis. Once this baseline was assessed, the model was vertically tuned with the use of in-situ bottom elevation data to improve its absolute accuracy. For the analysis of this step, bathymetric derivation was done for multiple case studies under varying hydraulic- and environmental conditions. Finally, also the ability to use SDB on large spatial scale was investigated while only trained for a smaller portion of the area.

4.1 Before Calibration: Light Attenuation Assessment

As explained in the literature review, the basis of empirical methods to derive bathymetry from multi-spectral images is the principle of light attenuation. In this section the results of the assessment of this theory are presented. First, the difference between the use of the blue and green wavelength band was investigated. After that, the reflectance of satellite images in an area with clear water and a highly reflective sea bottom was used to obtain the bathymetry. No calibration with ground-truth data was applied yet. In chapter 3.8 the research method was explained in more detail.

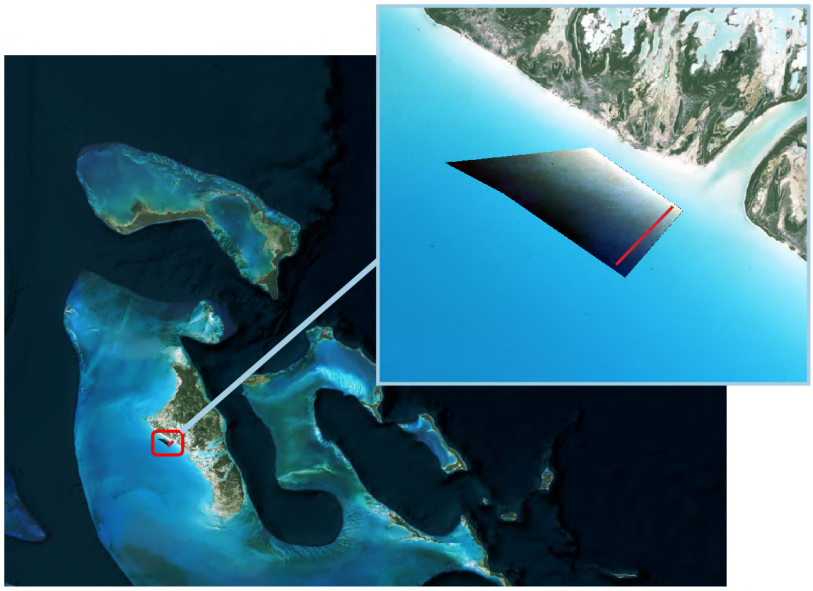

Figure 4.1: SDB location at the Bahamas, Background: Bing Satellite

A location on the west side of the island Andros was selected where the water is sufficiently shallow to be suitable for SDB (Figure 4.1). In this area, the water is very clear and the bottom consists of white sand, which is highly reflective. These should be good circumstances to perform the simplest derivation of bathymetry using only one wavelength band. A number of Sentinel 2 satellite images over the year of 2018 were collected and based on automatic filtering and visual inspection, images with clouds or other artifacts were removed from the collection. Next, one of the optically best looking images was used to derive the bathymetry. It was assumed that, because of the mild hydraulic conditions, morphological changes between the images were negligible or at least within the error margin of the empirical SDB technique.

After pre-processing the image (steps are elaborated in the methodology in chapter 3), the reflectance values represent the bottom reflectance. The water depth was derived by calculating the

natural logarithm for one wavelength band. The green or blue band are the bands to use, because of their deep penetration in the water, so a large portion of incident light is reflected from the sea floor. Light of lower frequency is attenuated in shallower water, resulting in a noisy signal. The resulting image represents an estimation of the water depth at the time the image was captured. This "pseudo-depth" does not necessarily coincide with the actual bottom level, because only the logarithm of a wavelength was used. No vertical tuning is applied in this step to assess the initial signal without addition of ground-truth data.

Based on visual inspection, one of the images (captured on 4 Dec 2018) was selected to determine the bathymetry by calculating the logarithm of the reflected radiance. As seen in Figure 4.2b both the blue and green band were used and a transect was sampled from the SDB to see the differences in their bathymetry. In both results, one can identify the bottom shape. They are shifted vertically by 20-30 cm because they are attenuated differently. The chart in figure 4.2a shows the local bottom elevation w.r.t. mean sea level. The log(Green) calculated bathymetry was closer to the chart data, but still had an vertical error of about 50 cm. In both transect, the sloping bottom is visible, so that indicates that the actual bottom reflectances are obtained in this image.

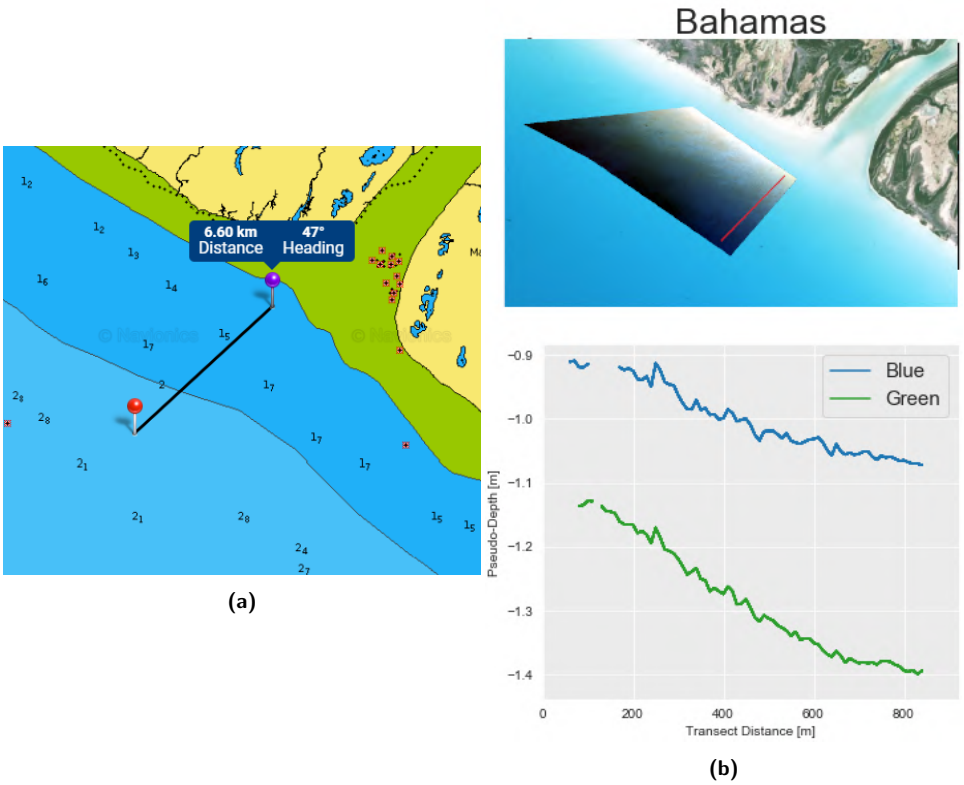

Figure 4.2: log(BLUE) and log(GREEN) on a transect at the Bahamas

An area where more accurate in-situ bathymetric data was available, is the south-coast of Sint Maarten. The sea floor around the island consists of large patches of sand, but vegetation and rock/reef can also be found. Because of the mild wave and current conditions, sediment hardly gets into suspension resulting in very clear water. A large bathymetric data set was acquired using single beam echo sounding measurements on transects with a regular spacing.

First, the SDB performance without any training was assessed. Therefore, only a sandy, high reflective part was selected to determine the SDB without calibration and validation using the available data set. After that, the bottom variation was taken into account. The area that was selected (Phillips Bay) has a large, nearshore patch of sandy bottom with vegetation and rocks starting at a

depth of around 8 meters. In figure 4.3, the location of the region of interest of the island is shown together with the satellite image that was used to derive the bathymetry. The sandy and non-sandy bottom is clearly distinguishable.

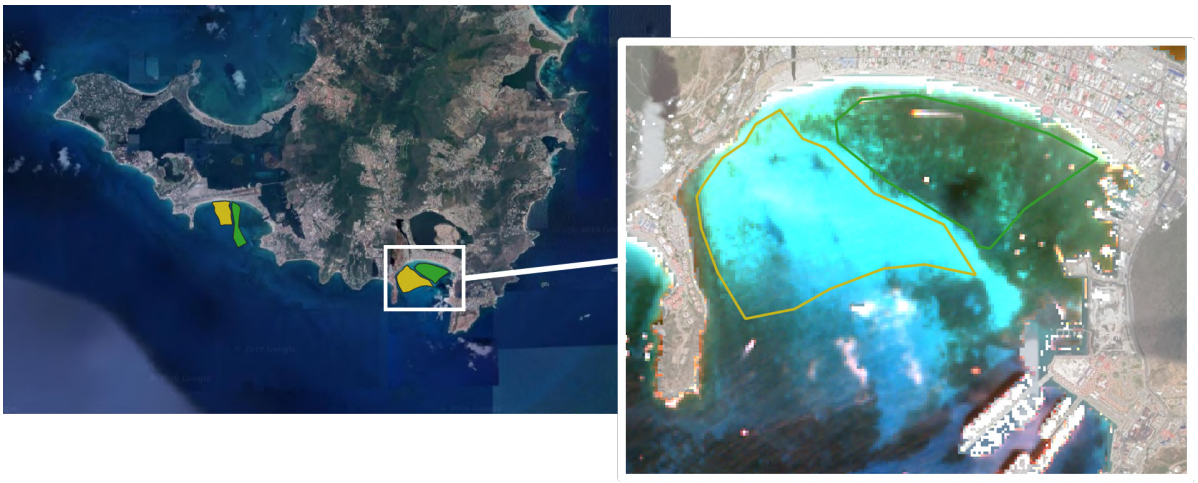

Figure 4.3: SDB location at the Sint Maarten, Background: Google Satellite

Just like in the Bahamas case, the natural logarithm of the green and blue wavelengths was used to determine the water depth without any additional calibration with ground-truth data. Figure 4.4 shows two bottom transects in this bay. The first one displays the SDB on a sandy part of the image. In this case, also the actual bottom profile is shown. Both green and blue bathymetries showed similar results, but in terms of absolute bottom derivation, they both have a large vertical error. However, a sloping bottom is distinguishable from both the green-band and blue-band SDB. The second bottom profile was chosen such that both vegetated, as well as sandy bottom were captured. At the transition between the two bottom materials, the actual, measured bottom had a depression of about a meter. After that, the sandy bottom was sloping gradually to a depth of about 6 meters below MSL. In both SDBs, the depth over vegetation was constantly estimated deeper than over the sandy part. On the interface between sand and vegetation, a clear jump in elevation was noticeable, which was higher than the actual change in elevation at that location. On the dark, low albedo bottom, there is hardly any difference between SDB obtained with the green and blue band. In the area with sand, on both transects, the blue depths were constantly estimated lower (less water depth) than the green one. This can be explained by the fact that vegetation causes more energy in the blue wave spectrum to be absorbed than in the green spectrum. On a sandy bottom, the fact that blue light is attenuated less than green light during its path through the water column, causes the blue SDB to be higher than the green SDB.

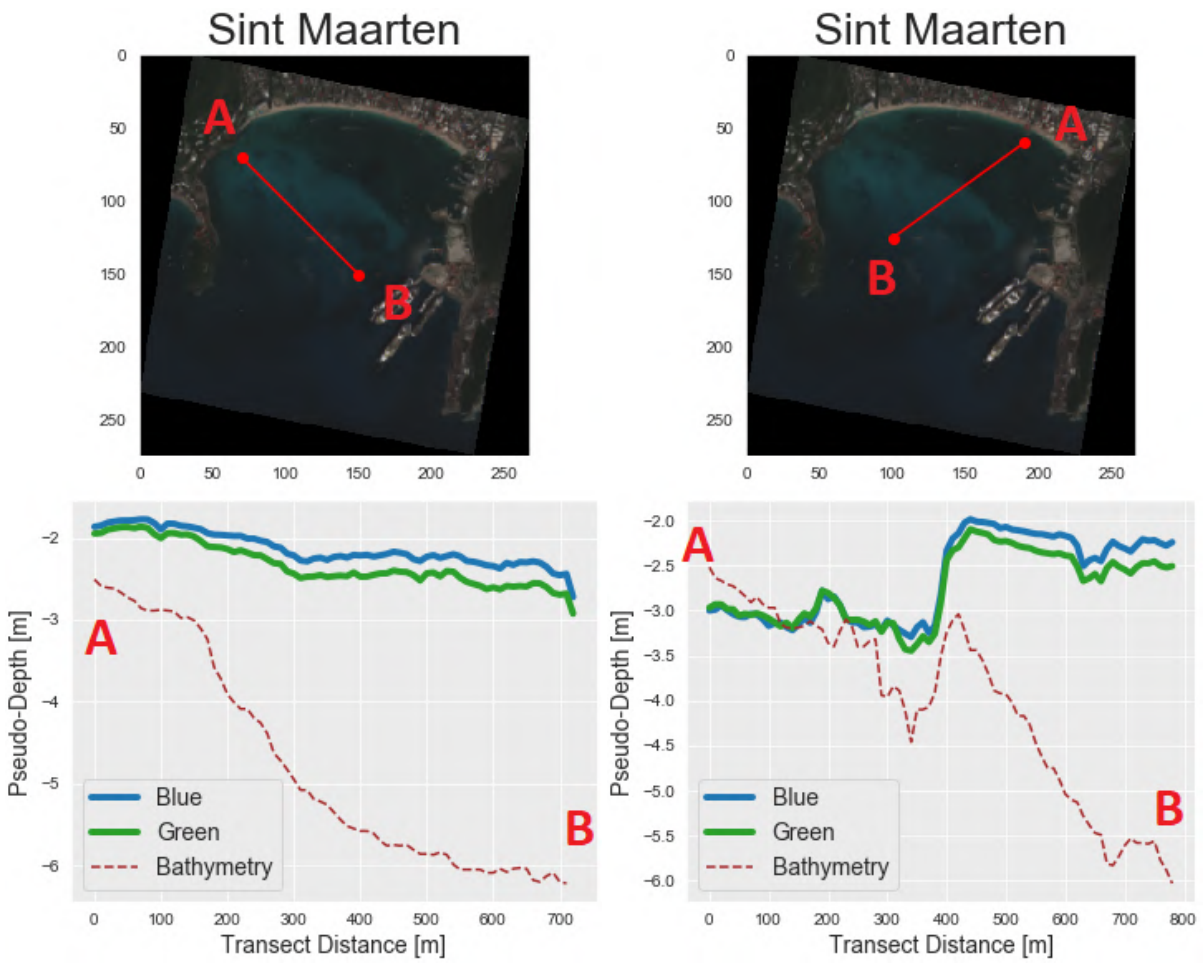

Figure 4.4: Bottom across Phillips Bay, Sint Maarten. Left: only sandy bottom, Right: Combination of sandy and vegetated bottom.

4.2 Temporal Analysis

Around the entire globe, Sentinel-2 satellites are acquiring images since 2015. In the investigation of morphological development of a certain area, data from the time series of these satellite images is extremely valuable. The applicability of SDB on different images in time was assessed in this section, and the results of the analysis described in chapter 3.8.2 are presented. At first, an assessment was made between multiple images at a location where the water was clear and bottom was homogeneous. which was found on the western part of the Bahamas. During the period of a year (January 2018 and December 2018), all usable images were acquired and pre-processed.
For eight images in this area, the SDB was determined by using the green band in the light attenuation principle ($Z = log(X_{GREEN})$). A bottom profile plot was created for all images and presented next to water level (LAT) values obtained from Navionics in figure 4.5. The Navionics values don't provide the most accurate validation data, but it provided sufficient information whether the order of magnitude is correct. In all plots, a sloping bottom was noticeable, but water depth values showed an absolute error of about 1 meter compared to the chart values. Also with respect to each other, the profiles had a maximum variation of about 20 centimeter. However, the vertical offset between the bottom profiles was not necessarily uniform over the entire transect. Therefore, vertical differences due to tidal elevation or wind setup, did not completely explain these differences. Actual data on water level elevation was not available to accurately assess the tidal influence. A tidal model was used to estimate the tidal level during the capture of each image (Table 4.1). It was found that the vertical differences between the SDBs did not correspond to the (small) tidal differences that were

obtained from the model,which can be caused by the inaccuracy of the model or because other, optical factors are affecting the bathymetry derivation more.

Table 4.1: Estimated tidal levels during the capture of images

Image	Estimated Tidal Elevation [m MSL]
2018-02-29	0.01
2018-03-19	0.12
2018-04-18	0.1
2018-06-22	-0.16
2018-07-17	0
2018-11-09	0.15
2018-11-29	-0.12

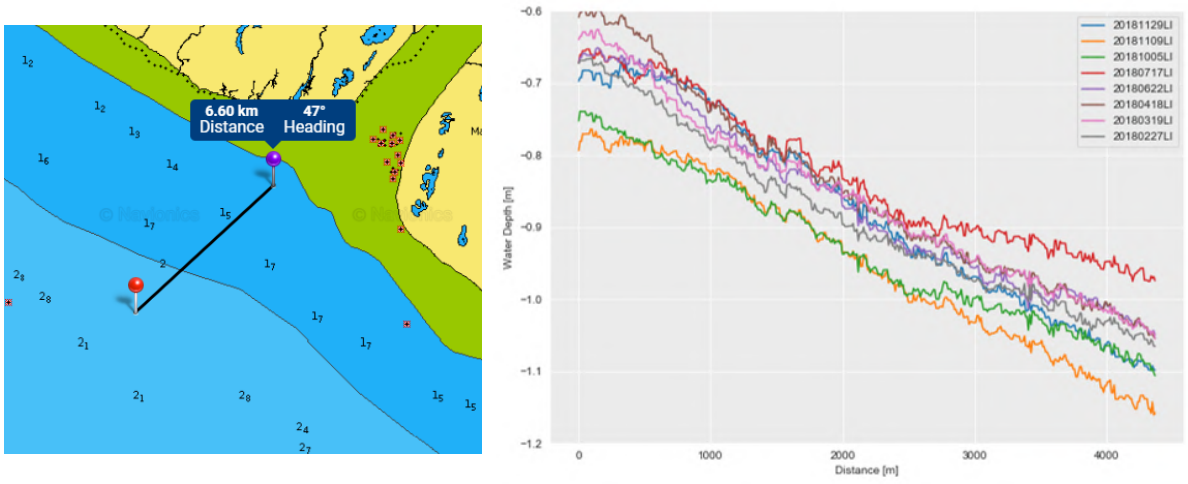

Figure 4.5: Bottom profiles of five different satellite images and location on Navionics chart

Due to the occurrence of hurricane Dorian in September 2019, the bathymetry around the Bahamas might have changed. Therefore, only images that were captured prior to this storm were used, so morphological changes were not the reason of differences in measured reflectance. Because of the absence of in-situ data pre- and post storm, an accurate analysis of the use of satellite images to derive the morphological impact of the hurricane, could not be done. To investigate if relative bottom changes could be detected, for 2019 two median composites were made in an area where hurricane Dorian hit hardest. The first is created from all the 2019 images prior to the storm (Januari-August) and the other used all images after (September-December). The same was done for 2018 to act as a reference without a storm. (Figure 4.6). Visually, not much difference on the sea floor can be determined. On land however, the destruction is visible along the coast. The bathymetry was derived using the logarithm of the green band. Comparison of both measurements resulted in similar differences between the images as found before on the multi-temporal image analysis in another part of the Bahamas. Therefore, using this technique, (small) changes in bathymetry can not be detected.

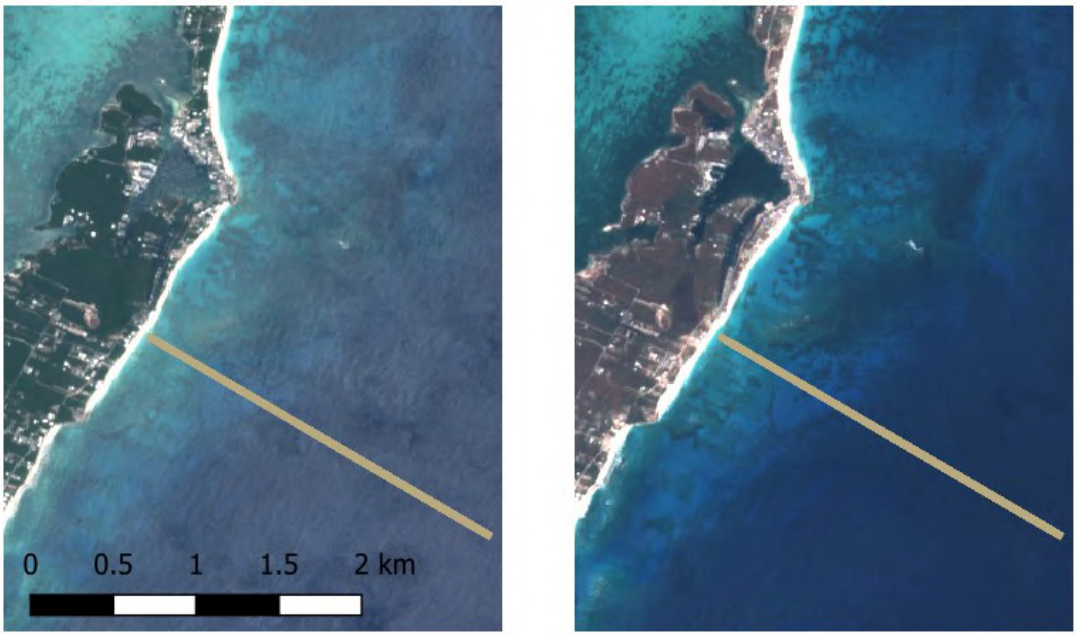

Figure 4.6: Elbow Cay [lat: 26.524720, lon: -76.965966], Left: pre-storm composite, Right: post-storm composite. Location of the transect that is plotted in Figure 4.7

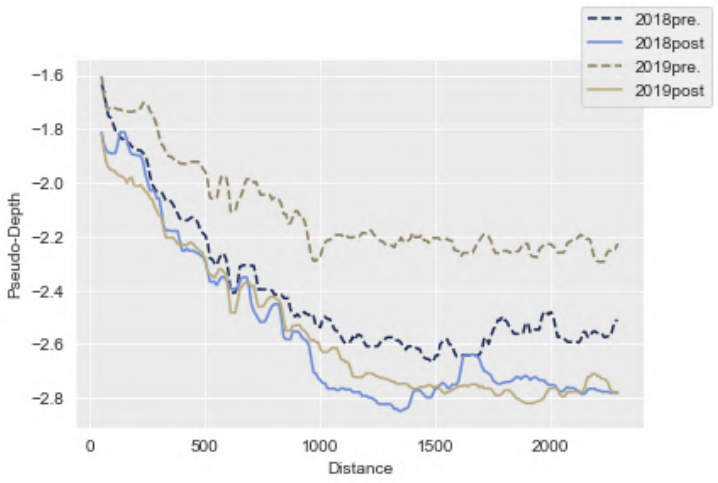

Figure 4.7: Pseudo-depth over a transect of Figure 4.6 the Bahamas

To assess the absolute error between SDB without calibration and known bottom elevation measured during a survey, on a sandy, highly reflective bottom in Sint Maarten, the bathymetry was defined. Here, data was available to make a more accurate comparison with the SDB. The bathymetry that was obtained from all three images gave about the same resulting bottom profile. In this case, no correction for tide was applied, because of the small tidal range on this location (0.2m), but it could be a cause of the minor vertical shifts between the lines. Compared with the in-situ measurement, the measured water depth from the satellite images showed a different pattern then the actual bottom. First of all, the vertical error, which increased with the water depth. In the shallow part the SDB results were deeper than the actual value, but if water depth increased, the SDB underestimated the depth.

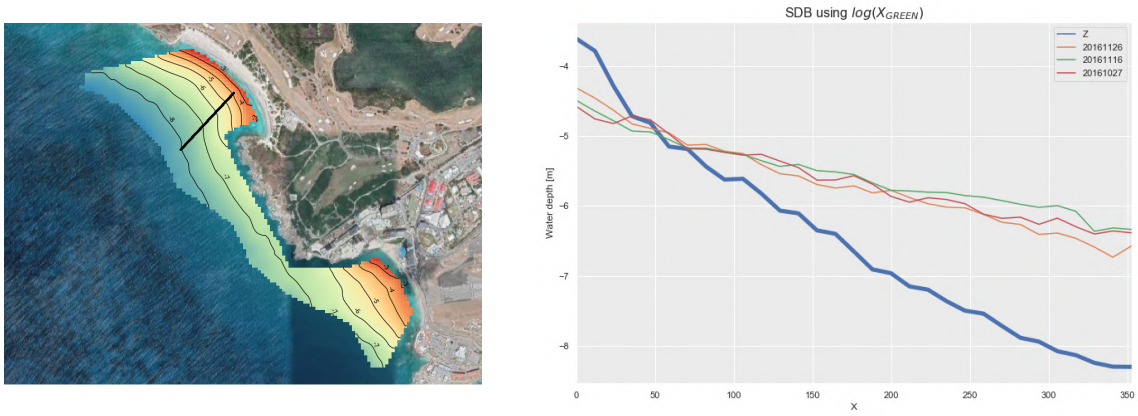

Figure 4.8: Bottom profiles of three different satellite images and location, Sint Maarten

The use of satellite images in temporal analysis is most valuable in areas where the sea floor shows morphological development.The coast of St. Louis, Senegal is such an area with rapid changes in coastal morphology. In two surveys, conducted 6 months apart, the changes were clearly noticeable. Also a comparison of satellite images showed changes in coastline and the southward development of a spit. For the investigation of the development under water, satellite images were obtained and light attenuation theory was applied to locate areas of erosion and sedimentation. In the two previous examples, it was already found that the derivation of an absolute bottom was not achieved without calibration of the models. To investigate if the relative changes between images can be identified in such a dynamic area, two images around the surveys were obtained. Differences in reflectance were compared with areas where sedimentation and erosion occured according to the survey.

However, due to the large quantities of transported sediments in these morphological dynamic areas, optical properties of the water are not sufficient for the use of SDB. A large portion of incident sunlight is not reaching the bottom because of the occurrence of suspended sediment. Per image, the amount of sediment and vertical location of this sediment cloud varies, which results in a different pseudo-depth measurement. Figure 4.9 shows the different pseudo-depth bottom profiles of all the cloud-free summer and winter images. Much more images were available in summer and their spread is smaller than the winter images. Therefore, a comparison on the dates of data acquisition (January and July) will not be reliable.

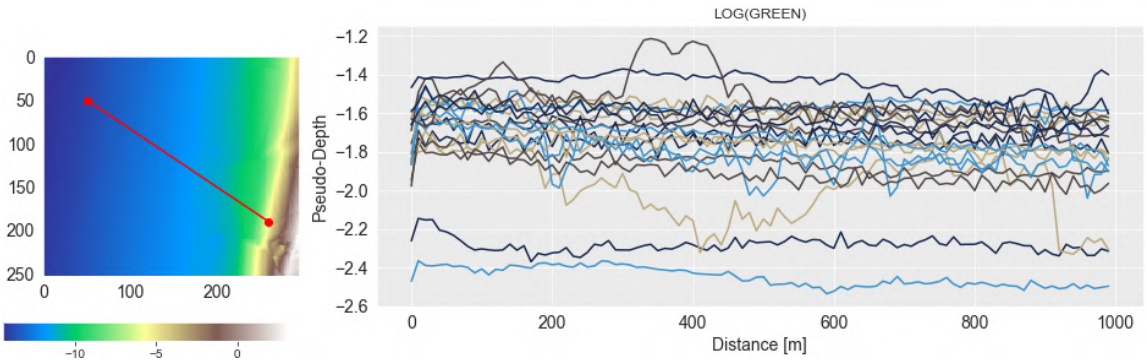

Figure 4.9: Bottom profile in St. Louis, Senegal

4.3 SDB after Calibration

The next step is applying in-situ measurements to train a model to derive the bathymetry. It was clear from the previous examples that in very clear waters the bottom shape can be extracted from a satellite image, but there were still errors in the Z-measurement. To overcome this, the addition of some ground-truth data points may increase the SDB accuracy. For the Bahamas case, no in-situ data was available, so the Sint-Maarten area was the area with the clearest water where training could be applied. In 2011 a large scale SBES bathymetric survey was conducted in this area. However, the earliest satellite images available were captured at late 2015 and the beginning of 2016, so there was a gap of about four years between the data acquisition and the moment of image capturing. In these four years morphological changes could have changed the shape of the bathymetry, but because of the moderate wave climate and the governing wave direction (east) it was assumed that the assessed area did not experience large morphological changes during that period and therefore it was possible to use the data set for calibration and validation of the model.

The survey data, that was acquired on cross-shore transects, was divided into calibration and validation data. Figure 4.10a shows the locations where training- and validation data were located. With the use of a jetski equipped with a single beam echo sounder (Figure 4.10b), transects were measured with a uniform spacing. The use of this technique makes it possible to acquire data at shallow parts. It was found that the use of training data on cross-shore transects resulted in a more uniform distribution of data points at all depths than when the data set was split randomly into training and validation data. The amount of data points was reduced to prevent that 1 pixel of the satellite image (10m x 10m) contained many different data points.

(a) Locations of training- and validation data, Sint Maarten

(b) Nearshore data acquisition using jetski

Figure 4.10

4.3.1 Method Selection

The two empirical methods that were used for SDB, are build upon the log-linear relationship between water depth and reflected radiance. Instead of using a single band, a variety of wavelength band combinations can be used. Therefore, analysis of the performance per band combination was done in order to select the method to work with in the other analyses. The first study was done in Sint Maarten on an area with a sandy bottom. For every combination, the root mean squared error, R-squared (which represents the proportion of variance) and the standard deviation (spread of the error) were determined. The results are listed in table 4.2. Below, the "building blocks" are shown for the linear method (4.1) and ratio method (4.2)

$$X_i = log(blue),\ X_j = log(green),\ X_k = log(red) \tag{4.1}$$

$$X_i = \frac{log(blue)}{log(green)},\ X_j = \frac{log(green)}{log(red)},\ X_k = \frac{log(blue)}{log(red)} \tag{4.2}$$

These values were used in the following linear regression equation:

$$d = a_0 + a_i * X_i + a_j * X_j + a_k * X_k \tag{4.3}$$

The parameters were obtained by applying linear regression using a set of training data points from an in-situ data set. The model calibration was described in more detail in chapter 3.7.

Method	Name	Combination	RMSE	R^2	std.dev
linear	L-B	log(blue)	1.32	0.59	1.02
linear	L-G	log(green)	0.51	0.84	0.68
linear	L-BG	log(blue) + log(green)	0.30	0.91	0.54
linear	L-BGR	log(blue) + log(green) + log(red)	0.31	0.90	0.52
ratio	R-BG	log(blue)/log(green)	0.94	0.71	0.96
ratio	R-GR	log(green)/log(red)	9.64	-1.92	2.75
ratio	R-BR	log(blue)/log(red)	17.59	-4.34	3.51
ratio	R-BGGR	log(blue)/log(green) + log(green)/log(red)	0.73	0.77	0.81
ratio	R-BRGR	log(blue)/log(red) + log(green)/log(red)	1.07	0.67	0.98

Table 4.2: Band combinations of Empirical SDB Methods

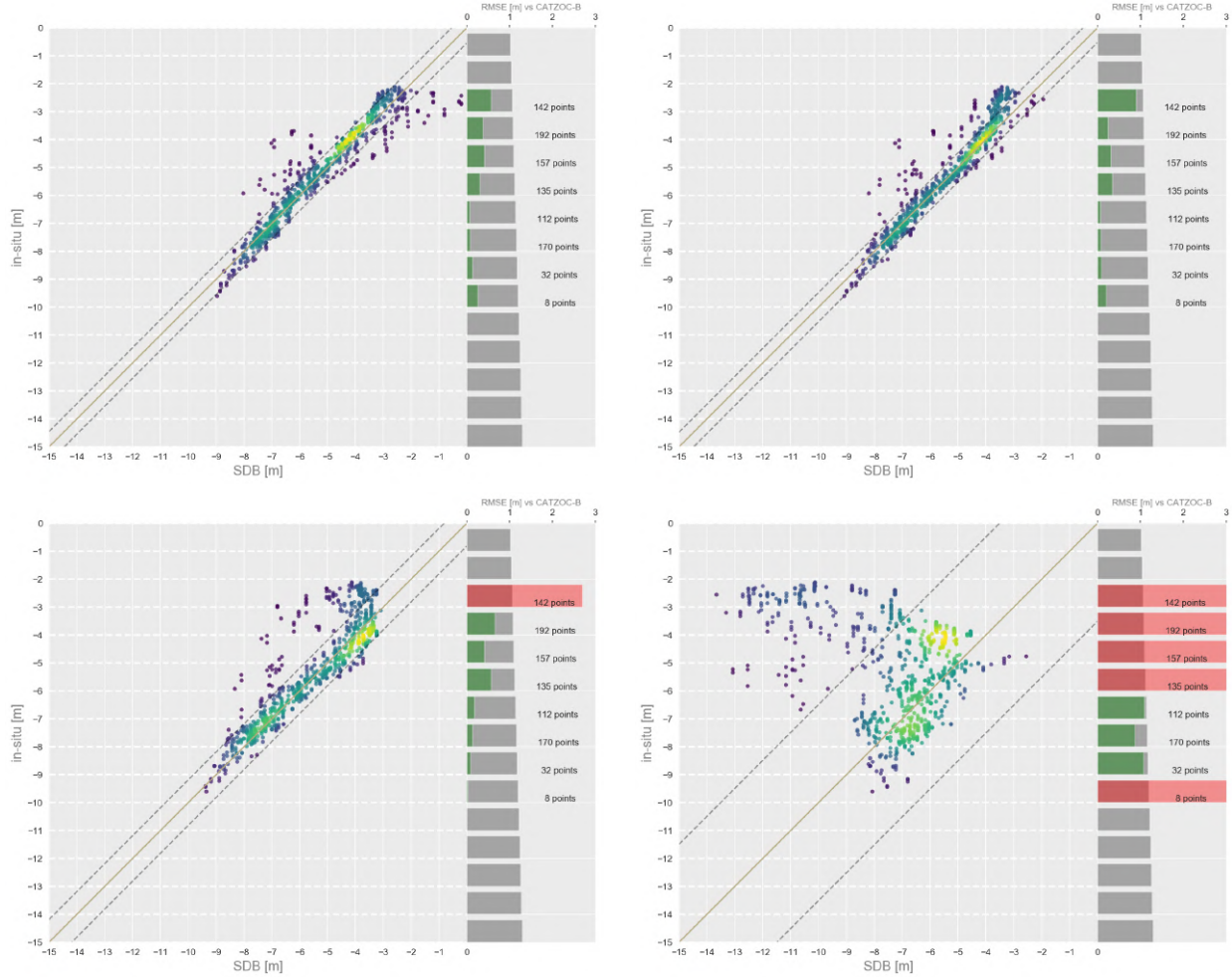

Figure 4.11: Score plot for four methods applied to Sint Maarten case: Top row: **L-BG, L-BGR**; Bottom row: **R-BGGR, R-BR**. Colors of the points correspond with the density (yellow high, blue low). Plots for other combinations can be found in Appendix A

In figure 4.11 for four assessed models, the bottom level according to the in-situ data was plotted against the SDB level. Some of these calibrated models show good correlation with the validation data, while in others the SDB results are less. To give an indication of the performance, for every depth class the RMSE of SDB was compared with the IHO CATZOC-B standard. Classes with an error smaller than CATZOC-B were colored green.
On this homogeneous bottom, the methods where the linear combination of bands was used showed the best correlation (R-squared scored close to 1) and the smallest RMSE (L-BG and L-BGR). The variants with the ratio of wavelengths are performing worse, especially if the red band is involved. Because the division of bands was used in the ratio method, erroneous values and noise were amplified. Therefore, the error and the standard deviation are significantly larger than for the ratio method. Addition of more bands leads to a better result for the linear method.

Next, the best performing linear and the best ratio method (L-BGR and R-BGGR) were tested in another area on Sint Maarten, where the bottom albedo varies due to the presence of under water vegetation and reef/rock. Phillips Bay (figure 4.12), which is located eastward of the previous assessed location, is an area where the bottom substrate varies strongly. From the satellite image, a clear distinction between bottom materials can already be made visually. The influence of these differences in solar reflection will be assessed by 1) analyzing the signal from the optical sensor, 2) apply in-situ data of the entire area to train the model without regarding the location of the various bottoms, and 3) applying training data to each patch individually.

Figure 4.12: Assessed area Phillips Bay (1) divided in a sandy bottom (1) and a patch of (vegetated) rock (2)

In an assessment on the influence of albedo on SDB results, calibration- and validation data from both sandy and vegetated area (fig. 4.12) was used. This data set was split into a training and validation set. After that, a separation was made between sand and vegetation data based on visually classification of the satellite image. The model was than calibrated and validated using respectively only sand and only vegetation data points. The resulting RMSE plots are shown in figures 4.13, 4.14 and 4.15. The case with both data on sand and vegetation shows poor results in the deeper located areas. This is because of the calibration on low reflective bottom in shallow parts. Deeper located sandy parts have similar low reflectance and their depths are therefore underestimated. In case of a homogeneous bottom, the resulting SDB shows good correlation with the validation data in both linear and ratio method.

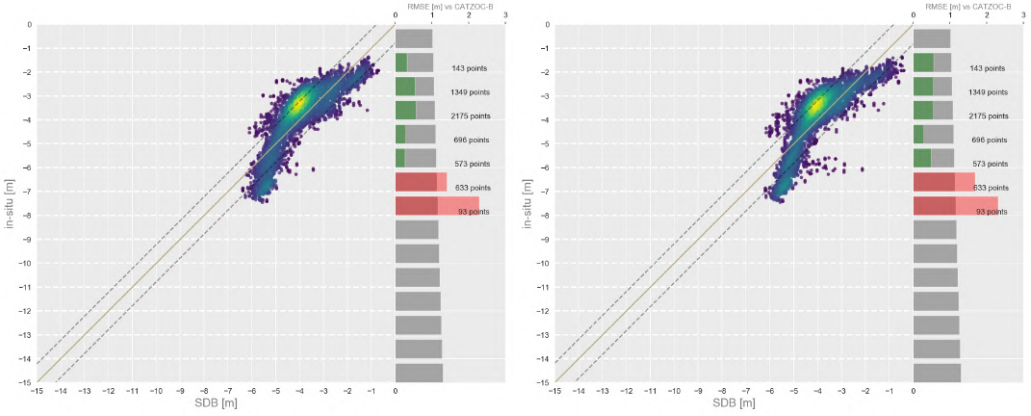

(a) Linear method with blue, green and red bands **(b) Ratio** method with blue/green and green/red

Figure 4.13: Region of interest containing **sand** and **vegetation** (Sint Maarten)

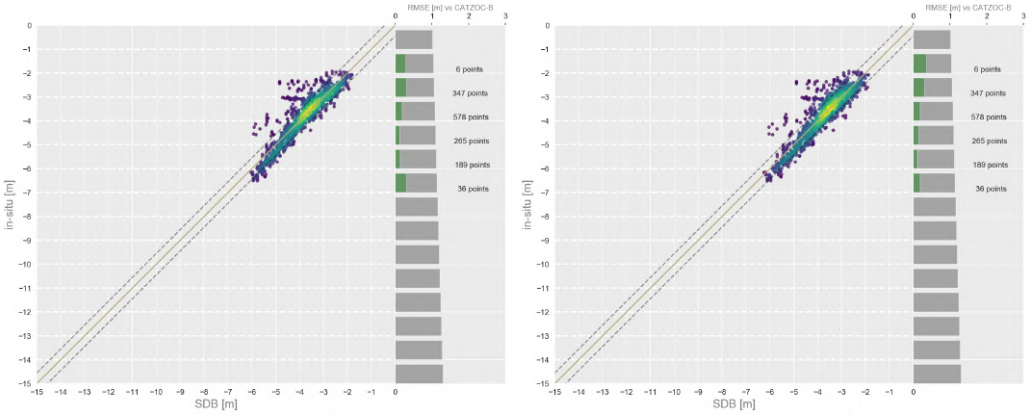

(a) Linear method with blue, green and red bands **(b) Ratio** method with blue/green and green/red

Figure 4.14: Region of interest containing only **sand** (Sint Maarten)

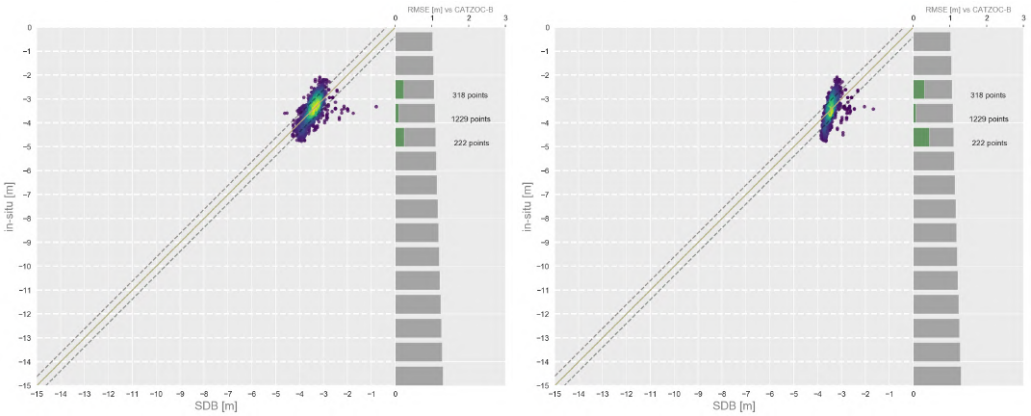

(a) Linear method with blue, green and red bands **(b) Ratio** method with blue/green and green/red

Figure 4.15: Region of interest containing only **vegetation** (Sint Maarten)

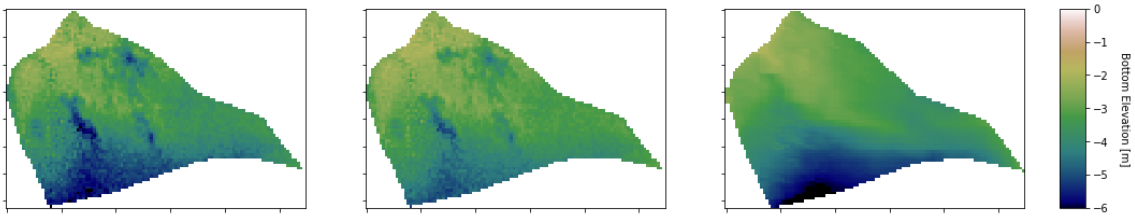

Figure 4.16: Results over a sandy area in Sint Maarten. **Left**: Linear, **Middle**: Ratio, **Right**: In-Situ Data

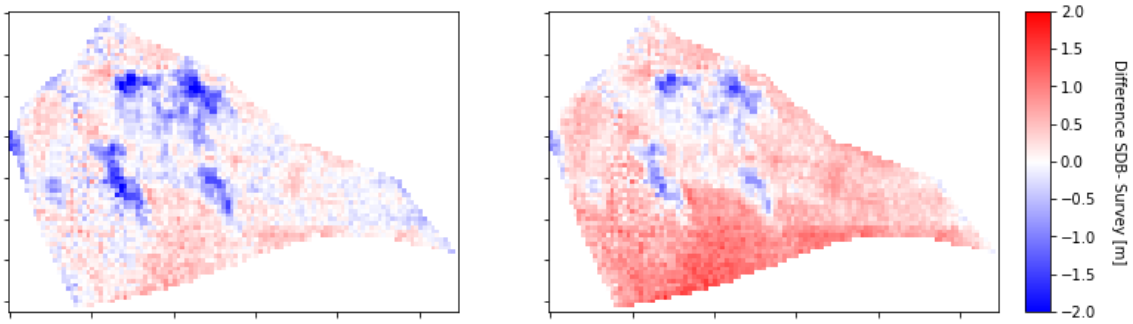

Figure 4.17: Difference with in-situ data. **Left**: Linear, **Right**: Ratio

Figures 4.16 and 4.17 show the SDB results of the sandy area and comparison with in-situ data set. The dark spots in the image (see satellite image in figure 4.12) correspond to the largest errors of the SDB. Therefore, the variations in sea bottom affect the results of SDB methods. Both the ratio and the linear method had similar performance over varying bottom type, but the linear method showed more consistent performance, so it was chosen to be used in the remaining of this research.

4.3.2 SDB case studies

After the different band combinations were assessed (section 4.3.1), the best performing method was used in other areas with varying environmental- and optical circumstances. All assessed locations were described earlier in chapter 3.8.4. The studies were performed in order of SDB difficulty. First, Key West, USA was used to clear water, bottom features. UAE, more turbid, deeper. Faro, more turbid, more development in morphology. Markermeer,

Key West, USA

Key West, Florida (USA) was another clear-water location that was used as case study. However, the water depth in this area was more shallow and some deeper channels and harbor basins were dredged to provide access for vessels. This case study was used to assess the detection of these under water features alongside the accuracy of the absolute bottom elevation derivation. Part of the satellite image of the considered area is shown in figure 4.18, where the dredged area is also clearly noticeable.

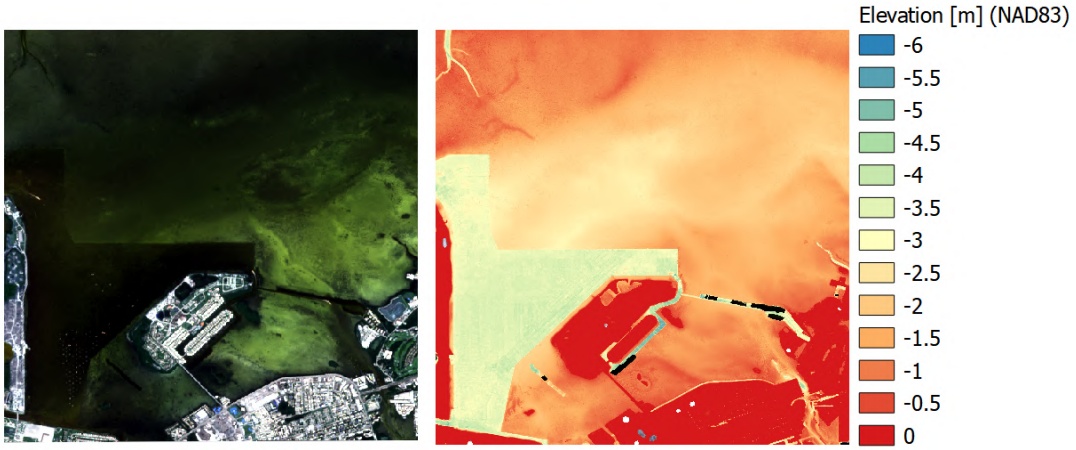

Figure 4.18: Overview of Key West, FL. Left: Satellite image (11-10-2016), Right: DEM of LiDAR survey 2016

A calibration data set of 60 in-situ data points and a validation set of almost 400 in-situ data points were sampled from the LiDAR survey and used to respectively calibrate and validate a SDB model.

The results are in line with the findings of Caballero and Stumpf (2019), who also used this data set for their SDB study. In the first 3 meters of water depth, SDB was closely following the in-situ data. In deeper areas, more noise is present in the image due to a large quantity of ships within the harbor basin. Figures 4.19 and 4.20 show the error between SDB and in-situ both on the validation data as well as spatially. Along the edges of the dredged channel, the errors are large, because of the difference in ground sampling distance between the satellite image and LiDAR.

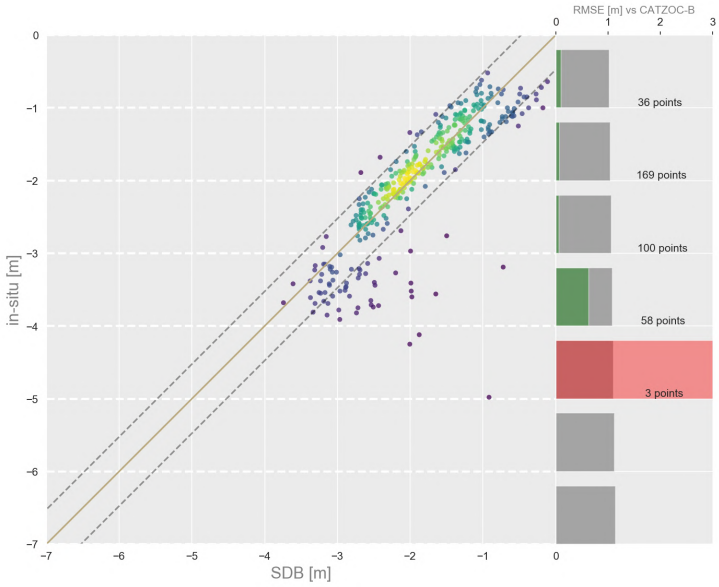

Figure 4.19: Observed vs. SDB depth values in Key West, FL. Bars on the right hand side show RMSE error. If green, CATZOC-B norm is satisfied and if red, the error is too large.

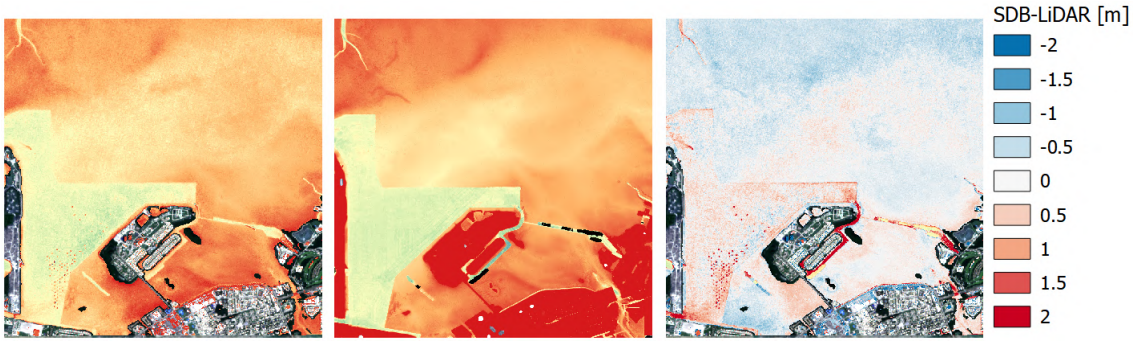

Figure 4.20: Left: SDB, middle: LiDAR, Right: Difference between SDB and LiDAR [m], (Key West, FL)

United Arab Emirates

The considered areas in the previous case were relatively shallow with maximum depths of around 8 meter. To assess the ability to obtain bathymetry on greater water depths, a location in the United Arab Emirates was used. The bottom of the Persian Gulf around the UAE has a relatively steep slope between 0 and -7m MSL. After that the slope is more gentle until -12m MSL which was the maximum depth within the area of interest.
Figure 4.21 shows the validation of this case study. Only few calibration and validation data points were available in the shallow areas, so this case is focused on the -7m to -12m MSL range. Again, the RMSE values per depth class meet the CATZOC-B norm. However, the spread of the error is wider than in the previous cases.

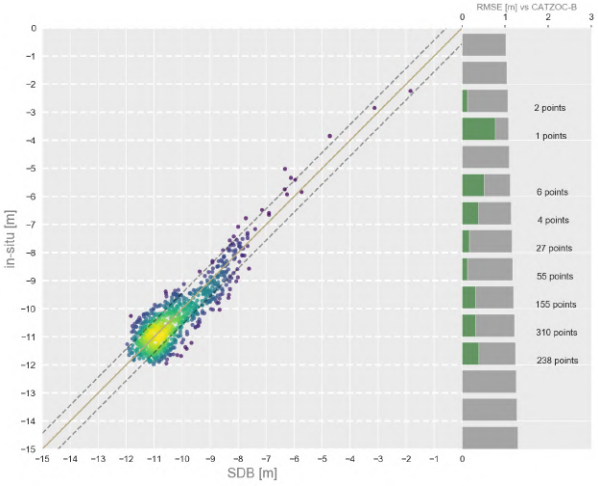

Figure 4.21: Observed vs. SDB depth values in UAE. Bars on the right hand side show RMSE error. If green, CATZOC-B norm is satisfied and if red, the error is too large.

To provide access to the harbor, a large dredged channel is present with a width of about 400m and a depth of 14 meters below mean sea level. The calibrated model did not have this deep bottom feature in the SDB. Therefore, a small research was done to the initial signal in this area. A selection of images was acquired, pre-processed and used. It is clear that from the original signal (Figure 4.22), the dredged channel can not be distinguished. Therefore, it is important to note that during calibration of the model, one might be calibrating the reflectance from a sediment cloud in stead of bottom reflectance. In this case, the bottom at -10m and -15m give exactly the same signal, so the reflectance is originating from suspended sediment at a depth that is smaller than 10 meter below MSL.

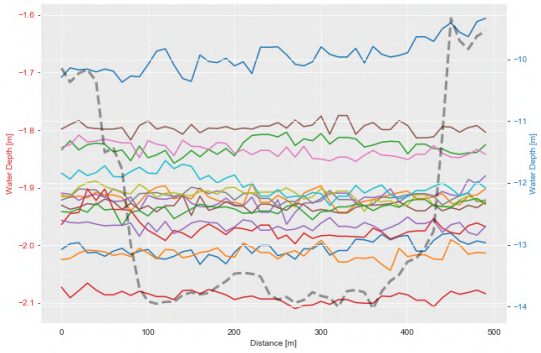

Figure 4.22: Signal of green band around the dredged channel (y-axis differ to mark the channel's position)

Faro, Portugal

In the previous section, the areas being assessed had both clear water and a highly reflective bottom. Hydraulic conditions were such that hardly any suspended sediments were present in the water column. This assured that the reflections were coming directly from the sea bottom. In the case where of some level of turbidity exists, sun light is scattered by the particles in the water and not all radiant energy reaches the bottom to be reflected. How much it influences the satellite derived bathymetry is treated in this section. A new location was used where the bottom material was homogeneous and reflective, but suspended sediment occurred approximately in the entire area. Rio Formosa, located on the south coast of Portugal, had these conditions. High sediment concentrations were found near the river outlets and the tidal inlets of the estuary, but reduced with distance from

these locations. An overview of the location and the area that was assessed is displayed in figure 4.23. The large data set (provided by the Portuguese Foundation for Science and Technology FCT) covering the entire coastline of the Rio Formosa area, including large parts of the estuary was acquired using bathymetric LiDAR from an airplane. The focus area was located on the west part. Pacheco et al. (2015) used this data set in their research on SDB in this area already. However, they used Landsat 8 images, but achieved an accurate derivation of the bathymetry.

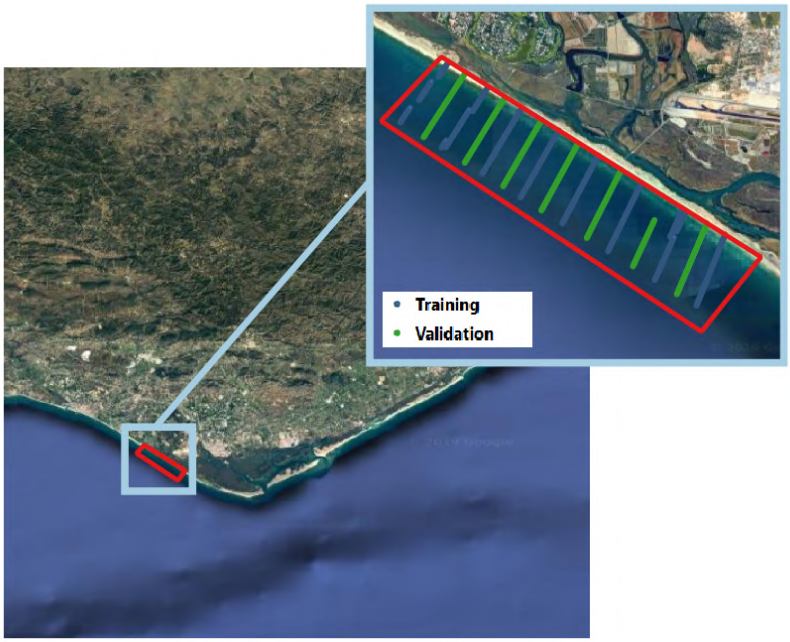

Figure 4.23: Overview of the assessed area on th Portugese coast near Faro with training and validation transects indicated in blue and green

For one year, from November 2015 until November 2016, the highest quality, cloud-free Sentinel-2 images were obtained and pre-processed. A SDB model was calibrated on every image using the linear-method. The validation plot of the image with the smallest RMSE errors across all water depths in shown in figure 4.24a. It is clear that the same performance as in the case of crystal clear water (Sint Maarten) is not obtained. However, these results still meet the CATZOC-B requirements. Figure 4.24b shows the pixels that deviated more than 1 meter (+ and -) from the actual measured bottom level. All other pixel were made transparent. These high-error pixels are mainly located near the water line. This is caused by the breaking waves that prevent light to be reflected from the sea floor. The other noticeable errors are the pixels with an overestimated water depth just offshore from the water line. It seems like a sand bar has developed in the period between data acquisition and image capture. Therefore, morphological effects might play a role, because of a three year gap between data acquisition and image capture.The remainder of pixels with a large error are the noise in the image that can be removed by applying a filter.

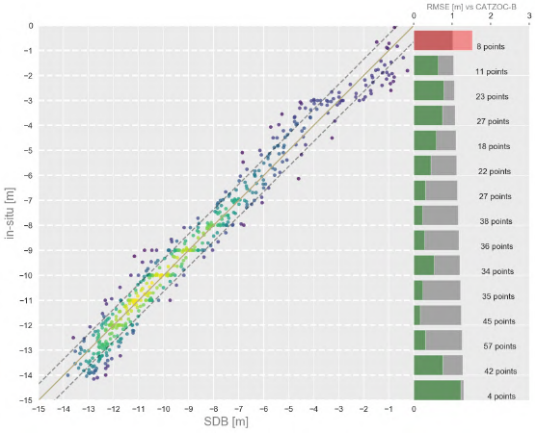

(a) class separated RMSE plot of the image of 17-09-2016

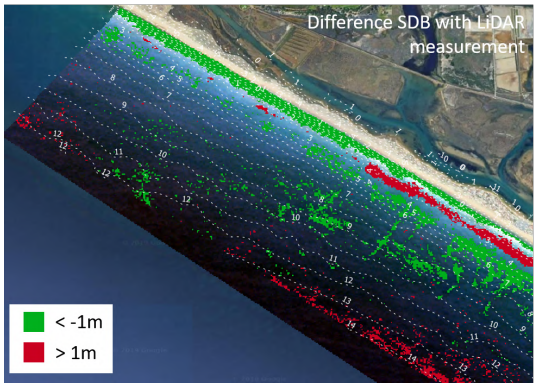

(b) Areas of large error (>1m)

Figure 4.24

St. Louis, Senegal

To assess the empirical SDB methods in the most challenging coastal conditions, the case of St. Louis in Senegal was used. The bathymetry in this area changes very rapidly, which also causes for a lot of water related issues in this city. Two bathymetric surveys were conducted 6 months apart that showed major erosion along the coast and at the river outlet and sedimentation downstream. Five images of the surveyed area captured within one month of the time of the survey were collected and a SDB model was calibrated on each of them to derive the bathymetry. Figure 4.25 shows the satellite derived elevations plotted against the observed validation points from the survey for an image taken on January 8 2019 (one week before the survey). This was the best resulting bathymetry among the five images, which can be observed from the RMSE values per depth class in Table 4.3.
In none of the images, the CATZOC-B norm is satisfied, because RMSE values are too high. In this area the turbidity levels fluctuate by river discharge and hydrodynamic forcing what results in alongshore sediment transport. Under these conditions, it is almost impossible to retrieve bottom reflectance values and thus derive an accurate bathymetry. All reflectance values are similar over multiple depths, so the model is trained to a particular depth. As seen in Figure 4.25, it performs well in one or two depth classes, but it underestimates the bottom elevation in deeper areas and over-estimates in shallower parts. Therefore, although in some classes the accuracy levels seems within the limits, the confidence in captured bottom reflectance and derived bathymetry is low. So for cases like St. Louis, empirical SDB is not a good method to retrieve the bathymetry.

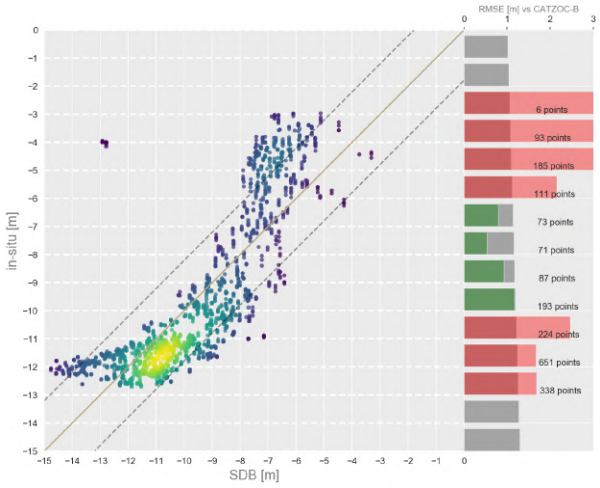

Figure 4.25: Observed vs. SDB depth values in St. Louis, Senegal. Bars on the right hand side show RMSE error. If green, CATZOC-B norm is satisfied and if red, the error is too large.

Table 4.3: Results of multiple images in St. Louis with RMSE per depth class (shallow, intermediate and deep water).

Image Date	RMSE[m] shallow (<5m)	RMSE[m] moderate (5-10m)	RMSE[m] deep (>10m)
12-09-2018	11.67	2.38	4.95
01-08-2019	12.75	1.21	1.37
01-18-2019	13.85	4.49	2.18
02-02-2019	7.48	2.49	1.23
02-22-2019	8.50	1.68	0.62

Marker Lake, The Netherlands

Hydraulic conditions in lakes often significantly differ from what is found in the coastal zone. To assess the applicability of SDB under these condition, a case study in the Markermeer lake was conducted. The Houtribdijk separates the two largest lakes of the Netherlands: the IJsselmeer and the Markermeer. Recently, this dike has been enforced by constructing a sandy foreshore. In a pilot project, that was conducted in the previous three years, the behavior of such a dike reinforcement was investigated and closely monitored.
Due to the absence of tides and swells, bottom material hardly gets transported, so the bottom is muddy. Wind does play a role in this system, because of the large fetch it can have depending on the direction it is coming from. This causes wind waves and water level set up at the dike. In the pilot, this resulted in the formation of a shallow plateau between two steep slopes. From the satellite images, this shallow part is sometimes visible. Therefore, it was investigated to obtain the water depth with the use of SDB. The survey of January 2016 was used to calibrate an image from that same time period.In figure 4.26 the location of the pilot is shown, together with the Sentinel-2 image that was used to derive the bathymetry. The difference map shows the performance of SDB in this area compared with the bathymetric survey. The RMSE plot is shown in figure 4.27. Training data on transects was used, because that was the way the data was acquired during the survey. Because the bottom profile is almost flat, many data points were collected at approximately 3 meters water depth. The model therefore performs best on those points. The slope of the foreshore is only a few pixels wide, so relatively little data is located there. The spatial resolution of Sentinel is not sufficient to accurately map the bottom features in these steeply sloping areas.

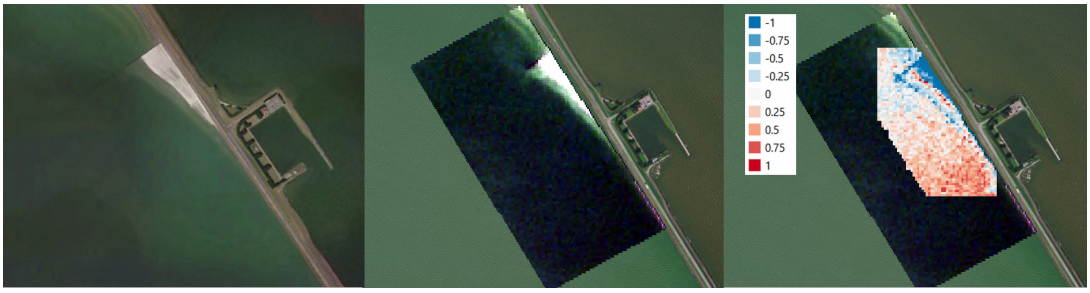

Figure 4.26: Houtribdijk (Markermeer side) with the pilot and the difference between survey and SDB [m]

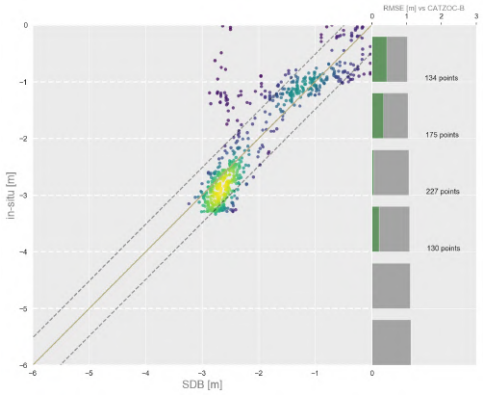

Figure 4.27: Observed vs. SDB depth values in Markermeer. Bars on the right hand side show RMSE error. If green, CATZOC-B norm is satisfied and if red, the error is too large.

4.3.3 Synthesis of Case Studies

In the previous chapters, the performance of SDB in a variety of cases was assessed. These cases were chosen such that they cover a wide spectrum of different coastal characteristics and therefore assess the robustness and performance of empirical SDB methods under different (optical) conditions. It was investigated under what circumstances it is possible to confidently obtain an accurate bathymetry and when not. Table 4.4 lists all the cases with the weighted average of the RMSE from the validation data in three different depth classes: shallow, intermediate and deep. Some cases did not cover all three classes.

Table 4.4: Results of case studies with RMSE per depth class (shallow, intermediate and deep water). For cells with "-", no data was available.

Location	Case	RMSE[m] shallow (<5m)	RMSE[m] moderate (5-10m)	RMSE[m] deep (>10m)
Bahamas	Clear water, reflective bottom	-	-	-
Key West	Clear water, less reflective bottom	0.26	-	-
Sint Maarten	Clear water, varying albedo	0.42	0.14	-
UAE	Deep water, bottom not visible	0.34	0.26	0.35
Rio Formosa	Deep, turbid water	0.78	0.35	0.38
St Louis	Deep, turbid, morphodynamic	12.75	1.21	1.37
Markermeer	Lake, turbid	0.39	-	-

In clear water, the optical conditions of the water column are optimal for the use of SDB. Therefore, the results in terms of vertical error were good. Also, because the bottom is already visible in the image, one can be certain that bottom reflectances were measured by the sensor. When spatial bottom variations occur, the results decreased slightly.For instance, areas with low reflectance (low albedo) that are located in shallow water were sometimes similar to deep areas with a well-reflecting bottom. Depending on the location of calibration data this resulted in an over- or underestimation of the vertical level of the sea floor. These results correspond with what was found in earlier SDB research

Areas that were not often threaten in SDB research yet are the ones where water is more turbid. In these areas, the resulting SDB was still good and within the defined norm. However, the signal consist out of both bottom reflectance and scatter from particles in the water column. The ratio between the two depends on the sediment concentration, but was not easy to quantify, what results in a higher uncertainty of the resulting derived bathymetry. The same applies for areas with deep ($> 10 - 15$m) waters, where the light might or might not penetrate all the way to the bottom. In the case of waves, in the shallow areas where waves are breaking light does not penetrate into the water, but is reflected directly from the whitewash of the wave. Do in these areas, no bathymetry could be derived with satellite images.

Because of the relatively steady water in lakes, the bottom consists of settled fine sediment like silt and clay. Some of these particles are so small that they are always in suspension in the water column. If these concentrations are large, light is not able to pass and won't reach the bottom of the lake. The signal the sensor measured is only coming from in-water scattering and surface reflectance and not from bottom reflectance.

In terms of CATZOC assessment, all the average errors satisfy the norm of CATZOC-B and some even CATZOC-A. However, this average over all values does not always gives a good representation of the true bathymetry. For example the Markermeer, one of the challenging cases with turbid water, only consists of shallow depths (below 5m) and has a good average RMSE value within the CATZOC norm. However, the bathymetry in the Markermeer is more or less flat. So when calibration is applied, the reflected signal from the turbid water is vertically tuned to the bottom level, which gives good results in terms of vertical error. Nonetheless, the confidence in the result is very low, because it is almost certain that the original radiance signal is not coming from the bottom,

but from particles in the water column. Therefore, when applying SDB in turbid waters with a flat bathymetry, the validation results might appear better than they truly are.

Table 4.5: Confidence in capturing the bottom reflectances in the satellite image.

Case	Description	Confidence in bottom reflectance
Clear water, high reflective bottom	Water is so clear that the bottom is visible in the original satellite image. Very little disturbances from particles in the water column. The bottom material is very reflective (white sand), so the reflected signal is strong.	★★★★★
Clear water, less reflective bottom	The bottom consists of patches of dark sand with some rock. Therefore, a large part of the light energy is being absorbed by the bottom instead of being reflected, which reduces the measured signal.	★★★★★
Clear water, varying albedo	Difference in bottom material that cause for difference in reflectance with the same water depth	★★★★☆
Deep water, bottom not visible	Water in some areas to deep to capture the bottom. Relevant for channels (harbor entrance or tidal channels)	★★★☆☆
Deep, turbid water, waves	Nearshore breaking waves result in scattering of light instead of reaching the bottom	★★☆☆☆
Lake, turbid water	Permanently suspended sediments hinder the penetration of light to the bottom.	★☆☆☆☆

4.4 Spatial Extrapolation

Until now, only a small section of the satellite image was used for deriving the bathymetry. This is mainly because often the in-situ retrieved data set does not cover the entire image. The calibration and validation points that were used in the previous sections were located within the same area of interest. The advantage of satellite images, is their large spatial coverage. A single Sentinel-2 image covers an area of 100km x 100km, which implies a great potential to map large coastal areas at once.

To assess the extensions of the use of SDB over a larger part of the image using the same amount of calibration data, two analyses were performed. In the first one, the calibration and validation data were still within the same area of interest. However, the number of points that were used to calibrate were reduced and the error per depth class was assessed. In a second analysis, an area some distance away from the training area was selected and validation points were sampled from the data set.

4.4.1 Amount of Calibration Data

To investigate the influence of the amount of training data, the number of points to train the model was reduced. The reduced training set was then used in the same manner as in the previous step to calculate the SDB. The validation data remained the same. Since the linear method performed slightly better in the previous examples, it was used in this analysis. An area in Sint Maarten with

a high reflective, sandy bottom was used for this analysis. The initial dataset consisted out of 300 points. By randomly selecting points, each step the set was reduced by half and the RMSE was calculated again. There was hardly an increase in the error noticeable until the set was only 5-10 points. Per depth class, the RMSE was calculated and displayed in table 4.6. This shows that in clear water with a high reflective bottom, only the addition of a small number of ground-truth values can get SDB results with decimeter order accuracy.

Depth	RMSE 100%	RMSE 50%	RMSE 25%	RMSE 12%	RMSE 5%	RMSE 1%
0	-	-	-	-	-	-
-1	-	-	-	-	-	-
-2	0.32	0.41	0.39	0.23	0.50	1.98
-3	0.13	0.11	0.10	0.16	0.25	1.00
-4	0.09	0.08	0.08	0.12	0.35	0.73
-5	0.11	0.11	0.10	0.11	0.43	0.57
-6	0.14	0.19	0.21	0.10	0.10	0.22
-7	0.10	0.15	0.21	0.07	0.08	0.11
-8	0.12	0.18	0.36	0.10	0.06	0.04
-9	0.45	0.60	1.02	0.43	0.15	0.10

Table 4.6: RMSE values per depth class for decreasingly amount of calibration points. Percentages show the amount of data relative to the first assessment. Location: Sint Maarten.

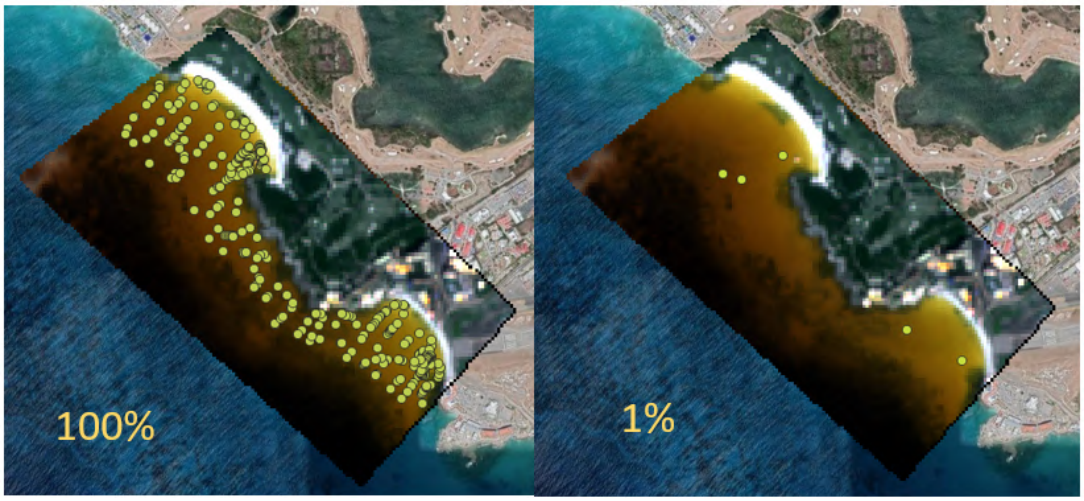

Figure 4.28: Locations of the data points for the first and last assessment (100% and 1% of the data). Figures of other percentages can be found in Appendix B. Location: Sint Maarten

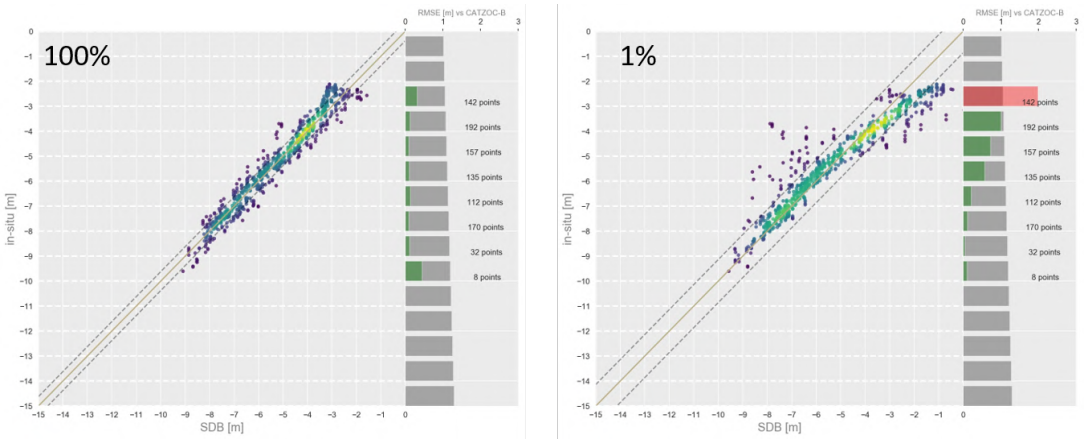

Figure 4.29: Observed vs. SDB depth values in Sint Maarten with 100% and 1% of the amount of calibration data. Bars on the right hand side show RMSE error. If green, CATZOC-B norm is satisfied and if red, the error is too large.

In a practical application of the acquisition of calibration data, one would not obtain randomly spaced point. This data set consists of cross-shore transects with a spacing of about 50 meters. In figure 4.30 two transects were used to calibrate the model (100 data points), which leads to similar results as the randomly selected points. Acquiring data on a transect is how one would do it in a practical situation and therefore this situation is more representative for the real-world application of SDB combined with some in-situ data.

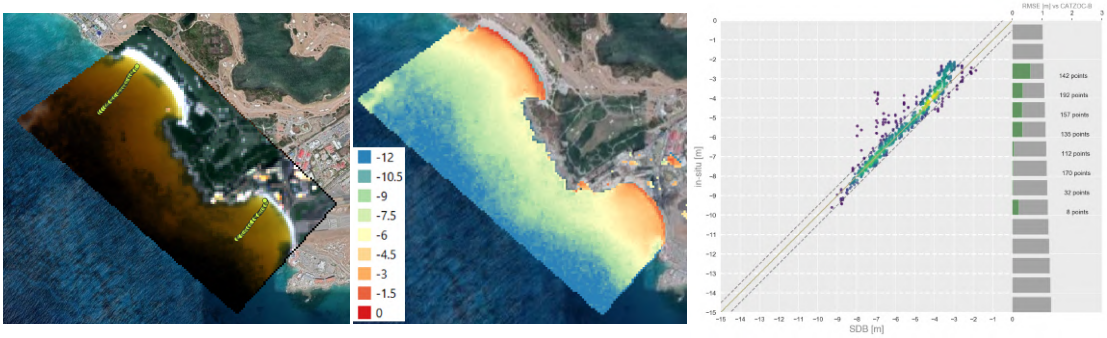

(a) Two calibration transects **(b)** Bathymetric map **(c)** RMSE plot

Figure 4.30: Transect based data reduction. Reduced data set to two transects and displayed results in elevation map and RMSE plot. Location: Sint Maarten

4.4.2 Distance from Calibration Data

As explained in 3.8.5, the bathymetry of large stretches of coastline can potentially be covered with the use of satellite images. The data set of Rio Formosa, Portugal covered a stretch of coastline of about 65 km near the city of Faro. In section 4.3.2, the performance of the SDB at this location was already presented. However, the data used to calibrate and to validate the model were located within the same area of interest. To investigate the SDB performance beyond the region where in-situ data is available, the data set was divided into three areas (location shown in Figure 4.31). Initially, the model was trained with data from an arbitrary area (number 1). The validation plot in figure 4.32a shows comparable results that were found earlier on this location. The linear method was used and the regression parameters were saved to use in the same image in another area. Area 2 was located 10km eastward on the other side of a tidal entrance. In this area, 2000 validation points were obtained from the airborne LiDAR data, which were used to validate the results of the SDB. The same process was done in area 3, which is located about 20km from the calibration data. Besides the distance from the calibration data, the coastline in area 3 is also facing another direction,

which affects the beach profile. Also the occurrence of two tidal inlets, causes for more turbidity in area 3.

Figure 4.31: Locations of the areas considered in this spatial extrapolation analysis. Rio Formosa, Portugal

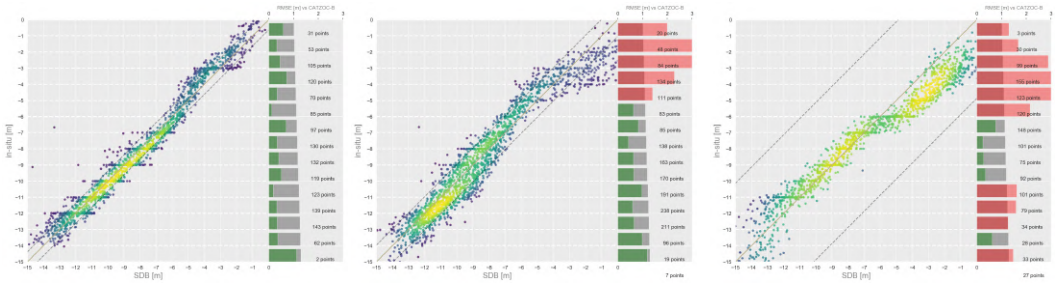

(a) RMSE plot of **Area 1** **(b)** RMSE plot of **Area 2** **(c)** RMSE plot of **Area 3**

Figure 4.32: Observed vs. SDB depth values in Portugal at increasing distance from calibration data. Bars on the right hand side show RMSE error. If green, CATZOC-B norm is satisfied and if red, the error is too large.

The performance of the SDB model reduces with increasing distance from the calibration data. Especially in shallow water (0-5m below MSL), the errors increase significantly. A cause of these errors might be the time difference between data acquisition and image capture (which is about three years) in which morphological changes might have occurred. These changes affected the quality of the initial calibration and are contributing more in the more dynamic areas. Increased turbidity near the tidal inlet in area 3 can also be a source of error that cause for the underestimation of water depth.Thus, spatial extrapolation of the calibrated model is only possible if the conditions in the new area are equal to the calibration area. If optical properties of the water column in remote areas are affected by, for instance, increased turbidity levels, the SDB model can not be successfully be applied.

5 Discussion

The former chapter showed the results of SDB application on a large variety of locations with different (optical) hydraulic properties. In this chapter, some of the findings will be discussed in more detail and possible explanations are given to the performance of SDB methods under certain circumstances.

5.1 Empirical SDB Before Calibration

Empirical SDB methods require calibration with ground-truth data to give an accurate bathymetry, which is also found in previous research mostly performed under clear-water conditions. In this research, it was investigated what those methods can provide without the calibration step. At most locations around the world no data is available, but the satellite images might still contain valuable information about bathymetry and bathymetric changes. To investigate what the possible applications are without calibration, only the theory of attenuation of light was used in combination with various wavelength bands of the satellite images (section 4.1). This theory assumes that there is a linear relation between water depth and the natural logarithm of the reflected wavelength, which is a simplification of the complex radiative transfer theory. In none of the cases where this logarithm was applied, the true bathymetry was derived accurately, which makes sense because no attenuation coefficient was used. This coefficient is wavelength dependent and should shift the resulting depth values such that they correspond with the real bottom elevation. However, in all assessed cases, not only a vertical offset was found, but also the slope of the satellite derived bathymetry was significantly different than the slope of the surveyed bathymetry, so a coefficient to correct for the vertical error is not enough to obtain an accurate result.
Another problem with vertical correction without ground-truth data occurred when multiple images of the same area were analyzed. It was found that, even after atmospheric- and water column correction, the measured reflectance differs between every image. Partly, this can be assigned to tidal elevation, what results in a longer path for light to travel in water, hence more attenuation occurred. However, also in areas with limited tide these differences between images were present, which makes it not possible to derive a single value to correct for the vertical offset for all images.
So when only satellite images are available, the absolute vertical position of the bottom can not be derived with empirical SDB methods. However, for coastal research, the relative changes could also already contain valuable information on morphological development. Comparing two "bad" results can also give insight in the areas where vertical bottom changes occur, so it indicates erosive and accreting locations under water. To investigate if changes in signal could possibly be related to the vertical changes in bottom level, in section 4.2 an analysis was performed on a number of images over the year. It was found that there were significant differences in measured reflected radiance per image that could not be accounted to changes in bottom level. The analysis was initially performed at a location where the bottom was assumed to be steady because of mild wind and wave conditions (Bahamas), but between the images that were gathered over one year, significant fluctuations occurred. The vertical differences were not uniform over the entire area, so it could also not be caused by tidal levels. Because of these fluctuations, it is hard to confidently assign locations where the bed is eroding or accreting and therefore not possible to derive an absolute bottom change from that. In areas that were more dynamic (St. Louis, Senegal), the turbidity concentrations were so high that no bottom reflectances were measured. Only the morphological development above the water could be monitored using satellite images, but only in horizontal direction, like the changes in shoreline position.
Because of the high temporal resolution of satellite images over the same area, they have great potential to be used in the monitoring of coastal areas either in absolute as well as relative sense. However, because of the differences in reflectance per image, changes in measured reflectance could not be confidently assigned to bottom level changes. An elaborate investigation to these fluctuations was performed to gain understanding of their origin and possibly find ways to correct.

5.1.1 Seasonal Fluctuations

In chapters 4.1 and 4.2 it was shown that the measured reflectance of a single location had a vertical offset that varied per captured image. Because of that, by applying only the log-linear method, without any calibration, the resulting bottom levels also showed temporal variations. However, these were not caused by morphological changes, but were the result of a number of factors that were contributing to an error in measured bottom reflectance. In order to use SDB for multi-temporal sea bottom analysis, a good understanding of the reflectance fluctuations is necessary. Therefore, an analysis of all Sentinel-2 images over multiple areas was carried out in this research.
Initially, at an location around Abu Dhabi an area was defined over water. Out of all images in the collection that captured that area, monthly median composite images were created, where every pixel is the median value of all images captured in that month (can be over multiple years). Of all these composites, the median value of the pixels within the area of interest was calculated. These monthly values are plotted in figure 5.2a. Per wavelength band (blue, green, red and NIR), a yearly representation of reflectance is presented. In all wavelengths, the measured values are higher in summer than in winter.
To assess the workings of the atmospheric correction, the same was performed over an area of (not changing) land. A part of desert covered by the same images as the water area was assessed and again the monthly median values were calculated from the entire Sentinel-2 collection. In this case, all months show approximately equal reflectance values every month (Figure 5.2b). So, these seasonal fluctuations should be caused by the characteristics of the water. The atmospheric correction models are able to convert TOA to surface reflectance on land. Those same algorithms were not designed to obtain the reflectance from the sea floor and therefore the optical properties of water column are still present in Level-2 (surface reflectance) satellite images.

Figure 5.1: Water and land region of interest. Abu Dhabi, UAE

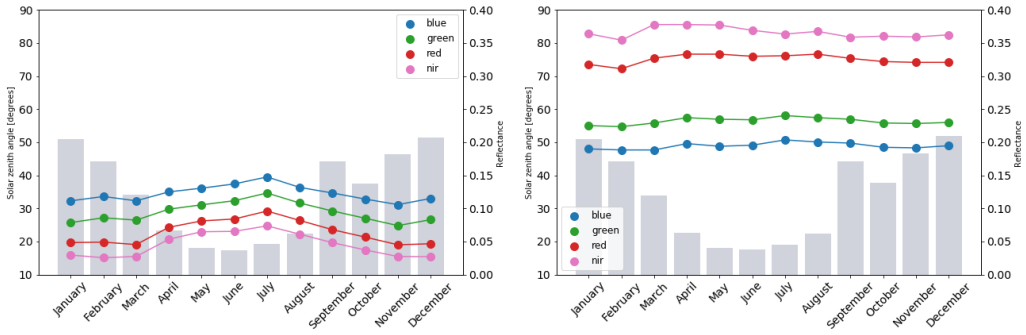

(a) Temporal analysis over water. Abu Dhabi, UAE **(b)** Temporal analysis over land. Abu Dhabi, UAE

Figure 5.2: Monthly median reflectance values over water and land. Gray bars represent solar zenith angle. Location: United Arab Emirates

On other locations around the world, the similar patterns in monthly median reflectance were obtained. Figure 5.3 shows the results of the analysis performed in Portugal (37°latitude) and Denmark (55°latitude). Between those two locations, the pattern significantly differs. In Portugal, just like in UAE, the high reflectances occur in the summer months and minimum values during the winter period. In Denmark, it is the other way around. Peaks of reflectance are occuring in winter and summer values are the lowest.

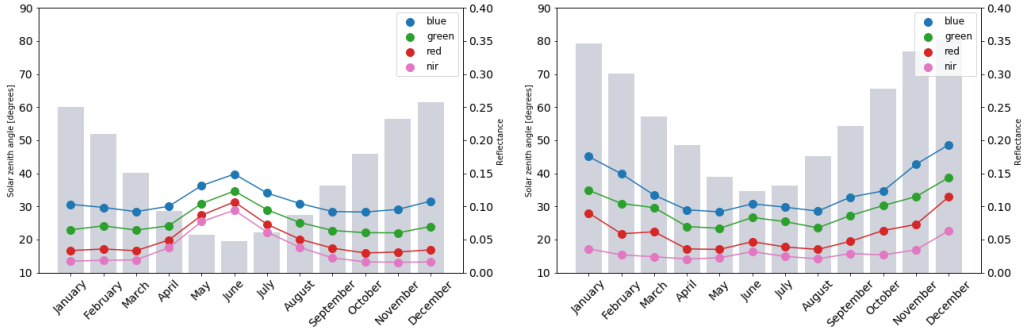

(a) Faro, Portugal 37°latitude **(b)** Denmark 55°latitude

Figure 5.3: Monthly median reflectance values. Gray bars represent the solar zenith angle.

The influence of these seasonal fluctuations was also visible in the cross-shore transect analysis (Figure 5.4). From all the summer images (April-September) a median composite was created. The same was done for all winter (October-March) images. The reflectances on the transect in Portugal are higher in summer than in winter and in Denmark it is opposite. It also seems that the higher value corresponds with more noise in the signal, which is especially noticeable in the winter images of Denmark.

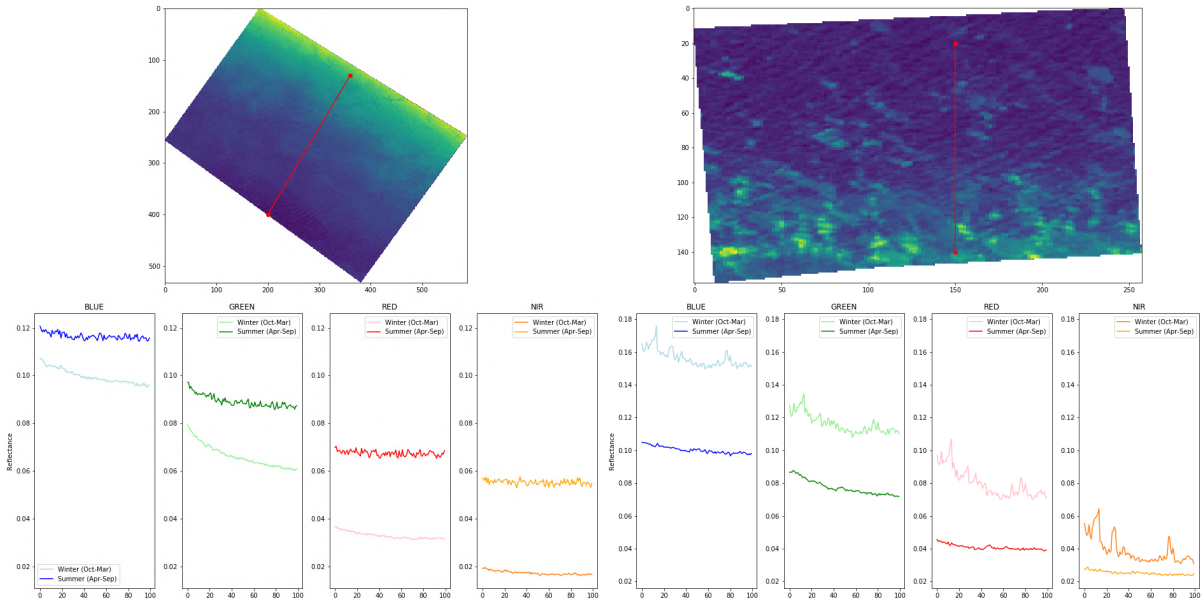

(a) Portugal **(b)** Denmark

Figure 5.4: Difference in reflectance values between summer and winter at two locations (Portugal and Denmark) with varying latitude. Note the switch in season with highest values between the locations

5.1.2 Solar Zenith Angle

Because the latitudinal position on earth relates to the seasonal pattern that was found (for both northern- as well as southern hemisphere), this effect is further analyzed. A contribution of temporal error that has not been reported by other SDB studies yet is the influence of the angle by which sunlight hits the surface of the water. Sunlight hits the earth's surface at an angle depending on the position of the sun relative to the earth. The solar position is defined by the the azimuth and zenith angles (Figure 5.5).

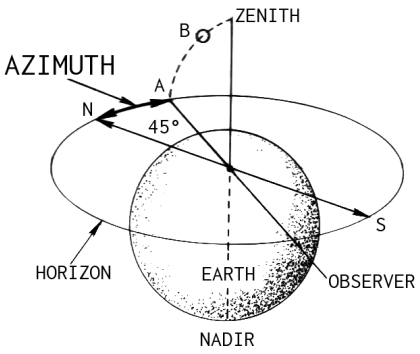

Figure 5.5: Illustration of Solar zenith and azimuth

The zenith angle indicates the height of the sun and the azimuth the horizontal position with respect to a horizontal plane at the location of the observer. The satellite records its own zenith and azimuth angles with respect to the earths surface, but, for Sentinel-2 satellites, these are more or less equal at every overpass. However, because the time of satellite overpass is approximately equal, the solar angles change during the year. In summer, zenith angles are low, which means that the sun is located high in the sky from an observer's perspective from earth (See the monthly median solar zenith angle indicated by the gray bars in figure 5.3 and 5.4). Therefore, the angle the sunlight

makes with respect to the water surface is small to almost perpendicular.Therefore, the influence of light refraction is negligible. In this situation, the light has the shortest path to the sea bottom. In winter, the zenith angle is higher, so the light hits the water surface with an angle.

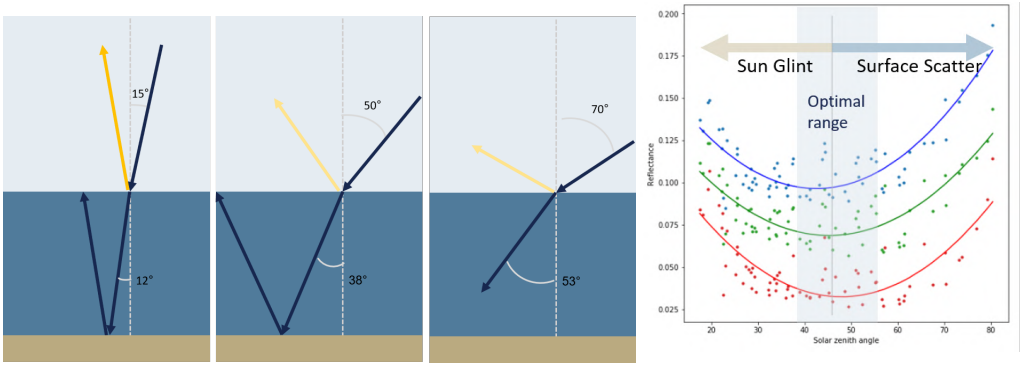

(a) Three regimes depending on incident solar angle.

(b) Analysis of 80 images: Reflectance vs. Solar Zeith Angle

Figure 5.6

Because of these variations in incident light angles, three regimes can be defined that cause for different manner of light reflection and absorption (Figure 5.6a). The first is when the sun's zenith position is highest ($< 40°$). The angle of both the sun and the satellite are close, which results in the direct reflection of sunlight from the water surface into the satellite's sensor. This phenomenon is called sun-glint and causes for high reflectance values, because the water surface is acting like a mirror for the sunlight. The other unfavorable regime is if the angle between the sun and the earth's surface becomes too large. A large portion of the light is refracted. Also the path that light has to travel in the water is becoming longer with increasing incident angle, so more light energy has been absorbed before it reaches the sea floor. Figure 5.6b shows the reflectance values for three wavelength bands (blue, green and red) of bout 80 images at different, non-turbid locations on earth plotted against the solar zenith angle. A typical pattern is visible minimum reflectance in the 40°-55°range.

The zenith angle depends on the latitudinal location on earth. Around the equator, the vertical position of the sun is more or less equal over the year, resulting in the absence of reflectance fluctuations. With increasing latitude, the differences in monthly solar angle become more prominent and are accompanied by an increase in reflectance fluctuations. At a location with an latitude of around 25°,during the summer the solar zenith angle is small and the reflectance that were measured were high. The opposite was observed in the winter period. Figure 5.7 shows the typical patterns that are measured over the year at different latitudes around the world. Similar (but opposite) patterns are noticeable on both northern- and southern hemisphere.

When satellite images are used to analyze temporal differences in water, this effect contributes significantly. Therefore, it is important to keep it in consideration or find a way to correct for it. Note that these analyses were performed in areas where turbidity levels were low. If turbid areas are considered, the median reflectances might show a different pattern based to the fluctuations of sediment concentration.

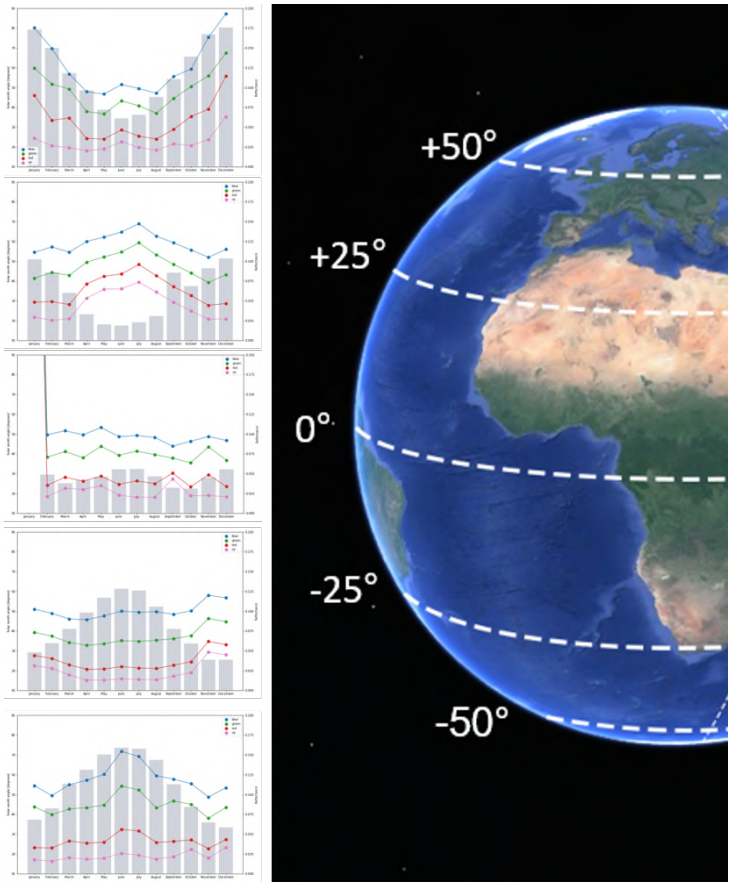

Figure 5.7: Typical patterns in measured reflectance over the year at different latitudes

5.2 Empirical SDB After Calibration

Empirical SDB methods are a simplification of the theory that describes the behavior of light in water, the radiative transfer theory. Therefore, they rely on the calibration with ground-truth data to achieve an accurate derivation of the bathymetry. Without the addition of that ground-truth data points in the area of interest, empirical SDB methods can not be used to obtain absolute bathymetry. When calibration is performed, understanding the raw signal from the satellite is key to achieve good and reliable results in water depth calculation. Especially in turbid environments, calibration should be performed with caution, because when calibrating the suspended sediment as sea floor, the SDB model will underestimate the water depth in those areas. Therefore, one should check if the bottom reflectance already shows the expected bottom shape. For empirical SDB methods applies "What you see is what you get". For instance, when deep channels are already not distinguishable from the raw reflectance signal because of turbidity or too large water depth, adding data does make them appear. Therefore, SDB must only be used if one is certain that the reflectance values of the image are representing the sea bottom.
Determining this level of certainty is key for a reliable SDB result, but is very complex to quantify. In the two extreme situations, very clear water and very turbid water, it is simple to determine the confidence in capturing the bottom reflectance just by looking at the image. However, for cases in between those situations, which occur in the majority of locations around the world, it is not so easy to distinguish a suitable image for SDB from an unsuitable one. Therefore, a more elaborate analysis on the importance of image selection was performed.

5.2.1 Image Selection

In chapter 4 the results of SDB with the addition of in-situ calibration data were presented. In various cases on different locations, resulting bathymetric maps were obtained with an accuracy within IHO CATZOC B (maximum vertical RMSE of about 1 meter). However, these results were obtained by performing calibration and validation on a single image, preferably one captured close to the moment of data acquisition. In the case calibration was applied to other images of the same area, the errors of the resulting SDBs fluctuated. For some images, the results were no reliable bathymetry derivation was obtained, even if the images were optically suitable for SDB (free of clouds and no visible suspended sediment). Because of sediments located in the lower part of the water column, the measurement of bottom reflectance might be disturbed. When vertical tuning was applied, the model was calibrated to the top of the sediment cloud, so no bottom shape was present in the initial reflectance signal. Also, the solar angle might be affecting the ability to use images for SDB in certain periods of the year.

When performing vertical tuning on images, it was found that, after filtering and pre-processing, some images gave a better resulting bathymetry than others. To analyze this, a number of images for the case study in Portugal were acquired. It was assumed that bottom changes were negligible in most depths in this area. A model was calibrated for every image using the same data points. In figure 5.8 the depth-separated RMSE values for the assessed images between 2015 and 2016 are presented next to each other. For every image, per depth (in bins of 1 meter), the RMSE was calculated. Per image, the errors differed, which meant that the SDB results strongly depended on the usability of the satellite image. Three images were selected from these time series (indicated by the numbers in the time series) to further analyze. One of which the bathymetry derivation was good (Figure 5.9b) and two images of which the vertical error with respect to the validation data was bad (Figure 5.9a and 5.9c). From the two "bad-performing" images, 5.9a could be visually distinguished as a non-suitable image because of high turbidity. However, 5.9c was visually not so different from the well-performing image apart from the increase brightness.
The occurrence of sediments in the water affected the results like the image in figure 5.9b. Another image with a large error (image figure 5.9c) visually seemed like a good image to use for the derivation of bathymetry. However, compared to "well-performing" images, the reflectance values in this image were higher, resulting in a brighter image.

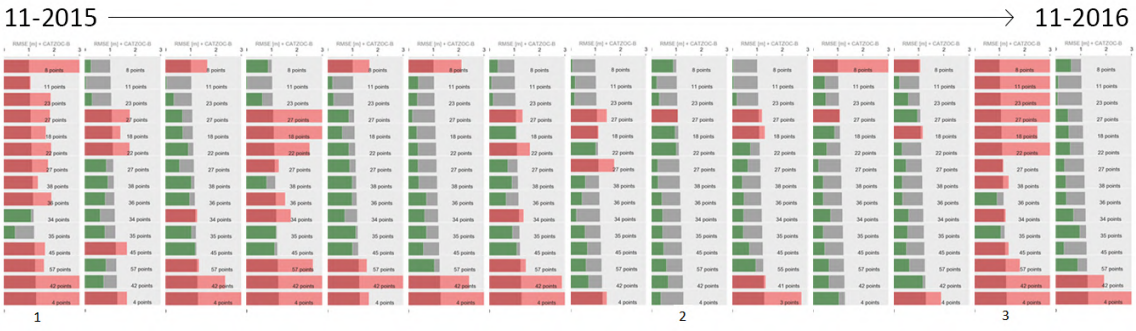

Figure 5.8: Faro timeline

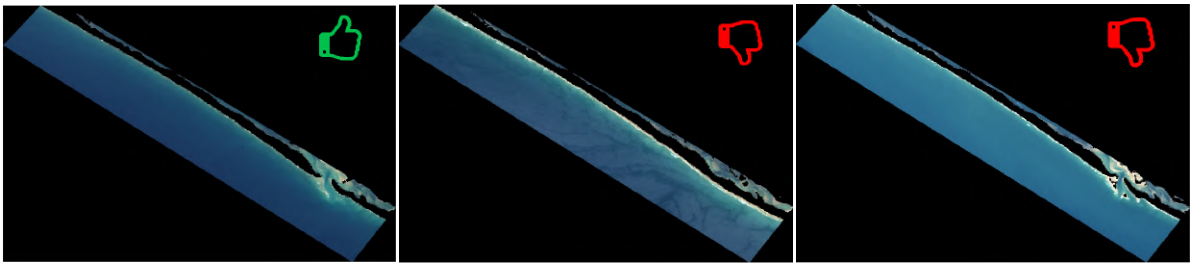

(a) Image 2 from fig 5.8 acquired at 17-10-2016 **(b)** Image 1 from fig 5.8 acquired at 04-11-2015 **(c)** Image 3 from fig 5.8 acquired at 11-06-2016

Figure 5.9: Left: Image resulting in a good bathymetry, middle and right image give the worst results

5.3 Applications of SDB

With calibrated SDB models one is able to derive the bathymetry at many locations on earth with a vertical accuracy that is smaller than 0.5 meter, which can be used in for instance the creation of nautical maps and as input for hydro-dynamical models. However, the optical conditions of water determine for a great part the confidence in the derived vertical bottom levels. Therefore, most of the research to (empirical) SDB focused on areas where water is clear enough to see the bottom. It was found in this research that even the addition of a small amount of data, distributed over a variety of depths, resulted in an accurate bottom derivation in clear waters. With these vertical errors and confidence in bottom levels, these SDB's could be a great contribution to smaller traditional survey. The small surveyed area can than be used to calibrate a model to derive the bathymetry of larger coastal areas within that image. One should consider the spatial differences in optical conditions when applying this technique, because with increasing the distance from calibration site, the uncertainty also increases. This is particularly significant in turbid water, where spatial differences can be large, which was covered in the assessment on spatial extrapolation in Portugal in section 4.4.

Without the addition of data, empirical SDB methods are not able to get close to an absolute bottom derivation. By using satellite images in the analysis on relative bottom changes, one should be aware of the temporal fluctuations that occur per image. Without knowledge on local conditions during capture of the image. Commercial parties found ways to derive bathymetry using other techniques than the empirical methods. These only apply for shallow, clear water areas and still have about the same accuracy as calibrated empirical methods under the same circumstances. If some ground-truth data is available and the optical conditions are suitable, empirical SDB method can provide an accurate representation of the bottom with decimeter accuracy.

Is satellite derived bathymetry using the presented methods in this thesis able to compete with established hydrographic survey methods? Not in terms of accuracy and spatial resolution. Unlike the data acquisition using echo sounding or ALS, SDB won't fulfill the accuracy requirements for IHO standards (special order or norm 1) in all waters. The application is highly depended on the local optical conditions of the water and can therefore not be used everywhere on earth. For instance for the detailed monitoring of sediment budgets or mapping of application in deep water, the accuracy and confidence achieved by SDB is not sufficient. Also in terms of spatial resolution, SDB can not always provide the desired specifications. Despite the increasingly amount of high resolution imagery, their GSD is still much larger than in-situ methods can achieve in area covering surveys. The application of SDB within the coastal zone management and monitoring lies more on the greater scale. Because of the large (and rapidly increasing) quantity of satellite imagery, and the increase in computational performance, on every location on earth some useful images are available to be used for SDB, shoreline derivation or other hydraulic research. Without actual visiting, one can obtain valuable information of even the most remote areas. With the use of satellite data, sea floor development of many years can be assessed.

Platforms like Google Earth Engine make the scientific research on satellite images even more accessible for researchers that didn't have the tools and knowledge in the past. The computation on global scale, long-term satellite data can be done from any laptop with access to the internet. No supercomputer is required for the user anymore. Global research on sandy coasts and shoreline change have already been performed using these tools and gave great insight in the global state of our sandy beaches. Information on bathymetry is always highly demanded, but hard to acquire and in most places around the world, not even available. In those areas, SDB can be a salvation to provide bathymetric information even at course accuracy and resolution. In many applications an indication of the bottom profile is already sufficient to be used in models, for instance in large-scale morpho-dynamic modeling.

6 Conclusion

Goal of this research was to obtain insight in the possibilities of empirical SDB applications and investigate the shortcomings of this technique, so one has realistic expectations in terms of vertical accuracy if SDB is applied in a certain area with typical (optical) conditions. A variety of analyses were done in order to provide answer to the research questions, which covered the use of SDB before and after calibration of the model, the multi-temporal use of satellite images and the spatial extrapolation of a calibrated model. To support these analyses, in multiple cases that all had specific environmental characteristics and optical water properties, the relatively simple empirical SDB models were assessed. In these cases was found that for waters where bottom reflectance is captured by the satellite's sensor, one is able to accurately (with an error smaller than 0.5m) obtain the bathymetry with empirical methods of SDB. In Sint Maarten, Key West and Portugal, a well derived bottom was obtained using some in-situ elevation data to calibrate the model, which is in accordance with other research in this topic. This research focused on the assessment of the applicability of empirical methods for satellite derived bathymetry under more challenging conditions more e. The following questions were formulated (chapter 1.2.2) to find the possibilities and shortcomings of empirical SDB methods:

Q1: What methods are available to derive bathymetric information from multi-spectral satellite imagery and how do they perform with respect to each other?

Before putting the calibrated empirical SDB technique to the test in a variety of conditions, a comparison was made between the linear- and ratio method. It was found that the use of either one of the two assessed empirical methods did not make a significant difference in the quality of the derived bathymetry. The most important factor was the choice of band combinations. Because multi-spectral satellite images contain a number of wavelength bands, a variety of combinations can be made in both methods. In the linear method, the more different bands added to the model, the better the resulting SDB. With the ratio method, the use of noisy bands like the red-band resulted in large outliers that affected the SDB result, but if only the blue and green band were used (in several combinations) results were comparable to the linear method. Because of the slightly better performance of the linear method, that one was chosen to be used in further analyses.

Q2 What are results of SDB methods without vertical tuning and are there SDB applications without providing calibration?

Empirical SDB methods rely on the availability of accurate ground-truth data for the calibration of the model. These data set are often not available, so an analysis on the use of satellite images without any calibration was performed to assess the performance in obtaining the water depth. It was found that, by applying the concept of light attenuation, the absolute water depth could not be derived accurately. This is caused by the many disturbances the light can find on its way to the satellite's sensor. For the disturbances caused by the atmosphere, a number of algorithms are developed to correct for them and leave the surface reflectance in the image. However, for the use of images in SDB, the sea floor reflectance is needed, which requires an additional correction of all the disturbances that take place within the water column. These have a large temporal- and spatial variability, so it is not possible to accurately correct for them without the availability of information on water clarity within the area of interest on the exact same moment the satellite image is captured. For this research that data was not available, so its influence on the depth retrieval could not be assessed.
For the use of satellite images in research hydraulic- and morpho-dynamics, the temporal differences between them were investigated. It was found that, despite hardly any bottom changes had occurred, images captured on different dates still gave different reflectance values. By applying an

atmospheric correction algorithm, the varieties of images should be corrected for. However, for areas over water, other factors play role in the reflectance of light. Besides the direct sources of light disturbance (clouds, sediments, algae, albedo), also a large seasonal effect was found that caused fluctuations in reflectance values of the period of a year. In an comprehensive temporal analysis, where the entire Sentinel-2 image collection was used, the seasonal reflectances were captured and a latitudinal influence became noticeable. The difference in solar zenith angle during capture of the images appeared to be a reason that caused a seasonal fluctuation in measured reflectance.
Due to these fluctuations, the temporal analysis of SDB is not possible without the availability of some calibration data. Because of the large differences between measured reflectance on images and the variations in inherent optical properties of water, a simple comparison between the images can not be made. Adding in-situ data per image is a way to make SDB inter-comparable, but requires the availability of data sets. SDB then is used to extend the spatial coverage of the acquired data. This leads to the analysis of spatial extrapolation of data.

Q3: What is the performance of the methods when they are extrapolated in time and space?

The great potential of satellite images lies in its temporal resolution and large area coverage. Therefore, it was investigated if a model can be used 1) for multiple images of the same area and 2) in areas within the calibrated image, but located at some distance from the calibration data. In this research those were called temporal and spatial extrapolation. For the temporal extrapolation it was found that a calibrated model was only applicable on the image that was used for calibration. The reflectances between images were varying too much to use the model also on other images of the same area. No correlation was found between the difference in reflectance and the difference in the model parameters, so also correction could not be applied.
The spatial extrapolation was assessed by selecting different study sites at varying distance from the calibration data. It was concluded that the result is very sensitive to differences in optical properties of the water at other location than the calibration site. Therefore, spatial extrapolation can only the done confidently if the optical properties are equal to the ones at the location of the ground-truth data, which hardly occurs in practice. Therefore, there is a limited application of spatially extrapolating the model which depends on the users allowed error margin.

Q4: How do water properties (turbidity, bottom type) influence the results of the SDB algorithms?

Increased levels of turbidity hinder the derivation of bathymetry. However, it is not always obvious that suspended sediments are present in the image. Therefore, SDB should be used with caution in areas where turbidity levels fluctuate. If the water is always turbid, SDB is not applicable, because it will calibrate the top of the sediment cloud to the in-situ bottom. A moderate level of turbidity however, can be dealt with using SDB, but only if the turbidity is uniform over the entire area of interest.
SDB works best on high reflective bottoms. If the bottom consists of reef or vegetation, only a small portion of the incident light is reflected. Therefore, it is difficult to obtain a reliable bottom from low reflective bottoms. In chapter 4.3.1, the results of an analysis were presented were a model was calibrated and validated with 1) only sandy bottom, 2) only rocky and vegetated bottom and 3) a mixed bottom consisting of both bottom types. It was found that if the bottom was mixed, it resulted in the worst performance in SDB. When dealing with a mixed bottom, the area should be divided (visually or automatically) into a sandy part and a rocky/vegetated part. When using a calibration data set covering both, SDB performs not as well as on a homogeneous bottom.

Q5: What is the applicability of the investigated SDB method?

Currently SDB is most frequently used in areas with clear water and reflective bottom to update the

charts and gain general understanding of the local bathymetry in these areas. In this research it was confirmed that in these situations with the empirical SDB technique a relatively accurate derivation of the bathymetry can be obtained with the addition of some ground-truth data. However, in these areas, the bottom can be assumed to be more or less steady (within the SDB error margin), so monitoring morpho-dynamic processes in these areas is not interesting. In areas where the bottom is developing, the optical conditions of SDB are mostly not optimal, because concentration of suspended sediments are higher it is harder for light to penetrate to the bottom. In these areas it was found that the selection of a suitable image is an important step in deriving a good bathymetry.

7 Recommendations

From this master thesis, and other researches that were done in the past, was concluded that it is possible to derive the bathymetry from satellite images using relatively simple empirical SDB methods. In earlier researches, this was mainly done in areas where the water clarity was good and wave action was limited. Also in this research it was found that in those areas the vertical position of the bottom can be derived within a margin of error in the order of decimeters. When the optical water properties were becoming more challenging, the vertical error of the bottom derivation increased and the calibrated model became less reliable. This research presented the possibilities and shortcomings of empirical methods for SDB by applying it in a variety of case studies. In this chapter recommendations for follow-up researches are presented that can append to the findings in this master thesis and can attribute to the SDB knowledge.

Calibration data from sources different than traditional surveys
It was found that, if either of the two empirical SDB methods were used, one requires (some) ground-truth data to obtain an accurate bottom derivation. In the areas where the bathymetry wants to be derived, this data is often not available or outdated, which makes it impossible to apply SDB. A valuable research would be to investigate the possibilities of using other data than the traditional in-situ survey data. For instance the satellite ICESAT-2, that acquires LiDAR data from space. When orbiting over water, it will receive a reflection from both the water surface and the bottom, so the local water depth on that scan line can be derived and used in the calibration of a SDB model. That way, an accurate bathymetry can be derived without visiting the area of interest.
Also other sources, like up-to-date charts (Navionics), could provide the necessary data to calibrate the model. In this research was found that only a few data points provided already sufficient vertical information to create an accurate model.

Pin the bathymetry on stable points
In this research was found that only a few ground-truth data points of the elevation could be sufficient to derive an accurate bathymetry (chapter 4.4.1). It is recommended to search for a few locations in the satellite image where it is known that the bed does not change and collect elevation data on these points. These can then be used as calibration points for the entire (dynamic) area on every image in the time series. It is still questionable if one can detect changes in sea floor because of spatial differences in water column properties. For instance, if a larger level of turbidity is present at one calibration location than another location, the calibration of the model is disturbed. Therefore, for these time series, using composite images might be a solution to eliminate the small scale water clarity effects.

Correct for monthly fluctuations
When a time series of satellite images is analyzed over an area of water, images show fluctuations in reflectance radiance. These can partly be assigned to the effect of incident angle of light in water (See Solar Zenith Angle chapter 5.1.2). A correction could be derived based on the seasonal (and therefore solar angle) fluctuations of reflectance. Because of the differences between single images, it may be useful to apply this to a monthly median composite image that includes all images collected during a month. Data from the entire collection can be used to derive typical monthly values (just as was done in chapter 5.1.1), which could be used to correct the reflectance values of single month composites in a time series. Plenty of cloudless images are required over an area where the satellite sensor is able to capture bottom reflectances to create proper composites. Similar to this research, the limitations for the technique could be assessed, but this time in terms of clarity and amount of required images could be assessed.

Use deep learning on entire collection

Because of the recent developments in cloud computing and the accessibility of large data set of satellite imagery, research of SDB has gained interest in the past few years. Despite the applied algorithms and techniques were often already developed many years before, they still work for today's applications. With increasingly more satellite data getting acquired and the availability of an archive of several years of data, applying artificial intelligence techniques to these large data set can give insights that were not found before. If hundreds of images of the same area are fed to an algorithm, it might be able to recognize if a difference in reflectance is caused by disturbances or by the actual change of the bottom level. Because Google provides the images and computational power with their Earth Engine, developing these algorithms has now become more accessible to researchers.

References

Caballero, I. and R. P. Stumpf
2019. Retrieval of nearshore bathymetry from sentinel-2a and 2b satellites in south florida coastal waters. *Estuarine, Coastal and Shelf Science*, 226:106277.

Chavez, Jr, P.
1988. An improved dark-object subtraction technique for atmospheric scattering correction of multispectral data. *Remote Sensing of Environment*, 24:459–479.

De Giglio, M., F. Goffo, N. Greggio, N. Merloni, M. Dubbini, and M. Barbarella
2017. Satellite and unmanned aerial vehicle data for the classification of sand dune vegetation. *ISPRS - International Archives of the Photogrammetry, Remote Sensing and Spatial Information Sciences*, XLII-3/W2:43–50.

Dekker, A. G., S. R. Phinn, J. Anstee, P. Bissett, V. E. Brando, B. Casey, P. Fearns, J. Hedley, W. Klonowski, Z. P. Lee, M. Lynch, M. Lyons, C. Mobley, and C. Roelfsema
. Intercomparison of shallow water bathymetry, hydro-optics, and benthos mapping techniques in australian and caribbean coastal environments. *Limnology and Oceanography: Methods*, 9(9):396–425.

Dekker, A. G., R. J. Vos, and S. W. M. Peters
2002. Analytical algorithms for lake water tsm estimation for retrospective analyses of tm and spot sensor data. *International Journal of Remote Sensing*, 23(1):15–35.

Donchyts, G., J. Schellekens, H. Winsemius, E. Eisemann, and N. van de Giesen
2016. A 30 m resolution surface water mask including estimation of positional and thematic differences using landsat 8, srtm and openstreetmap: A case study in the murray-darling basin, australia.

Durán, O. and L. J. Moore
2013. Vegetation controls on the maximum size of coastal dunes. 110(43):17217–17222.

Gao, J.
2009. Bathymetric mapping by means of remote sensing: methods, accuracy and limitations. *Progress in Physical Geography: Earth and Environment*, 33(1):103–116.

García-Rubio, G., D. Huntley, and P. Russell
2015. Evaluating shoreline identification using optical satellite images. *Marine Geology*, 359:96 – 105.

Gorelick, N., M. Hancher, M. Dixon, S. Ilyushchenko, D. Thau, and R. Moore
2017. Google earth engine: Planetary-scale geospatial analysis for everyone. *Remote Sensing of Environment*, 202:18 – 27. Big Remotely Sensed Data: tools, applications and experiences.

Hedley, J., A. R.Harborne, and P. J.Mumby
2005. Technical note: Simple and robust removal of sun glint for mapping shallow-water benthos. *International Journal of Remote Sensing*, 26(10):2107–2112.

Hodúl, M., S. Bird, A. Knudby, and R. Chénier
2018. Satellite derived photogrammetric bathymetry. *ISPRS Journal of Photogrammetry and Remote Sensing*, 142:268 – 277.

Kabiri, K.
2017. Discovering optimum method to extract depth information for nearshore coastal waters from sentinel-2a imagery - case study: Nayband bay, iran. *ISPRS - International Archives of the Photogrammetry, Remote Sensing and Spatial Information Sciences*, XLII-4/W4:105–110.

Kanno, A., Y. Koibuchi, and M. Isobe"
2011. "shallow water bathymetry from multispectral satellite images: Extensions of lyzenga's method for improving accuracy". *Coastal Engineering Journal*, 53.

Leah Moore
2010. Oceanography - light attenuation for various colors of light in water. [Online; accessed 20-April-2019].

Lee, Z., K. L. Carder, C. D. Mobley, R. G. Steward, and J. S. Patch
1999. Hyperspectral remote sensing for shallow waters: 2. deriving bottom depths and water properties by optimization. *Appl. Opt.*, 38(18):3831–3843.

Luijendijk, A., G. Hagenaars, R. Ranasinghe, F. Baart, G. Donchyts, and S. Aarninkhof
2018. The state of the world's beaches. *Scientific Reports*, 8.

Lymburner, L., E. Botha, E. Hestir, J. Anstee, S. Sagar, A. Dekker, and T. Malthus
2016. Landsat 8: Providing continuity and increased precision for measuring multi-decadal time series of total suspended matter. *Remote Sensing of Environment*, 185:108 – 118. Landsat 8 Science Results.

Lyzenga, D. R.
1985. Shallow-water bathymetry using combined lidar and passive multispectral scanner data. *International Journal of Remote Sensing*, 6(1):115–125.

Navionics
2019. Navionics chart. [Online; accessed 14-Juli-2019].

Ocean Optics Web Book
2019. Oceanography - light attenuation for various colors of light in water. [Online; accessed 8-May-2019].

Otsu, N.
1979. A threshold selection method from gray-level histograms. *IEEE Transactions on Systems, Man, and Cybernetics*, 9(1):62–66.

Pacheco, A., J. Horta, C. Loureiro, and Ó. Ferreira
2015. Retrieval of nearshore bathymetry from landsat 8 images: a tool for coastal monitoring in shallow waters. *Remote Sensing of Environment*, 159:102–116.

Poliyapram, V., V. Raghavan, M. Metz, L. Delucchi, and S. Masumoto
2017. Implementation of algorithm for satellite-derived bathymetry using open source gis and evaluation for tsunami simulation. *ISPRS International Journal of Geo-Information*, 6(3).

Sola, I. and R. Lloverí a
2018. Assessment of atmospheric correction methods for sentinel-2 images in mediterranean landscapes. *International Journal of Applied Earth Observation and Geoinformation*, 73.

Solazzo, D., J. B. Sankey, T. T. Sankey, and S. M. Munson
2018. Mapping and measuring aeolian sand dunes with photogrammetry and lidar from unmanned aerial vehicles (uav) and multispectral satellite imagery on the paria plateau, az, usa. *Geomorphology*, 319:174–185.

Stumpf, R. P., K. Holderied, and M. Sinclair
2003. Determination of water depth with high-resolution satellite imagery over variable bottom types. *Limnology and Oceanography*, 48(1part2):547–556.

Su, H., H. Liu, L. Wang, A. M. Filippi, W. D. Heyman, and R. A. Beck
2013. Geographically adaptive inversion model for improving bathymetric retrieval from satellite multispectral imagery. *IEEE Transactions on Geoscience and Remote Sensing*, 52(1):465–476.

Traganos, D., D. Poursanidis, B. Aggarwal, N. Chrysoulakis, and P. Reinartz
2018. Estimating satellite-derived bathymetry (sdb) with the google earth engine and sentinel-2. *Remote Sensing*, 10(6).

Tripathi, N. K. and A. M. Rao
2002. Bathymetric mapping in kakinada bay, india, using irs-1d liss-iii data. *International Journal of Remote Sensing*, 23(6):1013–1025.

Union of Concerned Scientists
2019. Ucs satellite database. [Online; accessed 28-August-2019].

United Nations
2017. The ocean conference factsheet.

Vinayaraj, P., V. Raghavan, and S. Masumoto
2016. Satellite-derived bathymetry using adaptive geographically weighted regression model. *Marine Geodesy*, 39(6):458–478.

Yrigoyen, C., I. García Rodríguez, and J. Otero
2008. Modeling spatial variations in household disposable income with geographically weighted regression. *Estadística española, ISSN 0014-1151, Vol. 50, Nº 168, 2008, pags. 321-360*.

Appendix A

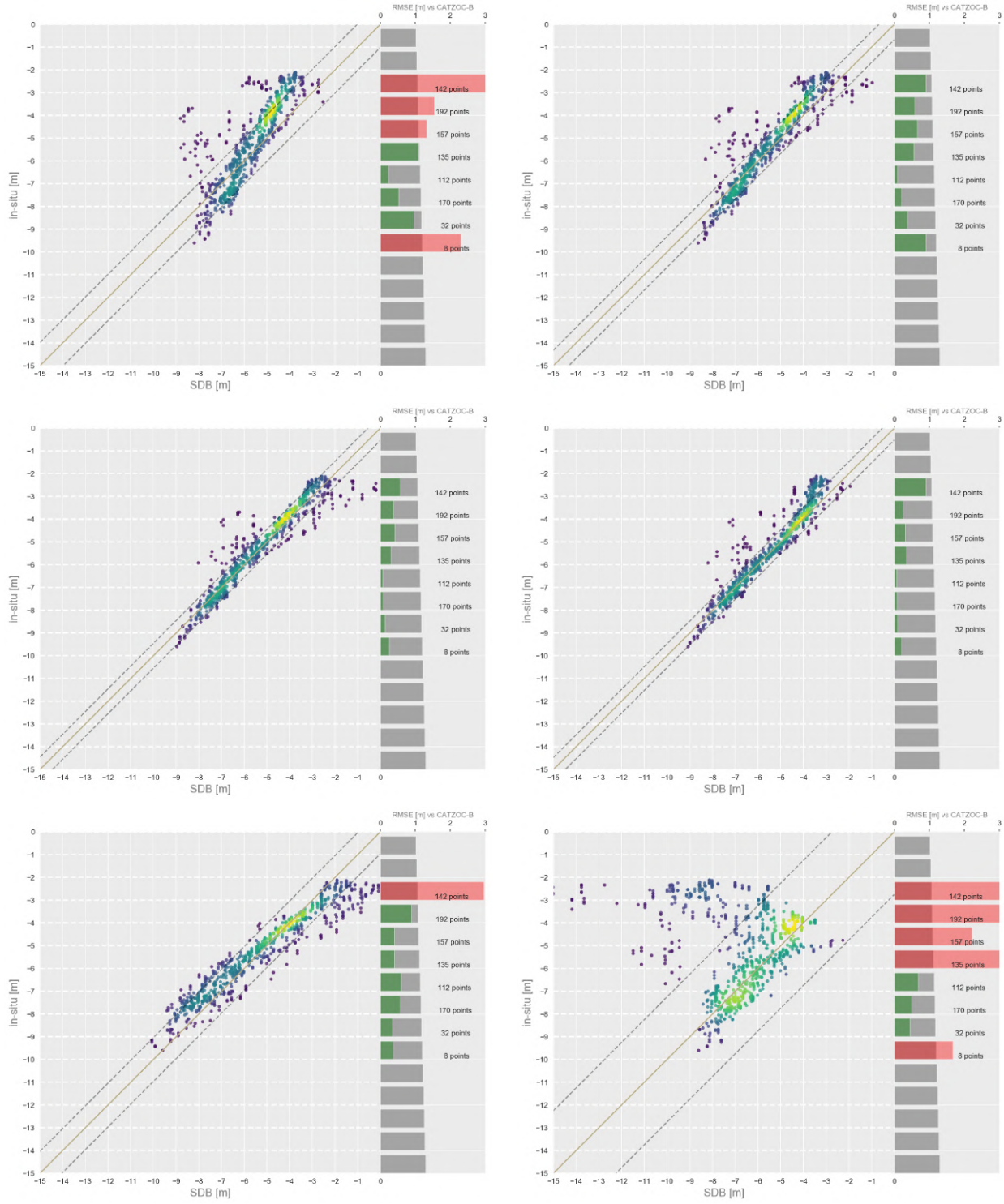

Figure A.1: Score plot for all methods: Top row: **L-B, L-G**; Middle row: **L-BG,L-BGR**; Bottom row: **R-BG, R-GR**. Colors of the points correspond with the density (yellow high, blue low)

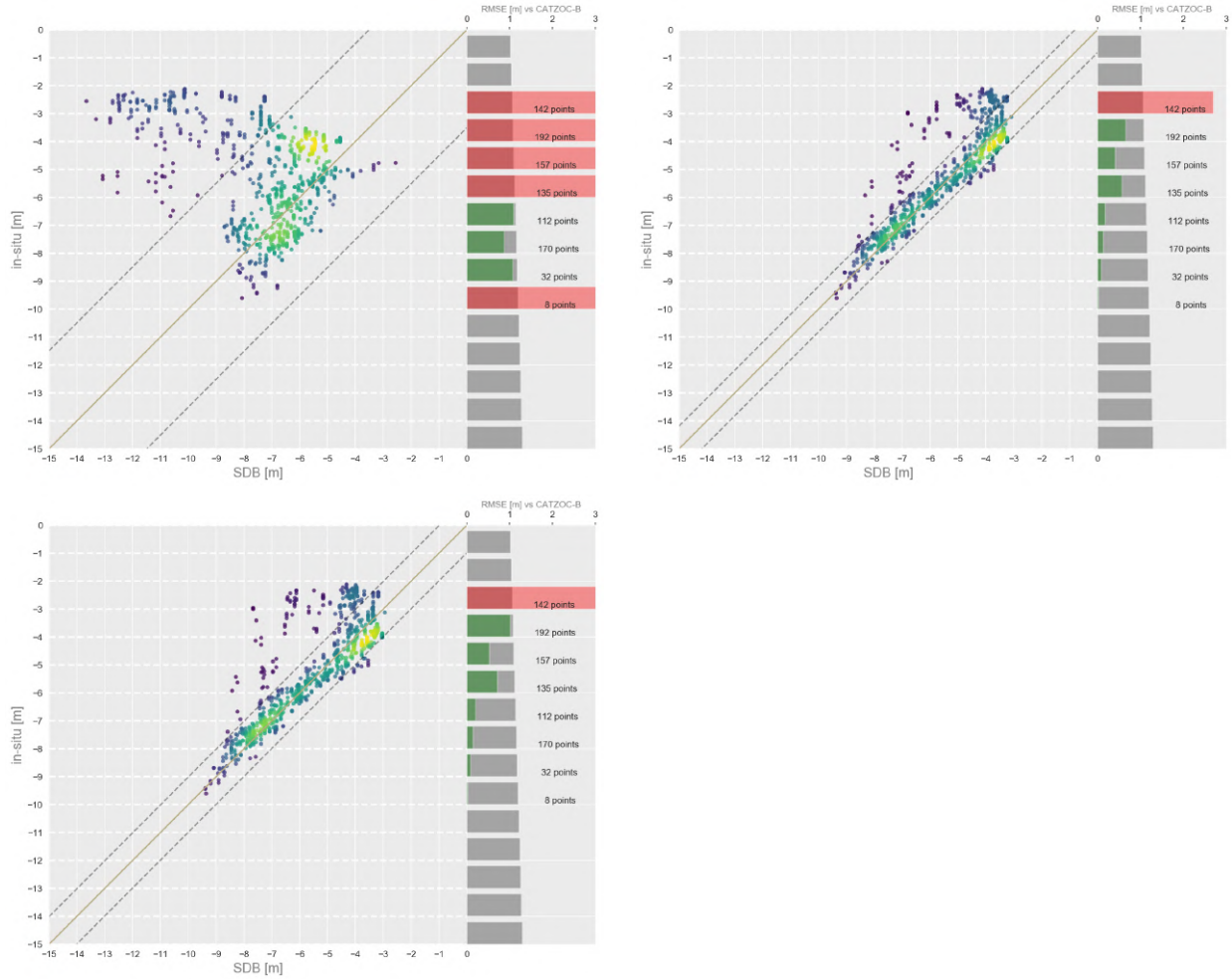

Figure A.2: Score plot for all methods: Top row:**R-BR, R-BGGR**; Bottom row: **R-BRGR**. Colors of the points correspond with the density (yellow high, blue low)

Appendix B

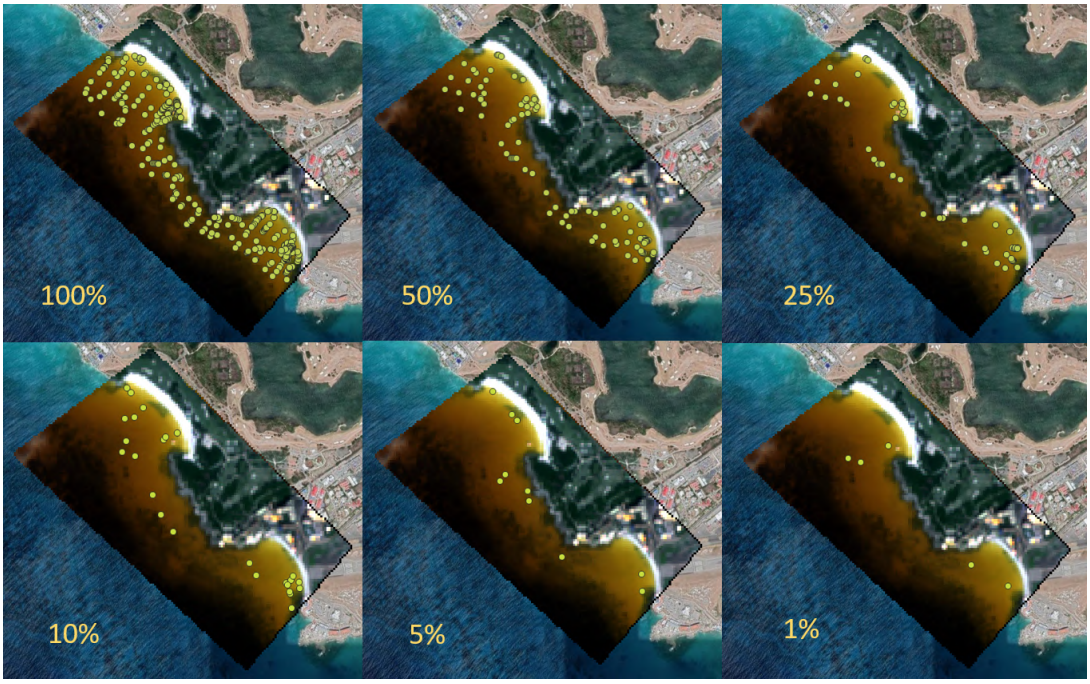

Figure B.1: Locations of the data points with decreasing amount of calibration data. Location: Sint Maarten

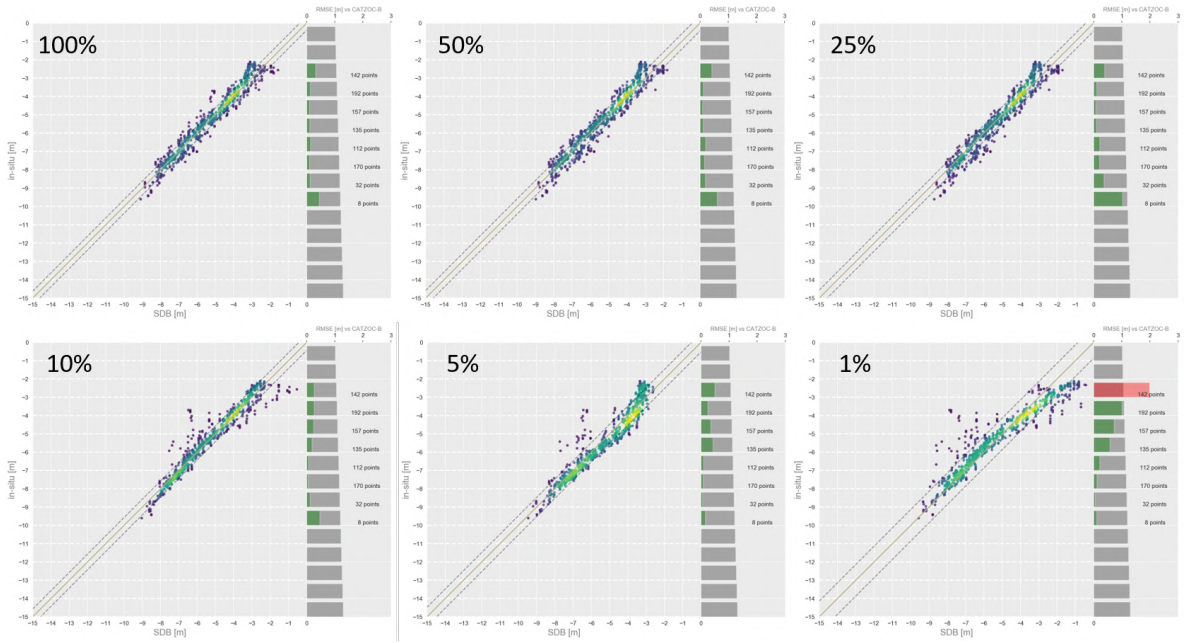

Figure B.2: Observed vs. SDB depth values in Sint Maarten with decreasing amount of calibration data. Bars on the right hand side show RMSE error. If green, CATZOC-B norm is satisfied and if red, the error is too large.